



Terms and Conditions of Use of Digitised Theses from Trinity College Library Dublin

Copyright statement

All material supplied by Trinity College Library is protected by copyright (under the Copyright and Related Rights Act, 2000 as amended) and other relevant Intellectual Property Rights. By accessing and using a Digitised Thesis from Trinity College Library you acknowledge that all Intellectual Property Rights in any Works supplied are the sole and exclusive property of the copyright and/or other IPR holder. Specific copyright holders may not be explicitly identified. Use of materials from other sources within a thesis should not be construed as a claim over them.

A non-exclusive, non-transferable licence is hereby granted to those using or reproducing, in whole or in part, the material for valid purposes, providing the copyright owners are acknowledged using the normal conventions. Where specific permission to use material is required, this is identified and such permission must be sought from the copyright holder or agency cited.

Liability statement

By using a Digitised Thesis, I accept that Trinity College Dublin bears no legal responsibility for the accuracy, legality or comprehensiveness of materials contained within the thesis, and that Trinity College Dublin accepts no liability for indirect, consequential, or incidental, damages or losses arising from use of the thesis for whatever reason. Information located in a thesis may be subject to specific use constraints, details of which may not be explicitly described. It is the responsibility of potential and actual users to be aware of such constraints and to abide by them. By making use of material from a digitised thesis, you accept these copyright and disclaimer provisions. Where it is brought to the attention of Trinity College Library that there may be a breach of copyright or other restraint, it is the policy to withdraw or take down access to a thesis while the issue is being resolved.

Access Agreement

By using a Digitised Thesis from Trinity College Library you are bound by the following Terms & Conditions. Please read them carefully.

I have read and I understand the following statement: All material supplied via a Digitised Thesis from Trinity College Library is protected by copyright and other intellectual property rights, and duplication or sale of all or part of any of a thesis is not permitted, except that material may be duplicated by you for your research use or for educational purposes in electronic or print form providing the copyright owners are acknowledged using the normal conventions. You must obtain permission for any other use. Electronic or print copies may not be offered, whether for sale or otherwise to anyone. This copy has been supplied on the understanding that it is copyright material and that no quotation from the thesis may be published without proper acknowledgement.

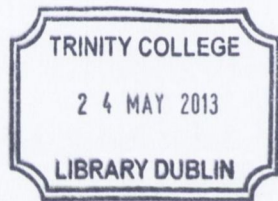
Zygomatic implants –
a finite element analysis study

Thesis submitted in part
fulfilment of D. Ch. Dent.

Oral Surgery

2012

Michael Freedman

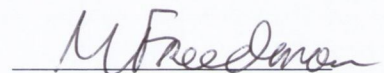


TX-1-944.

Declaration

This thesis

- has not been submitted as an exercise for a degree at the University of Dublin or any other University,
- is entirely my own work except where referenced in the text,
- may be lent or copied by the University Library upon request, subject to normal conditions of acknowledgement.


Michael Freedman

Summary

Alveolar bone resorption commonly occurs following the loss of teeth in the posterior maxilla. The placement of conventional dental implants is often difficult in this area when resorption has occurred. Zygomatic implants may be placed into the zygomatic bone and can support a dental prosthesis in the severely resorbed edentulous maxilla.

This study used a pre-operative CT scan of an edentulous patient undergoing zygomatic implant placement to create a computer model of half of an edentulous skull. Models of zygomatic implants and a fixed bridge were added to this. Finite element analysis models were constructed to study the effect of alveolar bone support, zygomatic implant position and additional bony support (bone graft) on the stress distributions in and around the zygomatic implants.

The results of this study consistently showed that stresses were dissipated through the zygomatic implants and the maxillary bone. Low stresses were noted in the zygomatic bone in all models. This finding is in contrast to previous research, but more accurately represents the stresses generated by masticatory loading. It was also demonstrated that the presence of alveolar bone support reduced the maximum stresses observed in and around the zygomatic implants. This finding has not previously been reported. Intra- and extra- sinus positions, as well as the presence of additional bony support had a variable effect on the maximum stresses observed.

Within the limitations of this study, the presence of alveolar bone support was shown to be beneficial for zygomatic implants. Masticatory stresses were predominantly distributed through the implants and the maxilla, with low stresses being transferred to the zygomatic bone.

Acknowledgements

This thesis was supervised by Prof. Leo Stassen and Mr Michael Ring. Without their assistance and guidance, it could not have been completed.

My thanks go to my parents, family, friends and especially to Laura, without whom this work would not be possible.

Contents

1. Terms and abbreviations	1
2. Introduction	5
3. Aim and objectives	8
3.1. Aim	8
3.2. Objectives	8
4. Literature review	9
4.1. Zygomatic implants	9
4.1.1. Introduction	9
4.1.2. Anatomical factors related to zygomatic implant placement	10
4.1.3. Protocols	15
4.1.3.1. Number of implants	15
4.1.3.2. Implant position	16
4.1.3.3. Loading	19
4.1.3.4. Grafting	20
4.1.4. Survival rates and complications	21
4.1.5. Alternatives	26
4.2. Finite element analysis	29
4.2.1. History	29
4.2.2. Theoretical method	32
4.2.3. Three-dimensional models	35
4.2.4. Application to implant dentistry	38
4.2.5. Material properties	40
4.3. Support of zygomatic implants	46
5. Materials and methods	48
5.1. Component Creation	48
5.1.1. Skull	48
5.1.1.1. CT scan	49
5.1.1.2. STL file creation (Mimics)	49
5.1.1.3. STL model editing (NetFabb)	50
5.1.1.4. Surface model (Rhinceros)	54
5.1.1.5. Solid model	54

5.1.1.6. Scaling	54
5.1.2. Zygomatic implants	55
5.1.3. Bridge	56
5.1.4. Grafts	57
5.2. Assembly of models	60
5.2.1. Model 1 - zygomatic implants in sinus, with alveolar support, no graft	60
5.2.1.1. Implant assembly and position	60
5.2.1.2. Implant placement in skull	61
5.2.2. Model 2 - zygomatic implants in sinus, with alveolar support, with graft	63
5.2.2.1. Implant, bridge and skull assembly	63
5.2.2.2. Graft positioning	63
5.2.3. Model 3 - zygomatic implants in sinus, no alveolar support, no graft	64
5.2.3.1. Implant, bridge and skull assembly	64
5.2.4. Model 4 - zygomatic implants in sinus, no alveolar support, with graft	65
5.2.4.1. Implant, bridge and skull assembly	65
5.2.4.2. Graft positioning	65
5.2.5. Model 5 – zygomatic implants out of the sinus, with alveolar support, no graft	66
5.2.5.1. Bridge, implant and positioning	66
5.2.6. Model 6 –zygomatic implants out of the sinus, with alveolar support, with graft	67
5.2.6.1. Implant, bridge and skull assembly	68
5.2.6.2. Graft positioning	68
5.2.7. Model 7 – zygomatic implants out of the sinus, no alveolar support, no graft	68
5.2.7.1. Bridge, implant and skull assembly	68
5.2.8. Model 8 – zygomatic implants out of the sinus, no alveolar support, with graft	69
5.2.8.1. Bridge, implant and skull position	69
5.2.8.2. Graft positioning	69
5.3. Finite element analysis	70
5.3.1. Material properties	70
5.3.2. Discretisation (Mesh Creation)	71
5.3.3. External forces	72
5.3.4. Boundary conditions	72
5.4. Analysis	72
6. Results	73
6.1. Distribution of stresses within models	73
6.2. Effect of force magnitude	83
6.3. Effect of force direction	87

6.4. Effect of alveolar support	88
6.5. Effect of implant position	89
6.6. Effect of additional bony support (graft)	90
7. Discussion	91
7.1. Model construction	91
7.2. Stress distribution in the skull	92
7.3. Alveolar bone support	94
7.4. Implant position	96
7.5. Additional bony support	97
7.6. Decision tree	98
7.7. Limitations	99
8. Conclusion	100
9. References	102
10. Appendix I - Model numbers and descriptions	112
11. Appendix II - Maximum stress tables	113
12. Appendix III – Stress distributions	117

1. Terms and abbreviations

The following terms and abbreviations are used in this thesis and are defined below for ease of reference.

Term	Definition
Boolean command	A task performed by computer software, which allows a logical operation to be performed on a number of bodies. This may allow two bodies to be joined, the shape of their intersection to be created, or for the shape of one body to be removed from another.
Cavity command	A task performed by computer software, where one solid body makes a hole in another.
CBCT	Cone beam computed tomography – a medical imaging technique that uses a cone of x-ray radiation to produce a three-dimensional image of a body.
CT	Computed tomography – a medical imaging technique that uses x-rays to produce a series of images as slices through a body.
DICOM	Digital Imaging and Communications in Medicine – a digital format used for storing, transmitting and printing medical images.
FEA	Finite element analysis.
FEM	Finite element method.
GPa (Giga Pascal)	Unit of pressure. One pascal is the pressure exerted by a force of one Newton over an area of one meter squared. A Giga

Term	Definition
	Pascal is 1,000,000,000 Pascals.
Hooke's Law	A law of elasticity that approximates the force exerted by a spring (or other linearly elastic material) when deformed. Hooke's Law states that the force exerted by a spring is directly proportional to its degree of extension.
Hounsfield unit	A value representing the radiodensity of an area of a CT scan. The radiodensity of distilled water at standard temperature and pressure is defined as 0 Hounsfield units, while the radiodensity of air is defined as -1000 Hounsfield units.
IGES	Initial Graphics Exchange Specification. A file format that allows the exchange of three dimensional computer models between different computer software packages.
Mass density	The mass of a body per unit volume.
Mimics	A software package that reads CT scans and other image data, allows selection of certain components of the images and creates a polygon surface model based on the scan data.
MRI	Magnetic Resonance Imaging – a medical imaging technique that uses magnetic fields to detect the nuclei of atoms (mainly water) in order to visualise the internal structures of a body.
N (Newton)	Unit of force. One Newton is the force needed to accelerate a mass of one kilogram at a rate of one meter per second squared.
Netfabb	A software package that allows editing and repair of polygon surfaces.

Term	Definition
NURBS	Non-Uniform Rational B Splines - a type of three-dimensional surface. It is defined mathematically by a number of control points to create a continuously curving surface. By changing the position and direction of the control points, the shape of the surface can easily be modified.
PET	Positron Emission Tomography – a medical imaging technique where the uptake of a radioisotope is measured by detecting the emission of gamma rays. This produces a three dimensional image, most commonly used to highlight areas of metabolic activity.
Poisson's Ratio	The ability of a structure to resist deformation in a direction perpendicular to that of the applied load.
Rhinoceros	A software package that creates and manipulates NURBS surfaces.
Simulation	A component of SolidWorks that performs finite element analysis.
SolidWorks	A software package that allows the creation and manipulation of three dimensional solid models.
STL	Steriolithography, a file type used to represent a surface as a series of triangles. Also known as Surface Tessellation Language.
Strain	The change in size of an object from one form to another.
Stress	The force per unit area applied to an object.
Von Mises Stress	The equivalent tensile stress used to predict the yielding of

Term	Definition
	materials, when they are placed under loads from different directions.
Yield Stress	The stress at which a material starts to deform plastically. At stresses lower than the yield stress, materials deform elastically.
Young's Modulus	The ratio of stress to strain, when a material deforms elastically. This is a measure of how easy it is to bend a material elastically.

2. Introduction

Zygomatic implants have facilitated the restoration of the edentulous maxilla with severe bone loss since 1990.¹ Following the loss of teeth, alveolar resorption and pneumatization of the maxillary sinus reduce the available bone volume. This can make the placement of conventional dental implants in the posterior maxilla difficult.² Traditional methods to overcome this problem include sinus lifting procedures and bone grafts.³ These traditional procedures aim to increase the volume of bone available. Despite a good overall success rate, these procedures are associated with significant morbidity and an increase in the treatment time.⁴ Zygomatic implants are placed into the zygomatic bone and may also be supported by the maxillary alveolar bone. They have shown success rates in excess of 90% for patients who are not suitable for bone grafting, or when bone grafting has failed.¹

Brånemark placed the first zygomatic implant in 1990, positioning the implants through the sinus into the zygomatic body.¹ This original protocol suggested that the implant should be supported at its coronal end by maxillary alveolar or palatal bone.¹ As the bone in the resorbed maxilla is very thin, it is easy to produce a bony defect in this area at the time of surgery, with consequent loss of alveolar support. Zygomatic implants have been designed that are supported only at their zygomatic end, with no support from the maxilla.⁵ Finite element studies have concluded that stresses applied to zygomatic implants are transferred mainly to the zygomatic bone.⁶ This study will investigate the validity of this conclusion and the effect that alveolar bone support has on zygomatic implants.

A variety of different zygomatic implant positions have been described. The original protocol placed the implants in an intra-sinus position, with implant threads exposed into the sinus cavity.⁷ Stella and Warner in 2000 proposed the sinus slot

technique where the implant is placed along the sinus wall.⁸ This along with extra-maxillary (sinus) positions have been advocated to aid visualisation and to facilitate the placement of the head of the implant in a favourable position for prosthetic restoration.⁵ While all implant positions have shown good results in case series, no clinical studies have been performed to compare implant positions. A finite element analysis has shown that both intra-sinus and extra-sinus implant positions produce favourable results, with the extra-sinus position yielding slightly lower maximum stresses in the implants themselves and the skull.⁹

Zygomatic implants are used to avoid the morbidity and delay of bone grafting. However, as the sinus lining may be preserved with careful surgical technique, the incorporation of a sinus lift procedure might be a logical extension of the zygomatic implant protocols. For extra-sinus implants, onlay grafting would also be a simple adjunctive procedure. This is routinely practiced for conventional implants that are not completely covered by bone at the time of placement.^{3, 10} Although bone grafting has not been reported for zygomatic implants, Chow *et al* in 2010 reported new bone formation around zygomatic implants when the sinus membrane was carefully preserved.¹¹ This is analogous to a sinus lift procedure. The value of this additional bone has not been studied.

Finite element analysis (FEA) has proven useful in the past to investigate the distribution of stresses in and around conventional dental implants.¹² FEA breaks down a complex body into smaller components, each of which can be modelled mathematically.¹³ Virtual forces are applied to the overall body of known material properties, allowing the internal stresses to be calculated at any given point.

This study investigated the importance of alveolar bone, implant positions and additional bony support (bone graft) in supporting zygomatic implants. It uses finite

element models to estimate the distribution of stresses throughout a bridge supported by two zygomatic implants per side, placed in the edentulous maxilla.

3. Aim and Objectives

3.1 Aim

To investigate the stresses in and around zygomatic implants placed with varying types of bony support and position.

3.2 Objectives

1. To create a computer model of a human edentulous maxilla / skull.
2. To analyse the stresses transferred to zygomatic implants and the skull with different implant positions.
3. To analyse the stresses transferred to zygomatic implants and the skull when the implants are supported by different elements of the zygomatic bone and maxilla.
4. To analyse the stresses transferred to zygomatic implants and the skull when additional bony support is provided for the implants.

4. Literature Review

4.1 Zygomatic implants

4.1.1 Introduction

Osseointegration is the direct structural and functional connection between living bone and the surface of the dental implant placed in bone.¹⁴ It was first developed by P.I. Brånemark in 1969.¹⁵ He was studying blood flow in an animal model using titanium chambers to provide direct visualisation of the movement of blood through bone. At the conclusion of the study, he found that the titanium chambers had become completely fused to the living bone. Instead of using another material to complete the study, he realised the significance of his accidental finding. This important scientific fact led to the development of dental implants as a means to support fixed and removable prosthodontics.

Dental implants are classically made from commercially pure titanium, which may be treated to give it various external surface characteristics.¹⁰ Originally, implants surfaces were milled resulting in a macroscopically smooth finish. Sandblasting, acid treating, plasma spraying and other techniques have since then been used to alter the milled surface. All of these treatments increase the surface roughness, leading to an increased bony surface contact area.. They have increased the bone to implant contact and reduced the incidence of bone loss around the implant.¹⁶ Titanium, as a metal, is highly reactive and on exposure to air its surface oxidises readily to form a very stable layer of inert titanium oxide.² The titanium oxide layer is biocompatible with bone and allows osteoblasts to grow onto and around it. This creates a direct connection between living bone and the implant.¹⁰

When an implant is initially placed into bone it relies on macro-mechanical retentive features to provide stability.¹⁷ Initial stability or primary stability is the

capacity of the implant to resist movements when it is first placed into bone. At this stage a microscopically thin layer of blood, which forms a clot, covers the surface of the implant. Osseous tissue treats the titanium oxide layer as if it were bone. The interface between an implant and the bone heals in the same way as a fractured bone.¹⁰ The blood clot is replaced initially by a callous and the callous is then infiltrated by osteoblasts, which form new bone.²

In order to achieve primary stability, a sufficient volume and density of bone must be present to provide initial stability.¹⁷ The maxilla and mandible, if treated early, can provide a sufficient volume of bone in the tooth bearing regions to place conventional dental implants.¹⁸ However, tooth loss, periodontal disease, infection, trauma and malignancy can result in bony deficiencies of the alveolar ridges.¹⁰ In the posterior maxilla, progressive pneumatisation of the sinus can reduce the amount of bone superior to the alveolar ridge, leading to an increase in the size of the sinus.¹ In these cases, or when bone augmentation procedures cannot be used or have failed, different options may be explored. The zygomatic bone provides an alternative site for the placement of implants bilaterally.¹⁹ These and other alternatives will be discussed in more detail below.

4.1.2 Anatomical factors related to zygomatic implant placement

The zygomatic bone forms the bony prominence of the cheek and makes up the lateral wall of the orbit (Fig 4.1).²⁰ It has three processes: frontal, temporal and maxillary. The frontal process extends superiorly forming the lateral wall of the orbit and connects the zygomatic bone to the frontal bone. The temporal process extends posteriorly to meet the zygomatic arch of the temporal bone. The term zygoma is often applied to both the zygomatic bone and the zygomatic arch of the temporal

bone.²⁰ This makes its use confusing, and it is therefore not used in this report. The most concave portion of the zygomatic bone between the frontal and temporal processes is known as the jugale.²¹ The maxillary process extends medially and inferiorly, making up part of the lower border of the orbit as well as forming the zygomatic buttress.

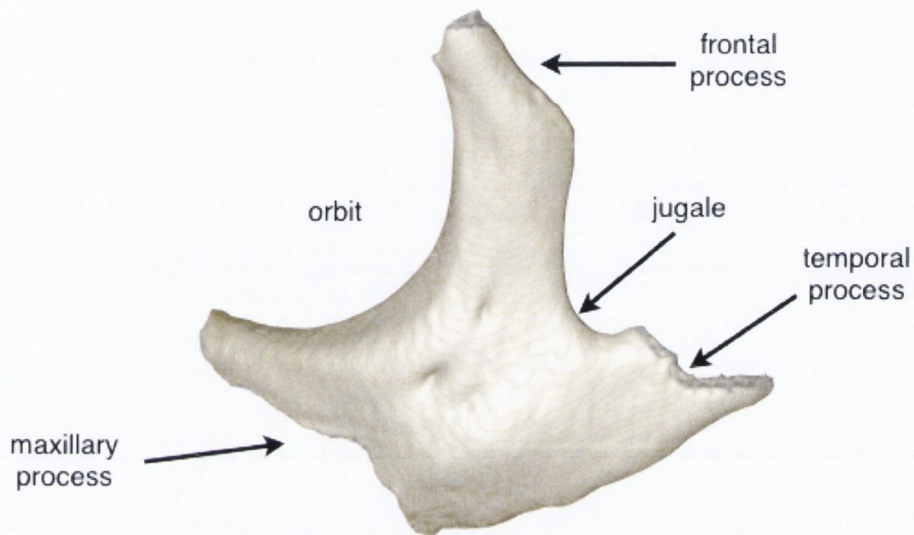


Figure 4.1 - Zygomatic bone

Two terminal branches of the maxillary division of the trigeminal nerve pass through the zygomatic body. The zygomaticofacial nerve exits the bone via the zygomaticofacial foramen and supplies sensation to the cheek. The zygomaticotemporal nerve exits the zygomatic body via the zygomaticotemporal foramen and supplies the skin to the side of the forehead.

The anatomy of the zygomatic body informs the placement of implants within it. Research has been conducted to evaluate the proportion of cortical bone available in the body of the zygomatic bone in order to estimate the average dimensions of the bone and to suggest anatomically ideal implant positions.

Nkenke *et al* in 2003 conducted a CT and histological analysis of thirty left zygomatic bones taken from edentulous cadavers.²² They investigated the radiographic bone mineral density, histological trabecular bone volume, histological cortical bone volume and histological trabecular bone pattern of the bones. They demonstrated that the bone mineral density was a useful predictive indicator for trabecular bone volume in the female zygomatic bones. They were unable to show the same correlation in the male samples, making its relevance questionable. In their study the percentage of cortical bone volume was $83.18\% \pm 8.87$ for the female zygomatic bones and $83.68\% \pm 6.35$ in the male zygomatic bones. The trabecular bone volume was $19.99\% \pm 7.60$ for the female zygomatic bones and $27.32\% \pm 9.49$ for the male zygomatic bones. This demonstrates that there is a large amount of cortical bone within the zygomatic bone that is available to support implants. This study compared male and female zygomatic bones. However, it also estimated the maximum implant length that could be supported within their zygomatic bone samples.²² They reported that $14.00\text{mm} \pm 3.10$ of length was available along the line of estimated implant position in the female samples and $16.53\text{mm} \pm 4.55$ was available in the male samples. Zygomatic implants are currently available in lengths from 30mm to 52.5mm.⁷ This suggests that a theoretical minimum of 20.8% of the implant (a 52.5mm implant in 10.9mm of bone) would be supported in zygomatic bone and a theoretical maximum of 70.3% of the implant (a 30mm implant in 21.08mm of bone) could be supported in zygomatic bone.

Kato *et al* in 2005 investigated the internal structure of the zygomatic bone using a micro-CT method.²¹ This is a small volume CT scan with resolution at the micron level rather than the millimetre level typically found in medical CT. They took twenty-eight zygomatic bones from edentulous cadavers and performed micro-CT

scans. They assumed that a zygomatic implant would be positioned along a line between the jugale and the most inferior part of the maxillary process of the zygomatic bone (Figure 4.1).

Along this line, they compared the bone volume density, trabecular plate thickness, trabecular plate number and trabecular plate separation on the micro-CT scans. They found that the mean bone volume density was lowest in the middle portion and highest at the upper (jugale) section of the zygomatic bone. There was a statistically significant difference between these two areas. The mean bone volume density in the area of bone at the maxillary process was lower than that at the jugale and higher than that at the centre of the zygomatic bones. These differences were not statistically significant. The findings of this study suggest that aiming the apex of implants towards the jugale, where they could engage this thicker bone should be beneficial.

The cephalic index is the ratio between the maximum transverse diameter of the skull and the maximum anteroposterior diameter of the skull. Rigollizo *et al* in 2005 investigated if the cephalic index was a useful predictor for zygomatic bone thickness using dried skulls.²³ They measured the maximum thickness of the zygomatic bones in 13 standardised positions and found bone thickness to vary from 1mm to 11mm in the same regions between samples. They were unable to show any useful correlation between bone thickness and the cephalic index. However, their results do show that there is a substantial variability in the thickness of different areas of the zygomatic bone and in the same areas between different zygomatic bones. They also found that the areas of zygomatic bone with greatest thickness were lateral and inferior to the orbit. They did not conduct any assessment of the cortical bone volume

or bone volume density. This would have been informative, as areas of greater bone thickness may not necessarily have correlated with areas of increased cortical bone.

The three studies described above have assumed that only one implant would be placed per zygomatic bone. However, loading protocols have been described supporting the use of two zygomatic implants per side.²⁴ The mean bone dimensions reported by Nkenke *et al* in 2003 are 25.4 x 7.6mm for females and 24.93 x 8mm for males.²² These measurements leave sufficient room for the placement of two zygomatic implants of 4mm diameter per side.

Rossi *et al* in 2008 therefore investigated the angle between two pairs of anatomical reference points to represent the ideal positions of a mesial and distal zygomatic implant.²⁵ They used a line between the two infra-orbital foramina as a reference plane that was neither dependant on the teeth nor changeable with maxillary resorption. They also measured the length of implants that would ideally have been required. A significant difference was found between the angulations of the mesial and distal implant positions in this study.²⁵ Although parallel placement of implants is preferred over angulated implants, this study suggests that parallelism is not achievable in the zygomatic bone when the implants are placed in an anatomically ideal position. The mean lengths required were 53.4mm (range 43.4-61.9mm) for the mesial implant and 42.5mm (range 34.9-51.5mm) for the distal implant. It is interesting to note that in many of these cases, longer implants than those that are currently available are required to achieve maximum bone support in the zygomatic bone, particularly for the mesial implant.

4.1.3 Protocols

Numerous protocols have been proposed for the placement of zygomatic implants. These differ in the number of implants placed, the positions of the implants and the timing of implant loading.

4.1.3.1 Number of implants

The original protocol for zygomatic implants was intended to restore the edentulous maxilla.^{1, 26} It used one zygomatic implant on each side with at least two conventional dental implants in the anterior maxilla. These are rigidly connected by a metal suprastructure in the restorative phase and allow forces, applied to one side, to be distributed to the other. This is termed cross arch stabilisation.⁷ Since then, protocols describing two zygomatic implants per quadrant have been described with and without conventional implants.^{24, 27}

Malavez *et al* in 2004 reported a case series based on their experience with zygomatic implants, where one zygomatic implant per zygomatic bone was placed with two to four anterior conventional implants.¹⁹ All of their 55 patients had edentulous maxillas, but in seven patients, only one side was suitable for the placement of zygomatic implants. This study showed a survival rate of 100% for the 103 zygomatic implants after an observation period of 12 to 48 months. In contrast to this, 16 of the 194 conventional implants placed failed, giving these a success rate of 91.75%. One patient in this case series developed a sinus infection, which responded to antibiotic treatment. No other complications were reported relating to the zygomatic implants.

Bothur *et al* in 2003 suggested that more than one zygomatic implant could be placed per side.²⁷ They noted that severe resorption may affect the anterior as well as

the posterior maxilla, requiring bone grafting procedures to place conventional dental implants. In this case, the placement of two to three zygomatic implants could be achieved without bone grafting, resulting in fewer surgical procedures for the patient and a quicker restorative result.²⁷

Miyamoto *et al* in 2010 conducted a finite element study investigating the effect of the number and position of implants in a maxillary defect model.²⁸ They used a CT scan of a patient following a hemi-maxillectomy to create a three-dimensional computer model. One or two zygomatic implants were simulated on the side with the defect and one to three conventional implants were simulated on the normal side. These were all connected by a gold alloy maxillary prosthesis. The results of their analysis showed better force distribution when two zygomatic implants were placed. The maximum stress noted in each zygomatic implant when two were used was roughly half that noted when one was used. The number and position of the conventional implants also have an effect on the maximum stress values noted, with more implants resulting in lower maximum stresses. This model may not be directly applicable to cases with normal anatomy, but it does demonstrate that multiple implants can be beneficial in spreading occlusal load when compared to single implants.

4.1.3.2 Implant position

Two different positions have been described for the placement of zygomatic implants.

The first is an intrasinus position.¹ This has the implant entering the maxilla palatal to the alveolar crest and passing through the sinus into the body of the zygomatic bone.⁷ A buccal window is opened into the sinus and the sinus membrane is elevated prior to implant placement.²⁶ The integrity of the sinus membrane is not

preserved in all cases, and is not considered essential to the procedure.^{7, 11} The apex of the implant is angled towards the jugale of the zygomatic bone, and may slightly exit the bone at this point.

The alternative technique involves an extra-sinus implant position. This concept was first proposed by Stella and Warner in 2000.⁸ They proposed the “Sinus Slot” technique, where the implant was positioned along the line of the lateral sinus wall. This drilling protocol produced a “slot” in the lateral maxilla, where the implant was placed, giving the technique its name (Figure 4.2). The advantages of this technique are that the implants may be placed under direct vision, a buccal sinus window is not required and it is quicker than the conventional procedure.²⁹ The sinus membrane is not raised during the procedure, and is perforated in all cases. The head of the implant is also closer to or on the alveolar ridge than with the conventional technique, facilitating restoration.



Figure 4.2 – The sinus slot implant position

Pennarocha *et al* in 2007 reported on the results of their case series of 40 zygomatic implants placed in 21 patients.²⁹ All of these implants were placed using the sinus slot technique and were supplemented by anterior conventional implants or pterygoid implants. Pterygoid implants are placed posterior to the maxilla into the pterygoid processes of the sphenoid bone. They are discussed further in section 4.1.5. The cases were followed up over an average of 29 months (range 12 – 45). In this series, the sinus membranes were perforated in all cases, with no attempt made to preserve them. Two patients reported post-operative sinusitis, which was treated with antibiotics. None of the zygomatic implants failed over the observation period. This shows similar results to the case series of intra-sinus zygomatic implants described by Malavez *et al* in 2004.¹⁹

Aparicio *et al* in 2010 produced a case series of 36 zygomatic implants placed in an extra-sinus position.³⁰ This group maintained the integrity of the sinus membrane during implant placement and reported no cases of sinusitis. They also had no zygomatic implant failures over the three-year follow up period. The stability of the zygomatic implants was assessed in this study using an electromechanical stability tester (Periotest).³¹ This percusses the implant and records the duration of contact between the instrument and the implant during percussion. This proprietary system produces a number, which increases with implant or tooth mobility. The Periotest values were found to be lower (more stable) for extra-sinus implants than those for similar implants placed in an intra-sinus position.³²

Chow *et al* in 2010 suggested a further alteration to the surgical technique, when the implants are placed in an intra-sinus position. They proposed an extended buccal window, allowing the sinus membrane to be fully lifted along the path of the

implant. By displacing the buccal bony window into the sinus, the membrane was protected from the rotary drilling instruments. They suggested that this technique would prevent sinus problems post-operatively, and reported no sinusitis in their series of sixteen patients (37 implants). Interestingly, when the patients had post-operative CT scans as part of the study protocol, new bone formation around the implants was noted inside the sinus.¹¹

Malo in 2008 used an extra-maxillary position that moved the zygomatic implant entirely out of the sinus.⁵ Using this technique, the implant was supported only by the zygomatic bone and had an implant survival rate of 98.5%. Migliorança in 2011 reported only two failures out of 150 zygomatic implants placed in addition to conventional implants with this technique.³³ Chrcanovic in a 2012 review, suggests that the decision on whether to place the implant in an intra-sinus or extra-sinus position should be based on the local anatomy.³⁴ In patients with large buccal concavities of the lateral maxilla, the extra-sinus position may be favoured. In cases where the lateral maxilla has a more convex shape, the intra-sinus position is suggested.³⁴

4.1.3.3 Loading

Different loading protocols have been developed for zygomatic implants, as they have been described with conventional implants. Delayed or late loading of zygomatic implants allows a period of five to eight months prior to the construction of a fixed prosthesis.^{1, 19, 35, 36} During this time, no functional forces are applied to the implants and they are allowed to osseointegrate.¹ As high success rates for this procedure were reported, immediate and early loading protocols were investigated to reduce the amount of time the patient spends without a fixed prosthesis.^{37, 38} Chow *et al* in 2006

first described an immediate loading protocol for zygomatic implants.³⁷ They used a guided surgery technique to place the zygomatic and conventional implants transmucosally. A buccal vestibular incision was made to allow visualisation of the implant through the sinus, but a mucoperiosteal flap was not otherwise raised. A provisional cobalt-chromium and acrylic prosthesis was connected to the implants immediately after the surgical procedure. This study showed a 100% success rate. It was a small study based on only ten zygomatic implants placed in five patients. The observation period was less than one year, leaving the long-term outcomes unknown.

Aparicio *et al* in 2010 reported on a case series of 47 immediately loaded zygomatic implants.³⁹ Their series was based on 47 implants placed in 25 consecutive patients and followed up from two to five years. Nineteen of these patients had temporary bridges placed after twenty-four hours and definitive restorations placed four to six months later. The remaining six patients had a definitive prosthesis placed and loaded five days after the implants were placed. This study reports a success rate of 100% for the zygomatic implants and no failures were noted in any of the 47 zygomatic implants two years post-operatively. However only eight of these implants were reviewed at the five-year follow up. Five-year results from the remaining 39 implants are needed in order to make long-term conclusions about this technique.

4.1.3.4 Grafting

Bone augmentation around the zygomatic implant, either with autogenous grafts or xenografts, is not described in any of the zygomatic implant protocols.^{1, 7, 11, 26, 27, 38} Indeed one of the advantages of zygomatic implants is that bone grafting does not appear to be required.²⁶ However, if the sinus membrane is maintained during zygomatic implant placement, carrying out a simultaneous bone augmentation is an

obvious extension of the procedure. Chow *et al* in 2010 placed zygomatic implants using an intra-sinus position and maintained the sinus membrane integrity.¹¹ As described above, their aim was to reduce the incidence of sinusitis post-operatively. However, they found that new bone formation was present around the body of the implants on follow up radiographs when no grafting material was used. They reported a 100% success rate at two years with this technique. This study demonstrates the ability to create additional support for the implant inside the sinus if the sinus membrane is maintained. This finding has not been reported by any other groups when the sinus membrane was either perforated or maintained.^{8, 26, 35, 36, 38-42}

4.1.4 Survival rates and complications

The survival rates for zygomatic implants have been reported in numerous case series and range from 90.3% to 100%.^{1, 30, 35} These high survival rates have been reported regardless of the number of implants placed, their position and the integrity of the sinus membrane. Most studies, however, report on a small number of patients observed over short time frames.

Brånemark *et al* in 2004 published a study that followed up 52 zygomatic implants for more than five years.¹ Their results showed a survival rate of 94% for the zygomatic implants and an overall prosthetic success rate of 96%. Kahnberg *et al* in 2007 published the largest case series of zygomatic implants. They followed up 145 implants over a three-year period in a multicentre study. The survival rate in their study was 96.3%.⁴³ Hirsch reported on 145 zygomatic implants over a shorter time frame (one year) with a survival rate of 97.9%.⁴² In all studies, the survival rate for the zygomatic implants was greater than the survival rates for the conventional

implants placed in the anterior maxilla at the same time.^{1, 19, 32, 35, 39, 43} This indicates the usefulness of the zygomatic bone as an alternative to conventional implant sites.

The most commonly reported complication related to zygomatic implants is sinusitis and is described in most case series.^{19, 32, 35} The incidence of sinusitis following zygomatic implants ranges from 0.7% to 19%.^{35, 43} The aetiology of this complication may be linked to the presence of the implant inside the sinus or the presence of an oroantral communication.^{30, 35} Petrusen, in 2004, conducted sinuscopy for patients treated with zygomatic implants who exhibited symptoms of sinusitis post-operatively.⁴⁴ He found healthy sinus membranes in all cases, leading to the conclusion that the sinus membrane is not irritated by the titanium surface of the implants.

Davo *et al* in 2008 studied sinus reactions to immediately loaded zygomatic implants.⁴⁵ They placed 71 implants in 36 patients, using an intra-sinus position or the sinus slot technique. The patients were followed up over a 13 to 42 month period. In all cases the sinus membrane was perforated, but they reported no cases of clinical sinusitis or oro-antral communication. Some thickening of the sinus lining was noted radiographically when post-operative CT scans were taken. As these did not cause clinical problems, sinus surgery was not performed for any of these patients.

The reported rates of sinusitis following zygomatic implant placement range from 2% to 27%.^{35, 42} Sinusitis has been reported when either an intra-sinus or an extra-sinus implant position has been used.^{1, 19, 29} It has been reported when the sinus membrane was kept intact.³⁵ Oro-antral fistulae have been reported even when the surgical protocol aimed to keep the membrane intact, suggesting that perforations may have occurred despite careful surgical techniques.^{35, 36} Results from Malo *et al*'s study in 2008, where all four cases of sinusitis occurred in patients where the

membrane was perforated, would suggest that it is prudent to maintain the integrity of the sinus membrane, if possible.⁵

Other complications reported include oroantral communication and altered sensation to the cheek or face^{1, 42, 43}. A case report of intracerebral placement of a zygomatic implant has been described⁴⁶.

When all studies investigating the success rates of zygomatic implants over a time frame of greater than one year are pooled, a total number of 1,189 implants have been reported, with 19 failures. This yields an overall survival rate of 98.4% of published cases as shown in table 4.1. A meta-analysis could not be carried out on these data as none of the published studies are randomised controlled trials.

Author	Year	Implants	Observation Period	No. per side	Position	Loading	Sinus Membrane	Survival Rate	Complications (number of cases)
Bedrossian ⁴⁷	2002	44	34 months	1	Intrasinus	6 month	Perforated	100%	Not reported
Brånanemark ¹	2004	52	5-10 years	1	Intrasinus	6 month	Perforated	94%	Recurrent sinusitis (4)
Malavez ¹⁹	2004	103	42 months	1	Intrasinus	Not reported	Not reported	100%	Sinusitis (5)
Hirsch ⁴²	2004	145	1 year	1	Intrasinus	Delayed	Perforated	97.9%	Paraesthesia (6), sinusitis (3), OAF (5)
Becktor ³⁵	2005	31	9-65 months	1	Intrasinus	5-8 months	Maintained	90.3%	Sinusitis (6), OAF (5)
Aparicio ³²	2006	131	0.5 – 5 years	1	Intrasinus	5-6 months	Not reported	100%	Sinusitis (3)
Bedrossian ⁴¹	2006	28	>12 months	1	Intrasinus	Immediate	Not reported	100%	None
Kahnberg ⁴³	2007	145	3 year	1	Intrasinus	6 months	Not reported	96.3%	OAF (3), Sinusitis (10), Paraesthesia (1)
Duarte ³⁸	2007	48	30 month	2	Intrasinus	1 day	Maintained	95.8%	None

Author	Year	Implants	Observation Period	No. per side	Position	Loading	Sinus Membrane	Survival Rate	Complications (number of cases)
Davo ⁴⁵	2008	71	13-42 months	1 or 2	Intra-/extra-sinus	Immediate	Perforated	100%	None
Peñarrocha ²⁹	2007	40	12 months	1	Extrasinus	2-4 months	Perforated	100%	Sinusitis (2)
Mozzati ⁴⁸	2008	14	2 years	1	Intrasinus	12-24 hours	Maintained	100%	None
Aparicio ³⁹	2010	47	2-5 years	1	Intra- /extra-sinus	1-5 days	Not reported	100%	None
Malo ⁵	2008	67	1 year	1 or 2	Extrasinus (no maxillary support)	Immediate	Perforated in some cases	98.5%	Sinusitis (4 - all in perforated membrane cases)
Aparicio ³⁰	2010	36	3 years	1	Extrasinus	4-5 months	Maintained	100%	None
Chow ¹¹	2010	37	6-24 months	1 or 2	Intrasinus	0-8 days	Maintained	100%	None
Migliorança ³³	2012	150	3 years	1	Extra-sinus	Immediate / Delayed	n/a (extramaxillary position)	99%	None

Table 4.1 - Case series reporting zygomatic implant survival rates over an observation period of greater than 12 months (continued from previous page).

4.1.5 Alternatives

A number of alternatives exist to zygomatic implants, each of which has advantages and disadvantages. These are summarised in table 4.2.

Technique	Advantages	Disadvantages
Tissue Supported Denture	Cheap, no surgery needed, no special training required	Removable, often poor retention in the resorbed maxilla, decreased oral function, palatal coverage
Implant supported overdenture	Requires small number of conventional implants	Removable, dependant on sufficient bone volume
Bone augmentation and conventional implants	Conventional procedure	Numerous surgeries needed, may not yield sufficient bone, unpredictable results
Pterygoid Implants	Does not involve the sinus	Needs to be supported by other conventional implants

Table 4.2 – alternatives to zygomatic implants

Conventional (tissue supported) dentures were the only option for the restoration of the edentulous maxilla prior to the availability of osseointegrated implants. They require no surgery and have none of the associated risks and morbidity.⁴⁷ However, retention of maxillary dentures in many cases, and particularly in the severely resorbed maxilla is poor.⁴⁸

Implant supported overdentures aid retention and have been shown to improve function and quality of life when compared to conventional dentures.⁴⁹ Despite this, some patients cannot tolerate a removable prosthesis and require a fixed option.

Bone augmentation procedures have been widely used to allow the placement of dental implants in the resorbed maxilla and mandible, which can support a fixed prosthesis.¹⁰ While autogenous bone grafts remain the gold standard, predictable results have also been shown with bone xenografts.³ No one technique has been shown to be superior to others in sinus lift procedures.⁴ Any augmentation procedure requires an initial surgery, followed by a period of healing before implants can be placed. For autogenous grafts a donor site is also needed and this is a surgical procedure with its own risks. It is generally safe, but should be best avoided, if possible.

No studies have directly compared a fixed restoration supported by zygomatic implants to one supported by conventional implants. In 2001 Jensen *et al* described a case series of immediately loaded fixed restorations supported by four conventional implants.⁵⁰ They followed up ten patients (40 implants) for a period of one year. All patients had resorbed maxilla with substantial pneumatization of the sinuses. The implants were angulated to engage the bone lateral to the nasal cavity using the M-4 technique (Figure 4.3).⁵¹ Where the implants crossed the maxillary sinuses, the sinus membrane was elevated and bone morphogenetic protein was placed. They reported a 94.8% implant survival rate and a 100% prosthetic success rate with this technique.⁵⁰ This method is comparable to a zygomatic implant option as it does not require a separate grafting procedure and results in a fixed prosthesis.

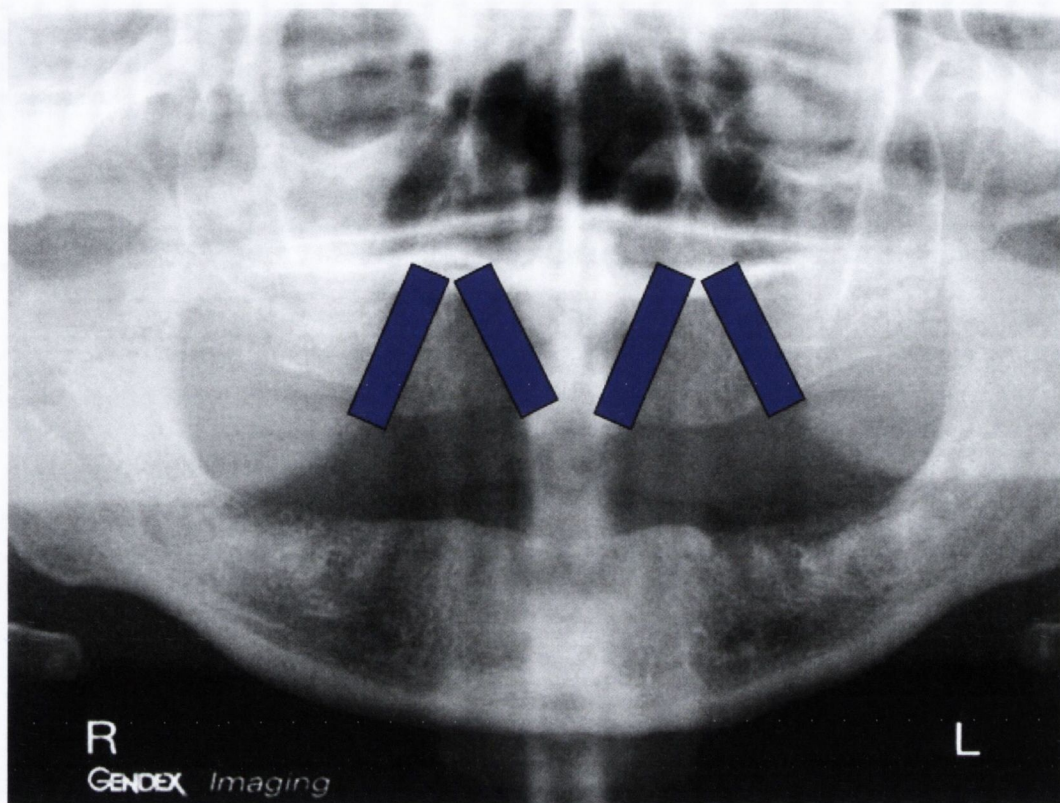


Figure 4.3 – Implant positions in the M-4 technique.

Placement of conventional dental implants in the pterygo-maxillary region or the pterygoid plates is a technique that can be used in the posterior resorbed maxilla (Figure 4.4). Candel *et al* in 2011 published a review of the success rates associated with these implants.⁵² They found that the weighted average success rate for pterygoid implants was 90.7%, which is similar to conventional implants. This success rate is lower, however than the reported success rates for zygomatic implants.¹ As with conventional implants, no studies have directly compared zygomatic implants to pterygoid implants.

While zygomatic implants have been placed since 1990, no direct comparisons have been made to alternative techniques. This is in part because zygomatic implants were initially used where all other techniques had failed.¹ All studies investigating the survival rates of zygomatic implants have shown better results when compared to

conventional implants placed at the same time. However long term, randomised controlled trials would be needed to directly compare the success rates of zygomatic implants to alternative techniques.

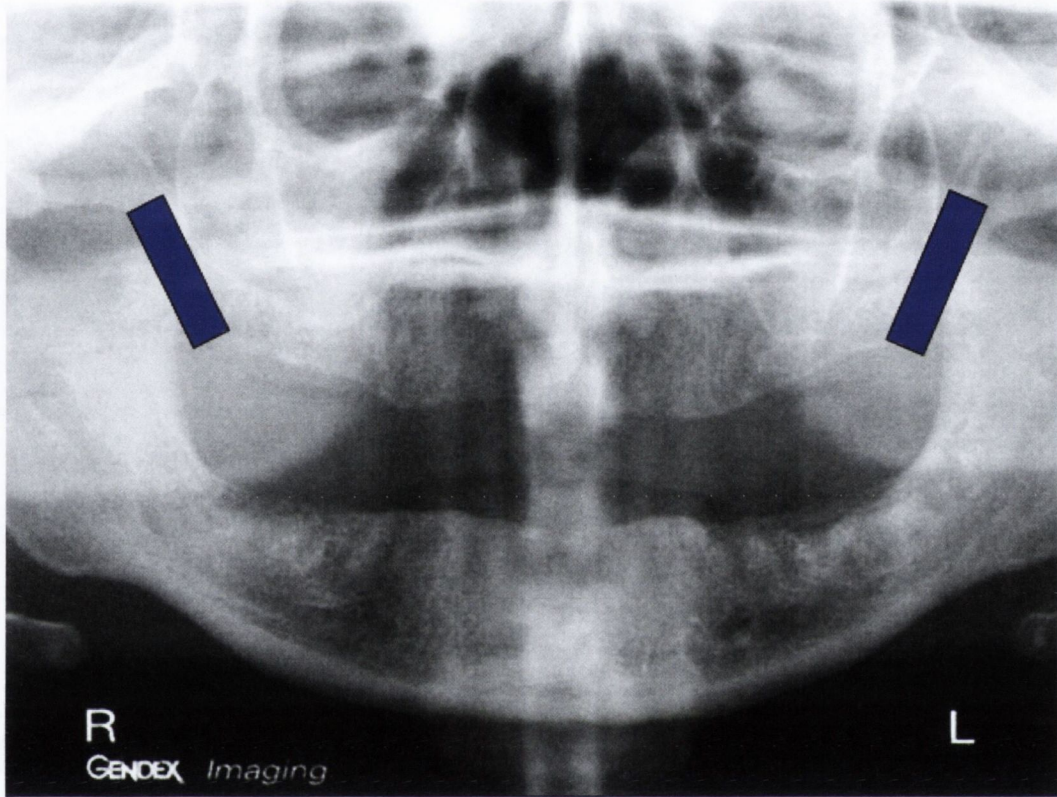


Figure 4.4 - Pterygoid implant positions.

4.2 Finite element analysis

4.2.1 History

The finite element method is defined as a numerical method for solving problems of engineering and physics.¹³ This definition is sufficiently broad to cover the large array of problems that the finite element method is applied to; however it does not satisfactorily explain what it is. The finite element method can be thought of as a way of mathematically describing complex shapes by breaking them down into smaller parts.¹² Finite element analysis (FEA) is the interpretation of the results of the finite

element method (FEM). The terms FEA and FEM are used interchangeably in the literature. For simplicity in this thesis FEA will be used to describe both the technique and the analysis.

The FEA method evolved over the past seventy years from the three fields of applied mathematics, physics and engineering as a result of problems that could not be answered using standard techniques available at the time.⁵³ In the 1930s and 1940s, the effects of forces on a plate were being examined by the engineering community. Using standard techniques it was possible to calculate the effect of a load on a body made out of a series of trusses (Figure 4.5). However, there was no way to evaluate the same forces on a solid plate of the same size and shape. Hrennikoff in 1941 developed the framework method, which proposed that a solid structure could be simplified by assuming that it was made from smaller, simpler components (Figure 4.6).⁵⁴ This method proved to be very successful and established the beginnings of FEA in the engineering community.



Figure 4.5 – a truss bridge

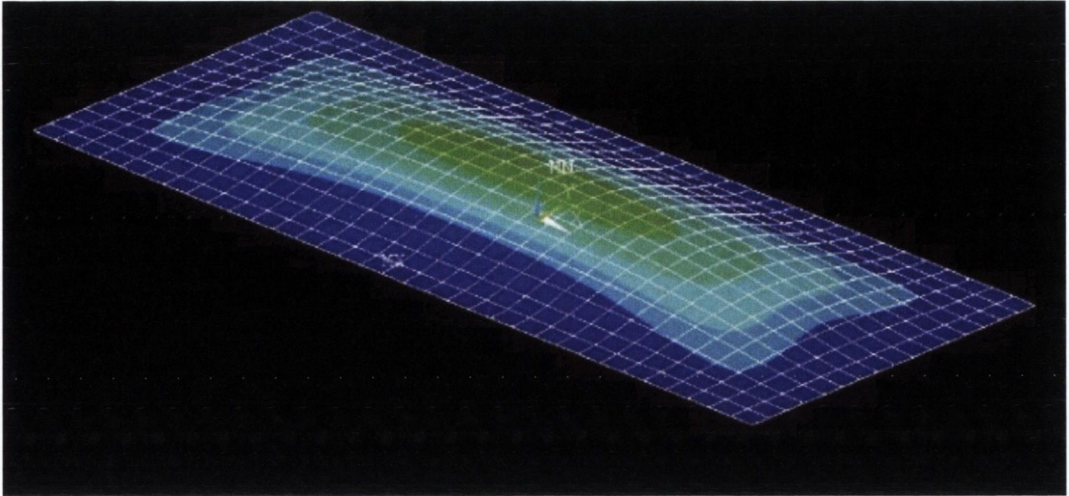


Figure 4.6 – A model of plate, made up of a lattice, undergoing bending.

In applied mathematics in the 1940s, Courant was investigating the Saint-Venant's principle (Figure 4.7).⁵⁵ He used a new approach to do this by conceptualising a structure as being made of a series of small triangles.

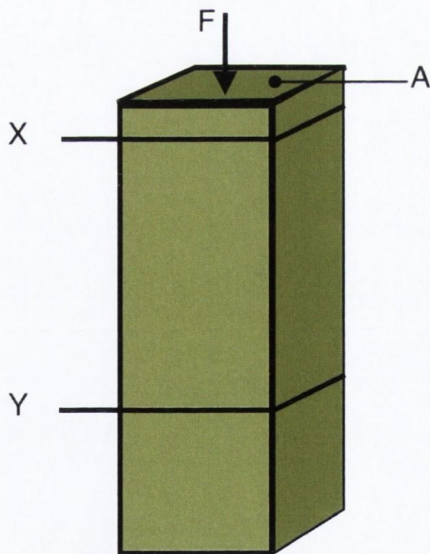


Figure 4.7 – Saint-Venant's principle states stresses far away from the point of application of a force (F) are not affected by the stresses close to point of application of a force. Stress is defined as force (F) per unit area (A). In the diagram above, this means that the stress at Y can be calculated as F/A , while this may not be true at X .

Advances in aeronautical and structural engineering in the 1950s and '60s were creating more and more complex shapes that needed to be studied. In 1956, Turner *et al* described stresses across a plane mathematically.⁵⁶ In 1959, Greenstadt described a method of breaking complex shapes into individual "cells". He was able to represent an unknown shape using a combination of mathematical functions, one for each cell that made up the overall shape.⁵⁷ These separate branches of similar work continued into the 1960s. It was Clough *et al* who in 1960 first coined the phrase "finite element method".⁵⁸

Since then, FEA has been used to study problems in numerous fields including structural analysis, heat transfer, fluid flow and electromagnetic potential.⁵³ The scope of its applications has increased significantly with the revolution in computer availability and power. This has allowed large and complicated models to be quickly broken down into components for analysis using FEA.¹³

4.2.2 Theoretical Method

FEA can be broken down into a series of steps.^{13, 53}

1. Discretisation

This process takes a large or complicated shape (a continuum) and breaks it down into simpler, smaller shapes (elements). The points where elements meet are called nodes. The number of elements used will dictate the accuracy and detail of the model. More elements will give a closer approximation of the continuum, but will be more complicated to solve. The choice of elements will vary depending on the problem or shape being studied and can include:

- a. 1-Dimensional elements e.g. a simple line

- b. 2-Dimensional elements e.g a triangular or quadrilateral plane
- c. 3-Dimensional elements e.g. a tetrahedral shape

2. Select a displacement function

This step involves looking at each type of element being used and selecting a mathematical model that describes its displacement when a force is applied to it. An example of a displacement function for a simple line element is shown in Figure 4.8.

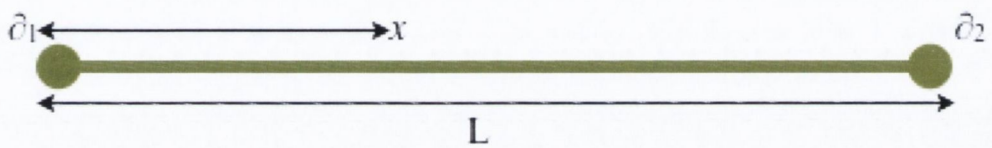


Figure 4.8 - The displacement function for a simple line element:

$\delta = (\delta_2 - \delta_1)x / L + \delta_1$, where δ is the displacement at point x , δ_1 is the displacement at node 1, δ_2 is the displacement at node 2, and L is the length of the line, all along the plane of the line element.

3. Define a stress / strain relationship

Stress is the force per unit area applied to an object. Strain is the change in size of an object from one form to another. The strain can be calculated from the displacement function in step 2 and the stress can be calculated using Hooke's Law. This can be developed into a formula to describe the stress / strain in a spring, elastic rod and a plane. It can also be applied to three-dimensional solids. The derivation of Hooke's law for an elastic rod is shown in Figure 4.9.

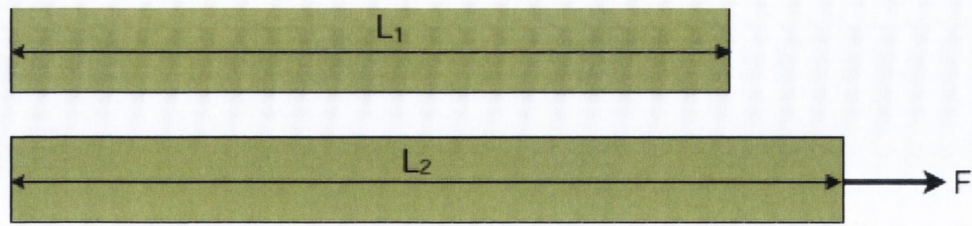


Figure 4.9 - Stress (σ) in a bar of original length L_1 , with a length of L_2 under a force F and a modulus of elasticity of E : $\sigma = E(L_2 - L_1 / L_1)$.

4. Derive the element stiffness matrices and equations

This step involves combining the formulae from steps two and three to produce a mathematical model for each of the elements within the continuum.

5. Assemble element equations

The individual mathematical models from step four are combined to form a mathematical model of the entire continuum. It is also necessary to establish some boundary conditions. This defines some elements as being fixed (cannot move). If no elements were fixed, when a force was applied to the system, the entire body would move, rather than deforming.

6. Solve equations for displacement

At this stage enough information is available to solve the displacement for the entire continuum. Using the solution, the displacement of any point within the continuum can be calculated when a force is applied.

7. Solve equations for stress / strain

Using the displacement calculated from step 6, a generalised formula for the stress at any point in the continuum can be calculated.

8. Analyse / Interpret results

As FEA is a mathematical method, the results that it produces will simply be a series of numbers. These can be displayed as graphs or overlaid as colours on the model being studied to assist with the interpretation of the results.

In practice, most FEA is carried out using computer software. Numerous packages are available, which can discretise any three-dimensional solid shape. This process is called mesh creation.¹² Displacement functions, stress-strain relationships and element equations can all be automatically derived and solved. This has allowed FEA to be carried out on very complicated shapes quickly and accurately.

4.2.3 Three-dimensional models

There are numerous ways to describe a three-dimensional object mathematically (Figure 4.8). Computer software can display these descriptions, creating a graphical representation of the object. The object can be represented graphically as a series of points, by points connected by lines or by a surface extending around the object.

A point cloud is the simplest method of describing a three dimensional object. A series of points that touch the object can be defined as having individual positions in an x, y, z axis. When these are all plotted together, they form the outline of the object that they represent.⁵⁹ A larger number of points will create a model with greater detail, but will use more memory and computer power. A CT scan is a version of a point cloud, which assigns each point (voxel) in the scan a value based on the radiodensity of the material being scanned.⁶⁰ The points are typically arranged as slices to aid interpretation, but when the slices are placed one on top of the other, they form a series of points in the x, y, z axes.

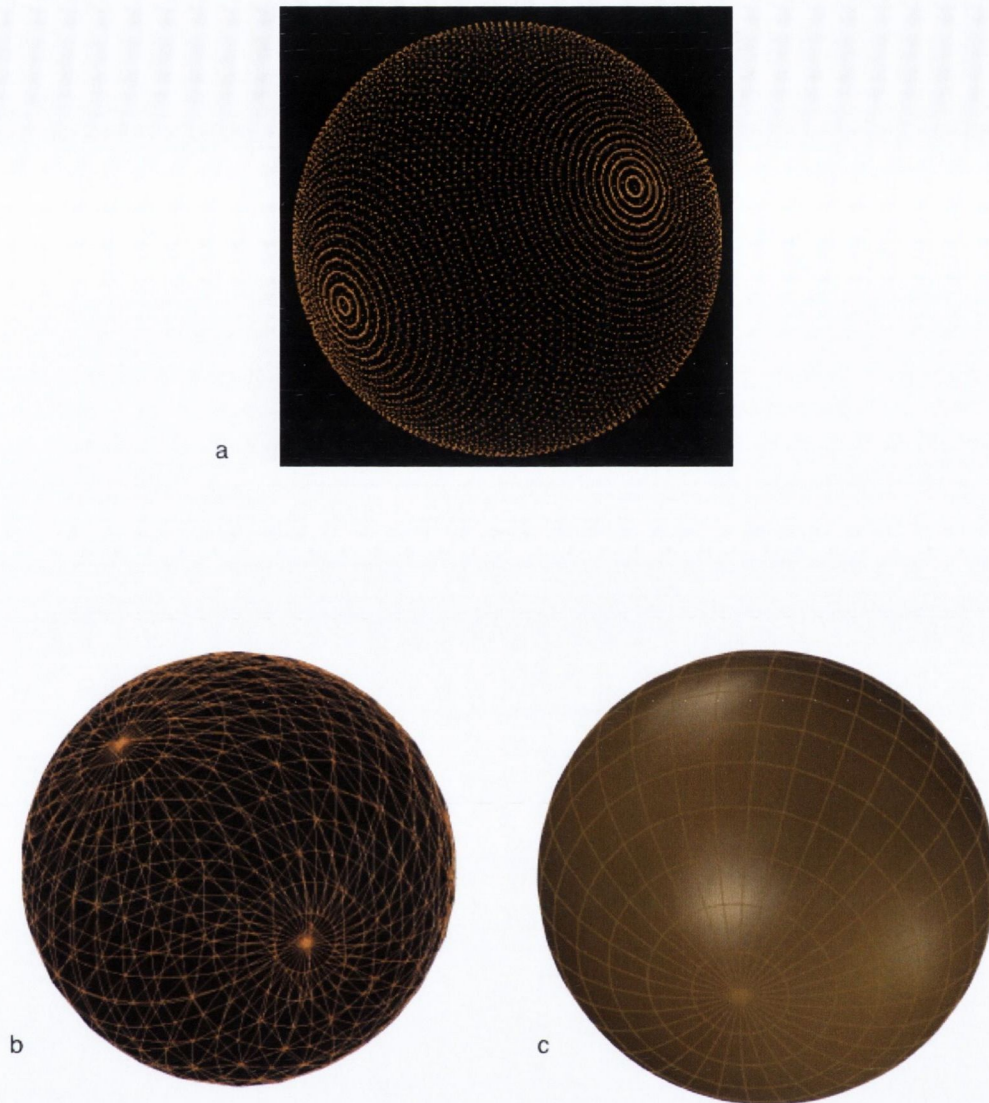


Figure 4.10 – A sphere represented by a point cloud (a), a polygon model (b) and a NURBS model (c).

As a point cloud only describes single points, it is difficult to see where the surface of an object is. A different method of describing an object is a polygon model.

This takes points on the surface of an object and connects them using simple polygons. This method's advantage is that it is not complicated to manipulate simple shapes, such as squares and triangles, in order to create a more complex three-dimensional object.⁶¹ As with the point cloud, greater detail (resolution) can be added

by increasing the number of polygons that describe a shape. This makes polygon models resolution dependant. An example of a polygon model format is the stereolithography (STL) file. This uses multiple triangles to form a polygon model of a shape (Figure 4.11).⁶²



Figure 4.11 - An STL model of a sphere

An alternative method to using polygons to create a surface is to use curved surfaces (Fig 4.10,c). A curved surface commonly used in computer modelling is the non-uniform rational B spline (NURBS).⁶¹ This is a surface that is defined mathematically by a number of control points, rather than the corners of a polygon.⁶³ The control points have a position and direction. They form a grid stretching across the surface and determine its curvature. NURBS models allow a surface to be created that is continuously curved when viewed at any resolution. These surfaces create complex organic and continuously curved shapes, using only a small number of

points.⁶³ By changing the position and direction of the control points, the shape of the surface can easily be modified.

Both the polygon and NURBS models define a surface in three dimensions. If this surface has a hole anywhere in it, or its edges do not meet, it is called an “open surface”. If it has no holes and no edges that do not meet another surface, it is called a “closed surface”. Open surfaces may be all that is required for some applications, such as in computer animation.⁶¹ However, for FEA, the model that is created needs to be defined as a solid structure. In order to do this, the surface must be closed. The computer software can then “understand” that the inside of the closed surface is solid. If the surface is open, there is no way to know where the inside starts and the outside ends.

Each computer software package has its own proprietary file format, which it uses internally to display and manipulate an object digitally. When objects need to be used in different software packages, they must be converted into a standard format, that can be understood by both pieces of software.⁶¹

4.2.4 Application to implant dentistry

FEA has provided a method for evaluating stress distribution throughout implants and their surrounding structures.¹² As it is a non-invasive tool, different implant geometries and positions can be modelled without the use of animal or human test subjects. This can then inform implant design as well as surgical and restorative techniques. As FEA is an approximation of a real system, its results must be taken in the context of the experimental method being used. Ultimately, these will either be supported or rejected by *in-vivo* research and clinical practice.

Geng *et al* in 2001 describe four different assumptions that are generally made in FEA studies relating to implant dentistry.¹² These are:

- a. the geometry of the model,
- b. the bone-implant interface,
- c. the boundary conditions and
- d. the material properties used.

Different model geometries have been used to represent the tissues that support dental implants. Some authors have used simplistic box or cylindrical shapes to represent the mandible.⁶⁴ While this is clearly an oversimplification, it may be sufficient, when stresses are not distributed over large distances in the bone, or when the area of interest is in the restorative components of the prosthesis. The development of digital radiographic techniques such as CT, cone beam CT, MRI and PET have allowed accurate computerised models of an individual patient's anatomy to be created.⁶⁵ In order to use these models for FEA, they must be carefully reformatted to yield anatomically accurate model geometries.

In FEA studies, it is assumed that the bone and the implant are perfectly interfaced.^{6, 28, 64} This means that the implant is fully in contact with the bone over the entire surface area that they meet, and that forces and displacements are the same in the two structures at this interface. In practice, this is not the case. Histological analysis of the bone implant interface have shown different proportions of bony contact with different implant surfaces.⁶⁶ Some FEA software can allow for an imperfect bone to implant interface, which may more closely mimic the clinical reality.¹² The percentage of bone to implant contact varies greatly in animal studies from 5% to 90%, depending on the surface characteristics of the implants and quality of the bone.⁶⁶

Boundary conditions need to be applied to an FEA model in order to generate force-displacement results. This is usually accomplished by fixing or restraining a number of surfaces of the model.¹² Without doing this, when a force is applied to an implant the entire model would move, rather than the implant being slightly displaced within the model. Some authors have incorporated the action of muscles into FEA models in an attempt to improve the model's accuracy.⁶ While this might more truthfully mimic the forces being applied to the structures supporting the implants, it could confuse the results. If the forces being applied by the muscles of mastication are large and are in close proximity to the implants being studied, it may be difficult to differentiate between the effects of occlusal (displacing) forces on the implant and the muscle's physiological effects on the bone. This is particularly important for zygomatic implants, if modelling the masseter muscle, as its origin lies close to the point of insertion of the implant.

The material properties used in FEA, when modelling craniofacial structures, have varied between studies.¹² Studies have investigated the material properties of human skulls.⁶⁷ These have shown that the bones often have different properties depending on how they are loaded. How the skull is modelled as part of the FEA is important and is discussed in the next section in detail.

4.2.5 Material Properties

Understanding the material properties of the substances, being tested using FEA, is required to formulate the stress/strain relationships for each element. Young's modulus of elasticity and Poisson's ratio are needed to calculate the distribution of forces, within an isotropic linearly elastic solid (Figures 4.12 and 4.13).¹² The yield

stress is valuable, if the forces being applied are likely to fracture the material being studied.

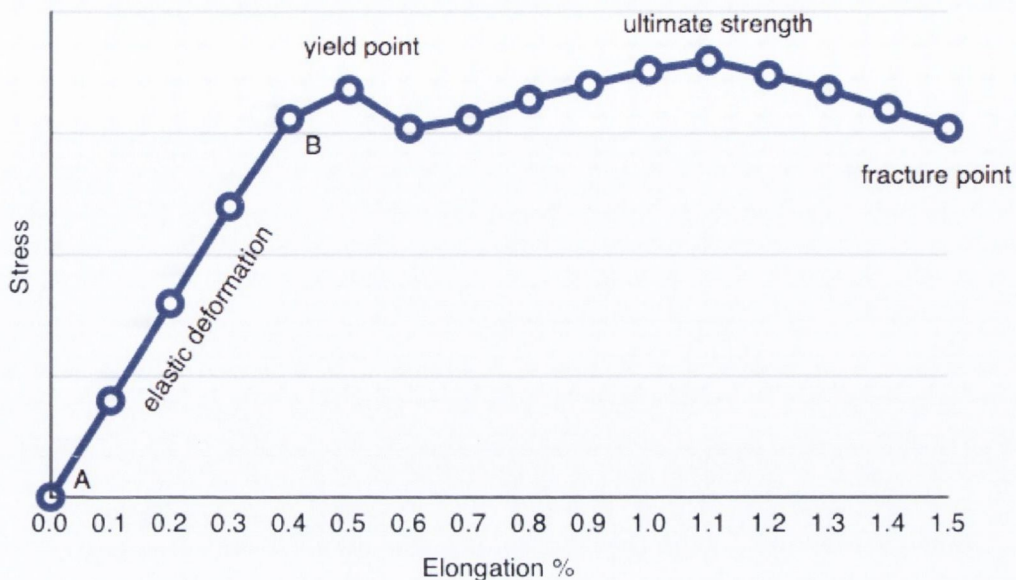


Figure 4.12 - A stress - strain relationship. Young's Modulus (modulus of elasticity) is calculated by measuring the slope of the graph from A to B above (i.e. during elastic deformation). As the material is stretched beyond point B the material reaches its yield point, when it starts to deform plastically. The stress continues to increase as the material is deformed to the material's ultimate strength, after which the stress reduces until the material fractures.

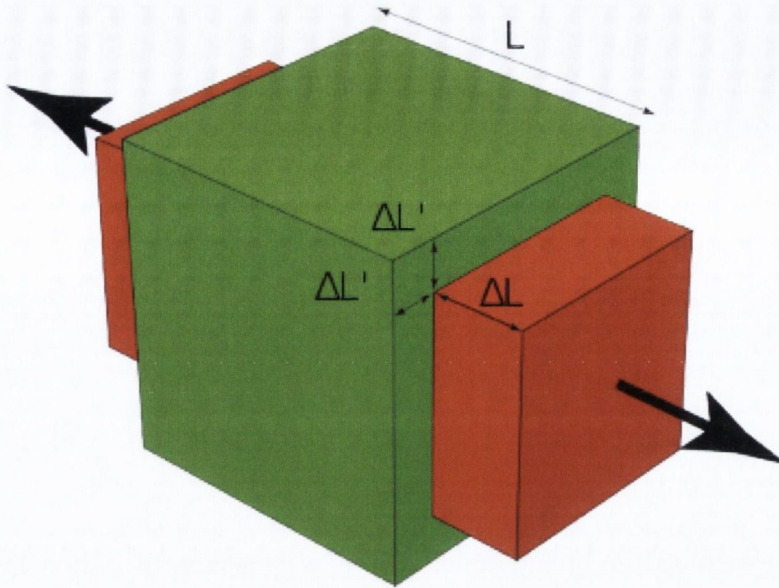


Figure 4.13 - Poisson's ratio is the ratio, when a body is stretched, of its contraction perpendicular to the direction of stretch in relation to its extension along the direction of stretch.

Outside of biological systems, material properties are often precisely known, having been studied by repeated measurements. For example, if a bridge is to be made of many steel beams, the material properties of steel are known and should be the same from one piece of steel to the next. These materials are also generally isotropic, meaning that they deform in the same way regardless of which direction the force is applied.

While this is true of a titanium implant, the same cannot be said for bone. Bone is a complex living tissue, formed from soft cancellous bone and harder cortical bone.²⁰ The bones of the skull have different properties at different sites.⁶⁸ Their properties also change depending on which direction forces are applied to them, making them anisotropic.⁶⁷ The bones may change over time due to growth, osteoporosis, remodelling and functional loading.⁶⁹ This creates a theoretical problem in using FEA in a biological system. FEA works well where materials are generally assumed to be homogenous and uniformly elastic.

Within implant dentistry, most FEA studies have assumed that the bone supporting the implant has a uniform amount of cortical bone and cancellous bone, which are also assumed to be homogenous¹² Values for cortical and cancellous bone have been estimated in animal and human studies. Mostly, data from the limbs have been used, showing an almost tenfold difference in the modulus of elasticity of the two bone types.⁷⁰

A small number of studies have evaluated the material properties of the facial bones in humans.⁶⁷⁻⁶⁹ In 2003, Peterson and Dechow investigated the material properties of the cortical bone of the cranial vault and zygomatic bone.⁶⁷ They passed ultrasonic waves through bone samples at various angulations. By measuring the changes in waveform, they were able to estimate the elastic properties of the bone. They found significant differences between the properties of different bones, in different sites within the same bone and in different directions within each sample. They found that muscle-bearing sites had different properties to sites that did not have muscle attachments.

Peterson *et al* in 2006 investigated the material properties of the maxilla.⁶⁹ They used the same ultrasonic pulse technique as was employed in the 2003 study.⁶⁷ This study used dentate maxillae and measured the material properties of the cortical bone. No measurements were made of the cancellous bone, a curious omission as the maxilla is a membranous bone and is predominantly formed from cancellous bone. Their results showed a wider variation in material properties from site to site within the maxilla when compared to results from the mandible. There was a wide variation in the axis of maximum stiffness for each sample, supporting other evidence, that facial and cranial bones are not isotropic.^{67, 69}

In 2009, Seong *et al* investigated the elastic modulus, mass density and surface hardness of the maxilla and mandible.⁶⁸ Unlike the mandible, the maxilla is a membranous bone. As a result, its cortical plates are thin giving the bone mainly cancellous rather than cortical behaviour. The study used a microindentation technique in contrast to the ultrasonic technique employed by Peterson's group.⁶⁷ Using this method, the elastic properties and mass densities for various sites in the mandible and maxilla were calculated. It was noted that the values recorded, using this technique, are generally higher than those found using other techniques. Unlike the ultrasonic method, they were not able to calculate the changes in material properties when forces are applied in different directions through the sample. This study investigated cortical and cancellous bone, yielding more useful results for the primarily cancellous maxilla. Interestingly, there was very little difference in the elastic modulus of cortical and cancellous bone in the maxilla. This finding is in contrast to the large differences that are often seen in FEA studies in implant dentistry.¹² Their study supports the variability of the material properties in the maxilla and mandible.⁶⁸ Generally higher values were found for the elastic properties of the mandible than the maxilla.⁶⁸

Strait *et al* in 2005 investigated the detail required to accurately model a skull using FEA.⁷¹ They created an FEA model of a monkey (*Macaca fascicularis*) skull, derived from a CT scan. They then created four separate models. The first assumed the skull to be made of an homogenous material and was based on the material properties of the human tibia. The second model assumed that the skull was homogenous, but was based on average values for the *M. fascicularis* skull. The third model divided the skull into individual isotropic regions, each with its own set of material properties. The fourth model was the same as the third but was orthotropic,

assigning different material properties to the bone depending on the direction that the force was applied. Interestingly, while there were differences between model one (based on human tibia data) and the other models, there was little difference between the second third and fourth models.⁷¹ The authors note that the detail required, when choosing which properties to use in an FEA model, will depend on the research question being asked. For example, if the precise amount of force that can safely be applied to an implant, prior to implant fracture, is being studied, detailed material properties would be required to get accurate results. If however one implant position is being compared to another to evaluate which is most favourable, less detailed information is required.

The mean values of the material properties found in the human maxilla and zygomatic bones are shown in Table 4.3.

Bone	Elastic Modulus (GPa)	Poisson's Ratio	Mass Density (g/cm³)	Shear Modulus (GPa)	Author
Zygomatic Bone (Cortical)	13.88	0.34	1.68	4.53	Peterson & Dechow (2003)
Maxilla (Cortical)	12.13	0.36	1.75	4.36	Peterson <i>et al</i> (2006)
Maxilla	14.9	Not studied	0.67	Not studied	Seong <i>et al</i> (2009)
Maxilla (Cortical)	17.7	Not studied	Not studied	Not studied	Seong <i>et al</i> (2009)
Maxilla (Cancellous)	15.4	Not studied	Not studied	Not studied	Seong <i>et al</i> (2009)

Table 4.3 – Material properties of the maxilla and zygomatic bone.

4.3 Support of zygomatic implants

Evidence for estimating where the support for zygomatic implants comes from is derived from two sources.

The first is anatomical data and CT scans of placed zygomatic implants. The anatomical studies described in section 4.1.2 by Nkenke *et al* in 2003 and Rossi *et al* in 2008 show that the zygomatic bone provides a larger length and surface area of bone to support a zygomatic implant, more so than the maxilla.^{22, 25} This concept is supported by post-operative CT scans in clinical case series.^{1, 19} However, the support provided by the zygomatic bone is at the apical end of the implant, furthest away from the location to which the force is being applied. The small area of bony support, supplied by the maxilla, is closer to the applied force, raising the possibility that it might have a significant role in supporting the implants.

The second source of information are the previously published FEA studies investigating zygomatic implants. Tie *et al* in 2005 and Miyamoto *et al* in 2010 studied the stress distribution when zygomatic implants were placed in models with large maxillary defects.^{28, 65} The defect was virtually repaired using a simulated fibula free flap in the 2005 study. Three conventional and one zygomatic implant were then virtually placed. A larger stress was shown in the zygomatic bone than in the fibula free flap.⁶⁵ Miyamoto *et al* in 2010 simulated one or two zygomatic implants in an unrepaired defect.²⁸ They showed that lower stresses were observed in the zygomatic bone when two implants were used.²⁸

Ujigawa *et al* in 2007 created an FEA study based on a CT model for half of an edentulous skull with normal anatomy.⁶ They used one zygomatic implant and two conventional implants to support a fixed bridge suprastructure. They modelled a single zygomatic implant, not connected to other implants. Their models incorporated

an occlusal force of 150N (Newton) and a lateral force of 50N on the bridge or implant. A 300N force was also applied to the zygomatic arch to simulate the muscular action of the masseter. The results of this study show different force distributions in the zygomatic and maxillary bone, depending on the direction of the force and on whether the bridge model with zygomatic and conventional implants or the single zygomatic implant model was used. When a 150N occlusal force was applied, higher stresses were noted in the maxillary bone than in the zygomatic bone for both the bridge model and the single implant model. When a 50N lateral load was applied to the bridge model, higher “von Mises” stresses were found in the zygomatic bone than in the maxillary bone. The opposite was found when the same lateral load was applied to the single implant model. This study suggests that in some cases the maxillary bone may carry a greater load from the implant than the zygomatic bone. However, as with other studies, a large force representing the masseter muscle was applied very close to the apex of the zygomatic implant. This makes it difficult to determine how much of the observed forces in the zygomatic bone are as a result of the implant, and how much are as a result of the masseter muscle.

The true relative contribution of the zygomatic and maxillary bones in supporting zygomatic implants is difficult to ascertain based on previously published literature. Brånemark in 2004 suggested the importance of maintaining bony support in the maxilla (at the cervical area of zygomatic implants).¹ However, as zygomatic implants have been described successfully in short-term studies without any maxillary support, the value of the maxillary bone in supporting zygomatic implants has been called into question.

5. Materials and Methods

5.1 Component creation

Computer modelling software was used to simulate the clinical situation of the placement of two zygomatic implants per side, which supported a fixed bridge. The components created were the skull, the zygomatic implants and the bridge. In order to reduce the complexity of the model, one half of the skull with two zygomatic implants and one half of the full arch bridge, were created. This approach reduced the model's complexity and the computational resources needed to analyse the model. A number of software packages were required in order to create and analyse the components (Table 5.1).

Software	Function
Mimics ⁷²	Reads CT scans and other image data, allows selection of regions of the images and creates a polygon surface model based on the scan data.
Netfabb ⁷³	Edits and repairs polygon surface models.
Rhinoceros ⁷⁴	Creates and manipulates NURBS surfaces.
SolidWorks ⁷⁵	Creates and manipulates three-dimensional solid models.
Simulation ⁷⁶	A component of "SolidWorks" that performs FEA.

Table 5.1 – Software used to create and analyse the FEA models.

5.1.1 Skull

The model of the skull used was constructed from the CT scan of a consenting edentulous adult female. This was formatted using the Digital Imaging and Communications in Medicine (DICOM) standard. In order to create the model, the

data from the CT scan was converted from the DICOM format via a number of software packages into a NURBS closed surface model, as detailed below. Once the closed surface model was created, it was interpreted as a solid model, representing the skull.

5.1.1.1 CT scan

The pre-operative CT scan of a consenting sixty-one year old edentulous female, who had previously undergone zygomatic implant placement, was used as the basis for the model for the skull. The scan was exposed using a Lightspeed VCT Scanner (GE Medical Systems). The scan extended from the maxilla inferiorly to mid-way up the orbits superiorly and included the zygomatic bones. The condyles and coronoid processes of the mandible were included. The scan was formatted as a series of DICOM images, with a slice thickness of 0.625mm.

5.1.1.2 STL file creation (Mimics)

The DICOM images were manually imported into the Mimics software package (version 10.01). The slice thickness was maintained at 0.625. Manual import settings were used with pixel properties set as signed short pixels, with low bite first bite swapping. These settings were chosen to match the format of the CT data. A threshold command was used to select only those voxels of the CT scan that corresponded to Hounsfield Values representing bone. These voxels were coloured and displayed as an overlay on the CT scan slices in Mimics. The components of the mandible that had been selected were removed. Some areas of bone, such as the lateral walls of the sinus and floors of the orbits were too thin to be selected by the threshold command. In

these cases, gaps were noted in the coloured overlay and were manually drawn in slice by slice.

A polygon model of the bony skull was made in Mimics using the selected voxels. This was exported as an STL file at low quality, which yielded a model of 149,304 triangles, sufficiently detailed to be anatomically accurate (Figure 5.1).



Figure 5.1 Initial polygon model constructed from CT scan.

5.1.1.3 STL model editing (NetFabb)

The STL model was opened using NetFabb for inspection and editing. At this point, the model was split down the midline, and the right side was discarded (Figure 5.2). Defects in the remaining model were noted including holes and overlapping polygon surfaces. Overlapping polygons were removed and replaced with continuous surfaces.

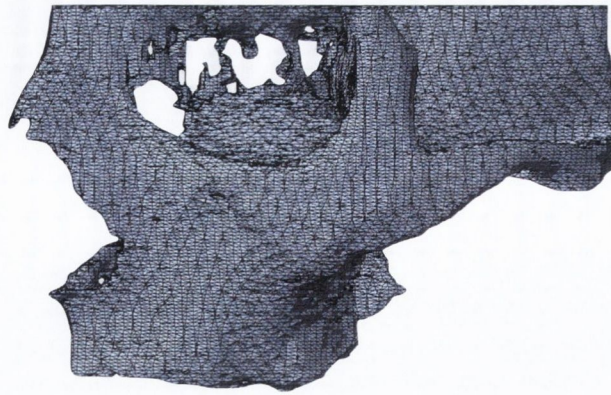


Figure 5.2 – Unrepaired STL model after removing the right side.

Two kinds of holes were present in the model (Figure 5.3). The first were gaps in the surface of the model. These needed to be repaired in order to treat the model as a solid. They were patched by adding additional polygons to produce a closed surface. The second kind of hole was not a defect in the surface of the model, but a hole in the model itself that was not anatomical. An example of this was a defect in the lateral wall of the sinus that extended all the way through to the sinus. The repair of this defect is shown in figure 5.4. In order to repair these defects, the polygons that made up the hole were removed leaving an open surface internally and externally. Both surfaces were then repaired by separately adding new polygons internally and externally and recreating a closed surface.

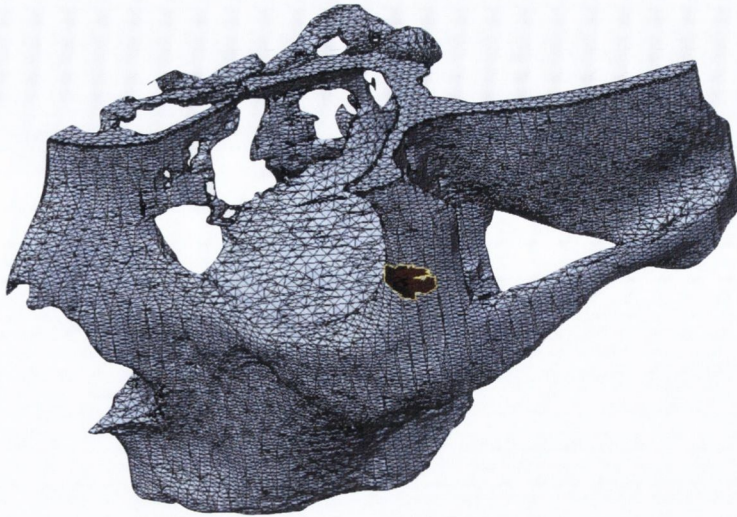


Figure 5.3 – Examples of defects present in the STL model. Non-anatomical holes in the medial wall of the orbit and a gap in the surface (yellow outline) on the lateral aspect of the frontal process of the zygomatic bone. Blue faces represent the external surface of the model, brown faces represent the internal surface of the model (only visible through gaps in the surface).

The repaired model was saved as a new STL file, made up of 72,818 triangles. While this was an anatomically accurate version of the left side of the CT scan, a polygon model is not compatible with the FEA software. It therefore was converted to a NURBS surface model.

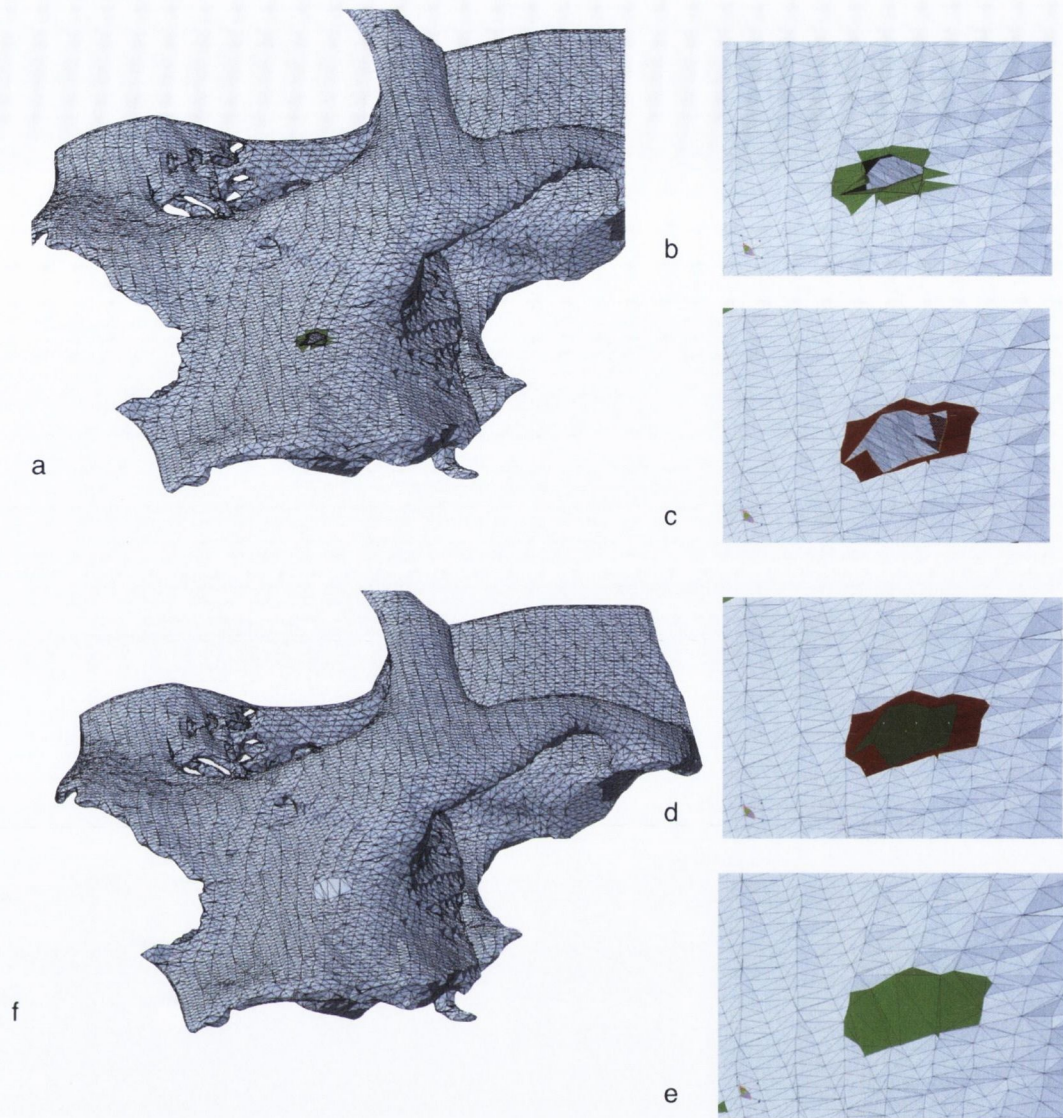


Figure 5.4 - Repair of a non-anatomical hole in the STL surface model – external faces of the polygons are blue, internal faces are brown.

(a) Hole in lateral wall of the sinus.

(b) Close up view of hole (green polygons) looking into the sinus.

(c) Faces forming hole removed, separating the inside and outside components of the wall of the lateral sinus.

(d) Inside wall patched with new (green) polygons.

(e) Outside wall patched with new (green) polygons, completing the repair.

(f) Wide view of the repaired hole.

5.1.1.4 Surface model (Rhinoceros)

The repaired polygon model was imported into the Rhinoceros software package. A series of NURBS surfaces were fitted onto the polygon surface using the T-Splines plug-in⁷⁷. This initially produced a NURBS model that was open (with gaps between some of the NURBS surfaces) rather than closed. The model was therefore carefully inspected and defects in the surface were noted. These defects took the form of gaps in the surface of the model. When a gap was found, it was manually repaired by adding a number of new NURBS surfaces that were continuous with the rest of the model. When this process was complete, a closed surface made up of 3,463 NURBS surfaces was formed, representing the left side of the skull. This was exported from Rhinoceros in the Initial Graphics Exchange Specification (IGES) file format for use as a solid model.

5.1.1.5 Solid model

The NURBS model was imported into the Solidworks software package. As it was a closed NURBS surface model, Solidworks was able to interpret it as a solid shape rather than a surface.

5.1.1.6 Scaling

As the model had been converted from the original DICOM CT data via a number of formats and software packages, the scale of the model was checked and adjusted at this stage. Measurements were made using fixed anatomical landmarks in all three planes on the original CT scan. These were compared to measurements made on the solid model in Solidworks and it was noted that the scale needed to be adjusted by a

factor of 0.5 in all dimensions. The model was then ready for assembly with the other components.

5.1.2. Zygomatic implants

Two virtual zygomatic implants were created in Solidworks. A circle of diameter 4.5mm was drawn and extruded to a length 13mm to form a cylinder. This represented the coronal portion of the implant. Another circle of diameter 4mm was created and extruded to form a second cylinder. This represented the apical portion of the implant. The two cylinders were connected together by lofting a surface of 2mm length between them. The length of the apical portion could be varied to fit the skull, corresponding to the different implant lengths available. A length of 35mm was chosen at the assembly stage, resulting in an implant length of 50mm.

To create the coronal end of the implant, which is angled, a curve was added to this portion of the cylinder. The angle of the curve could be varied in order to simulate angulated abutments, which facilitate the connection of the implants to the bridge. As the implant would be rigidly attached to the model of the skull during the FEA process, the threads were omitted to reduce the model's complexity and facilitate discretisation of the model (Figure 5.5).

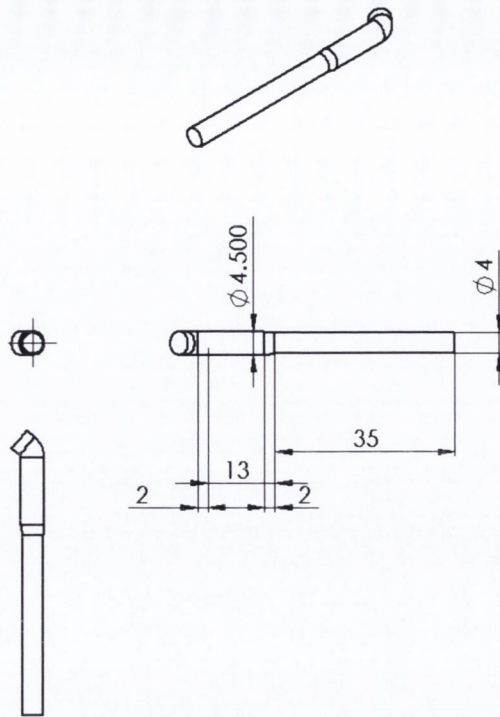


Figure 5.5. Implant schematic.

5.1.3. Bridge

A curved bar was made in Solidworks in order to mimic a rudimentary fixed bridge. The shape of this bar was based on a curve, drawn along the line of the residual alveolar ridge of the maxilla. This curve was expanded into a curved rectangle with a width of 6mm. The curved rectangle was extruded to a height of 10mm to form the bridge (Figure 5.6).

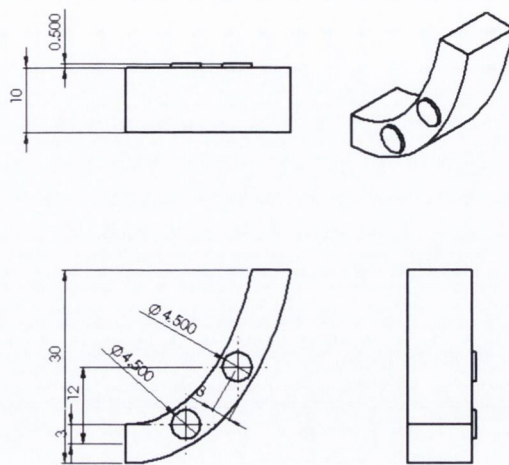


Figure 5.6 – Bridge schematic.

5.1.4 Grafts

Two bone graft models were required, one to cover the implants that would be placed inside the sinus, and the other to cover the implants that would be placed outside the sinus. Both grafts were constructed in Solidworks after the implants, bridge and skull were assembled and are described in this section.

For the implants in an intra-sinus position, a graft was created to cover the entire intra-sinus length of both zygomatic implants and was intended to simulate a sinus lift. To create this shape, a cylinder was created that surrounded both of the implants from their coronal to their apical end. This shape crossed the skull along the lateral sinus wall. A boolean command allows one shape to be cut away from another. This was used to remove the shape of the skull from the cylinder. The result was two

pieces of the cylinder, one that was inside the sinus, and the remaining part that was outside the skull. The internal part was retained and formed the intra-sinus graft, and the external part was discarded (Figure 5.7).

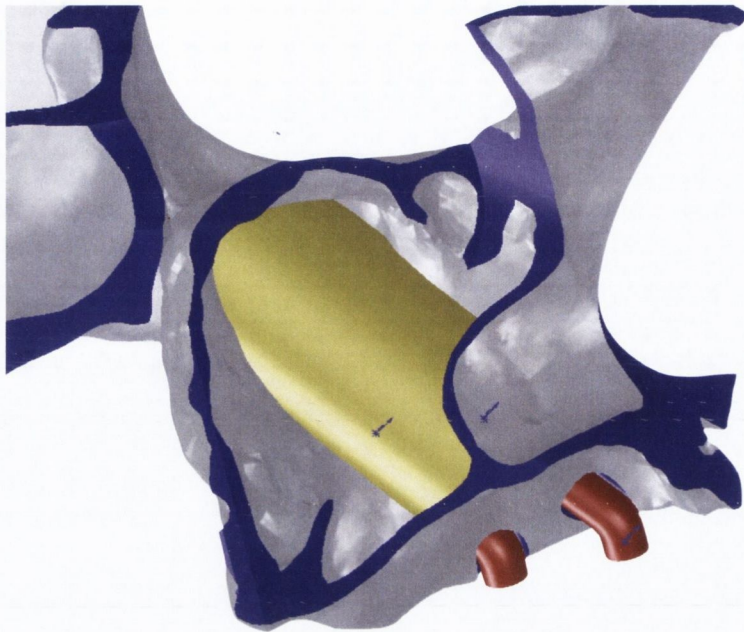


Figure 5.7 – graft for zygomatic implants with an intra-sinus position.

For the implants that were placed in an extra-sinus position, a graft was created to cover the implants outside the sinus from their emergence at the alveolar bone to their entry to the zygomatic bone. This was intended to mimic an onlay graft. As these implants all passed through the wall of the sinus at some point, an intra-sinus graft was also required for these implants (Figure 5.8). A cylinder was initially used as the basic shape to create the graft. While this approach would have been successful for the internal graft, it created too much graft on the external surface of the implants. As a result a different approach was taken. Three curves were drawn around the implants, one at the apical end, one midway along the length and one at the coronal end, all perpendicular to the long axis of the implants. A loft function was used to create a surface over these three curves, akin to a canvas covering the ribs of an

aeroplane wing. As with the intra-sinus graft, this shape crossed the lateral sinus wall. It was therefore removed from the skull using a boolean command, creating an internal graft covering the parts of the implant that were inside the sinus wall and an external graft covering the parts outside the sinus.

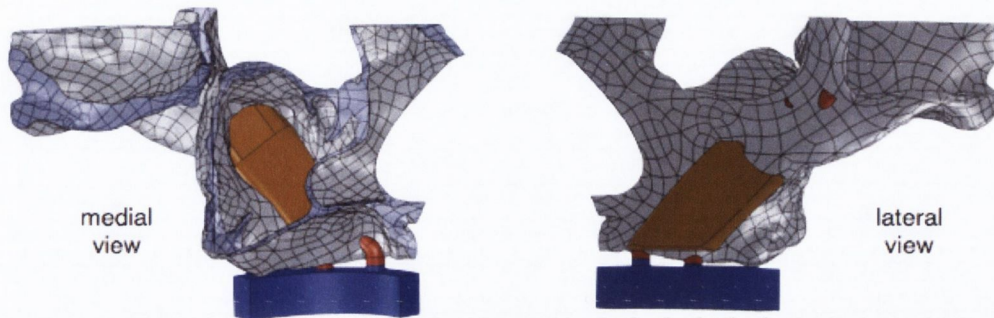


Figure 5.8 Graft for zygomatic implants in an extra-sinus position.

For both graft models described above, an intact sinus wall was necessary to divide the graft into internal and external components. Some of the models described below deliberately had defects in the sinus floor and wall to simulate a lack of alveolar support for the zygomatic implants. It was important for unbiased comparisons to be made, that the shape of the graft between similar models was the same. In the models with sinus defects, applying the technique described above would simply have filled the defects with the graft. To overcome this problem, the grafts that were constructed for the models without defects in the sinus floor or wall were exported as individual parts. These could then be incorporated into the models with defects, while maintaining the consistent graft shapes between different models.

5.2 Assembly of Models

The components created above were assembled to form a half skull with two zygomatic implants connected by a rigid bar. As three variables (implant position, presence of alveolar support and presence of graft) were being investigated, a model was created with each permutation of variables. This yielded eight models as shown in table 5.2 and are discussed in sections 5.2.1 to 5.2.8 below.

Model	Implant Position	Alveolar Support	Graft	Section
1	Inside Sinus	Yes	No	5.2.1
2	Inside Sinus	Yes	Yes	5.2.2
3	Inside Sinus	No	No	5.2.3
4	Inside Sinus	No	Yes	5.2.4
5	Outside Sinus	Yes	No	5.2.5
6	Outside Sinus	Yes	Yes	5.2.6
7	Outside Sinus	No	No	5.2.7
8	Outside Sinus	No	Yes	5.2.8

Table 5.2 – Models created for finite element analysis

5.2.1 Model 1 – with zygomatic implants inside sinus, with alveolar support, without graft

This model was intended to simulate the intra-sinus position of two zygomatic implants supporting a fixed bridge (Figure 5.9).

5.2.1.1 Implant assembly and position

The bridge and implants were assembled prior to their placement into the skull. The implants were connected to the bridge and were constrained by three variables in

order to allow their precise movement in all dimensions. The height of the implants off the bridge (simulated abutments), the position of the implants along the bridge and the angle that the implants made with the sagittal plane could be varied to achieve this.

Two circles were first drawn on the superior surface of the bridge and were extruded to form cylinders. These simulated the implant abutments. The height of these cylinders was the first variable described above. They were constrained so that their centre point was coincident with the midline of the curve of the bridge. Their position was also constrained relative to the anterior edge of the bridge's medial surface (at the midline of the skull). This distance made the second variable defining the implants' positions. The two implants were then added to the bridge. They were each constrained so that the midpoints of their coronal faces (the heads of the implants) were centred on one of the cylinders that had been created on the surface of the bridge. They were further constrained so that the angle made between the long axis of each implant and the sagittal plane could be defined. This angle was the final variable used to define the implant's position. This method allowed the position of the implant to be moved in a superior-inferior direction by changing the height of the abutment cylinders. It allowed them to be moved along the line of the arch by changing the distance of the cylinders to the anterior edge of the bridge, and it allowed the implants to be rotated about their heads by changing the angle that their long axes made with the sagittal plane.

5.2.1.2 Implant placement in skull

The implant-bridge assembly was positioned relative to the skull. The medial face of the bridge (at the midline) was constrained so that it was in line with the

midline of the skull. It was then moved so that the line of the bridge matched the line of the residual alveolar ridge antero-posteriorly. It was placed close to the surface of the skull in a vertical position to mimic the position of the dentition.

The three variables defining the positions of each implant relative to the bridge were adjusted to place the implants entirely within the sinus and maximising the amount of the implant that was in zygomatic bone. The apices of the implants were placed as close to the external surface of the zygomatic bone as possible, or just extruding through the surface. The coronal ends of the implants were placed as close as possible to the maxillary alveolar ridges, but were on the palatal side of the ridge.

A cavity command was applied to the skull so that, where the implants and skull intersected, a hole was created in the skull. This resulted in a model of half of the skull with two zygomatic implants placed in an intra-sinus position and connected by half of a fixed full arch bridge.

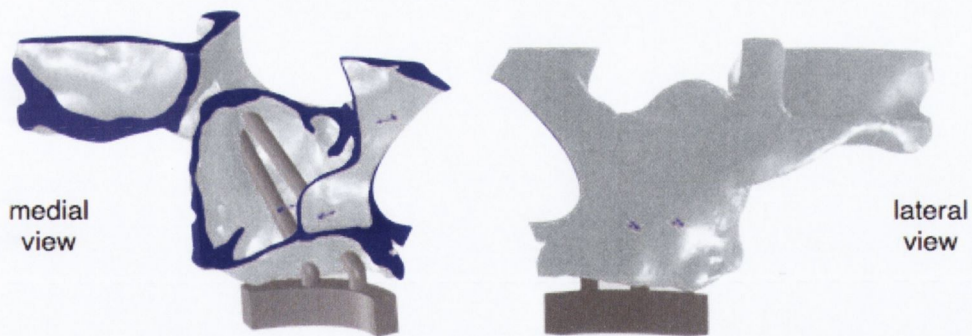


Figure 5.9 – Model 1 lateral and medial views.

5.2.2 Model 2 – with zygomatic implants inside sinus, with alveolar support, with graft

This model was intended to simulate the effect of a sinus lift, or new bone formation inside the sinus when zygomatic implants are placed in an intra-sinus position (Figure 5.10).

5.2.2.1 Implant, bridge and skull assembly

Model 1 was duplicated so that the positions of the bridge, implants and skull were identical in this model.

5.2.2.2 Graft positioning

The bone graft was constructed as described in section 5.1.4 and was positioned so that all of the surfaces of both implants that were inside the sinus were fully covered by the bone graft. A cavity command was applied to the bone graft so that where the bone graft and implants intersected, a hole was created in the bone graft.

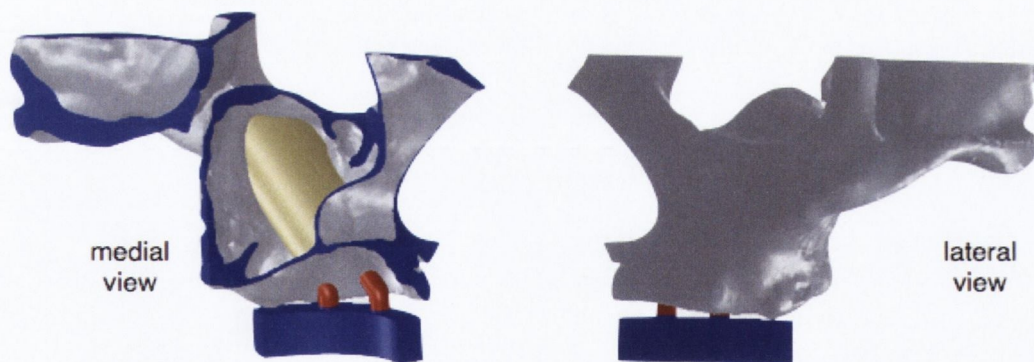


Figure 5.10 – Model 2 medial and lateral views.

5.2.3 Model 3 - with zygomatic implants inside sinus, without alveolar support, without graft

This model was intended to simulate the situation where zygomatic implants are placed in an intra-sinus position, but do not benefit from support from the maxillary alveolar bone (Figure 5.11)

5.2.3.1 Implant, bridge and skull assembly

Model 1 was duplicated so that the positions of the bridge, implants and skull were identical in this model. A modification to the skull was required in order to create holes in the alveolar bone surrounding the implants. For each implant, a circle with a diameter of 5.5mm was drawn, centred on the head of the implant. This was extruded along the line of the implant to create a cylinder of length 6mm. Using a boolean command, the cylinder was cut from the skull and then removed from the model. This created a uniform gap of 0.5mm in the maxillary bone around the implant (Figure 5.12). This process produced a model that was the same as model 1, except that the implant did not gain any support from the alveolar bone.



Figure 5.11 – Model 3 medial and lateral views.



Figure 5.12 – Model 3 from inferior view, showing the holes preventing the alveolar bone from supporting the implants.

5.2.4 Model 4 - with zygomatic implants inside sinus, without alveolar support, with graft

This model was intended to simulate the situation where zygomatic implants were placed in an intra-sinus position, where no support was available from the alveolar bone and where a sinus lift had been carried out (Figure 5.13).

5.2.4.1 Implant, bridge and skull assembly

Model 3 was duplicated so that the positions of the bridge, implant and skull were the same in this model. The holes created around the implants in the alveolar bone were also preserved by duplicating model 3.

5.2.4.2 Graft positioning

The bone graft was constructed as described in section 5.1.4 by exporting the graft used in model 2 and importing it into this model. The graft was placed inside the sinus

in the same position as in model 2. This was achieved making the surfaces of the implants coincident with the grooves in the graft cut that had been made by the implants in model 2. The holes created in the alveolar bone were preserved, and were not filled by the graft.

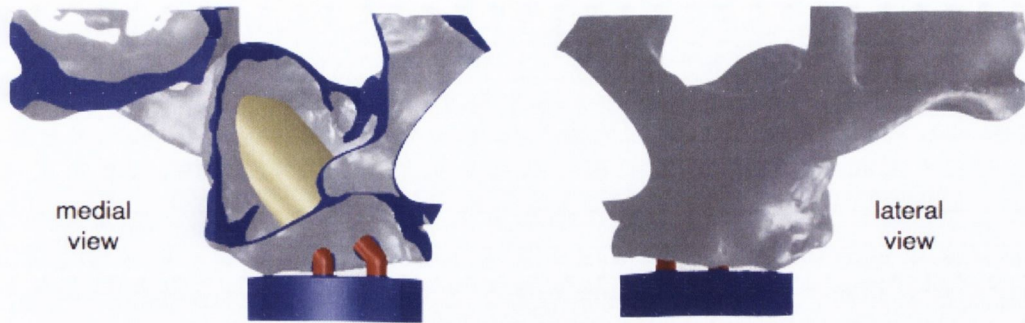


Figure 5.13 – Model 4 – medial and lateral view

5.2.5 Model 5 – with zygomatic implants outside of the sinus, with alveolar support, without graft

This model was intended to simulate an extra-sinus (sinus slot) approach to place zygomatic implants (Figure 5.14).⁸

5.2.5.1 Bridge, implant and positioning

The bridge and implants were assembled in the same way as described for model 1. The implants were altered in this model to place them in extra-sinus positions. The heads of the implants were placed more laterally than in models 1 to 4, to allow them to emerge in line with the alveolar crest. This was accomplished by moving the bridge-implant assembly laterally. The height of the implants above the bridge, their positions along the line of the bridge, and the angles that they made with the saggital plane were altered to place the apical ends of the implants in the zygomatic bone, while maintaining an extra sinus position. This placed the heads of the implants

further anteriorly along the line of the bridge than the implants in an intra-sinus position (models 1 to 4). As in the sinus slot technique, the implants grooved the sinus wall, leaving some of the implant surface just inside the sinus, and some outside.⁸ As in previous models, a cavity command was applied to create holes in the skull where the implants and skull intersected.

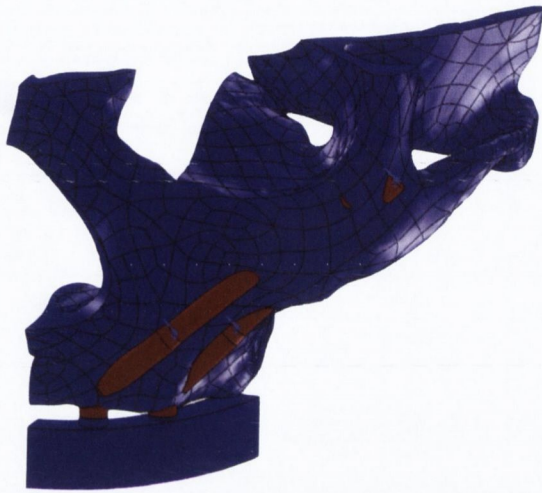


Figure 5.14 - Model 5 showing implants in an extra-sinus position.

5.2.6 Model 6 – with zygomatic implants outside of the sinus, with alveolar support, with graft

This model was intended to simulate the situation where an onlay graft was applied over zygomatic implants in an extra-sinus position. As the implants grooved the sinus wall, the graft was also placed to cover this internal surface of the implants (Figure 5.15).

5.2.6.1 Implant, bridge and skull assembly

Model 5 was duplicated in order to preserve the positions of the implants, bridge and skull in this model.

5.2.6.2 Graft positioning

The bone graft was created as described in section 5.1.4. It was placed in this model, so that all of the exposed internal and external surfaces of the implant were fully covered by the graft. A cavity command was applied, so that where the implants and bone graft intersected, a hole was made in the bone graft.

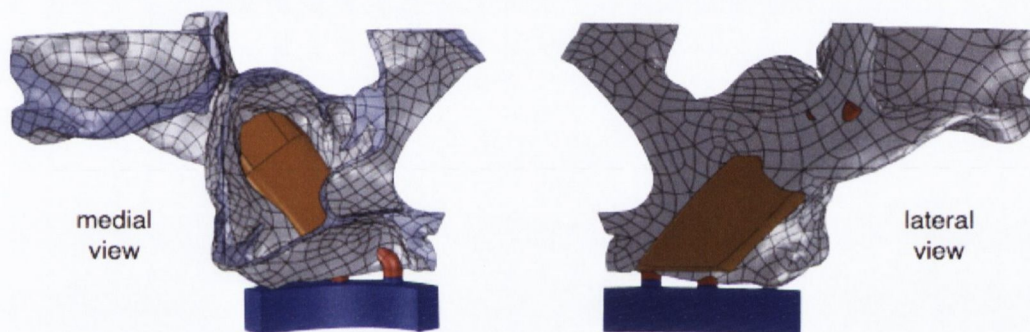


Figure 5.15 – Model 6 showing external graft to cover the surface of the implants.

5.2.7 Model 7 – with zygomatic implants outside of the sinus, without alveolar support, without graft

This model was intended to simulate the situation where a zygomatic implant was placed in an extra-sinus position without any support from the maxillary alveolar bone (Figure 5.16).

5.2.7.1 Bridge, implant and skull assembly

Model 5 was duplicated to create a model with identical positions of the bridge, implants and skull. As described for model 3, holes were made in the alveolar bone,

creating a uniform space of 0.5mm around the implants as they passed through the alveolar bone. This produced a model without alveolar support with the implants in an extra-sinus position.

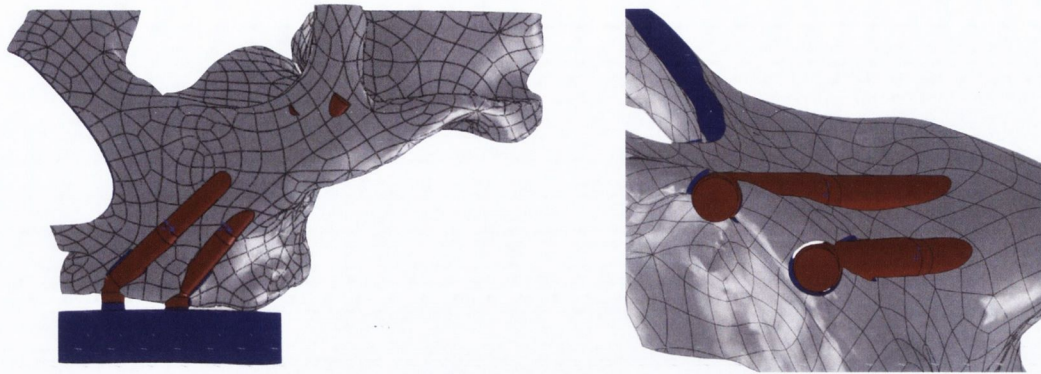


Figure 5.16 – Model 7.

5.2.8 Model 8 – with zygomatic implants outside of the sinus, without alveolar support, with graft

This model was intended to simulate the situation where zygomatic implants were placed in an extra-sinus position, where alveolar bone was not available for support and when an onlay graft was placed over the implants (Figure 5.17).

5.2.8.1 Bridge, implant and skull position

Model 7 was duplicated to create this model. This preserved the position of the implants as well as the holes in the alveolar bone between the two models.

5.2.8.2 Graft positioning

As for models 2 and 4, the bone graft for this model was exported from model 6. It was placed into this model so that the grooves made by the implants in the graft were

coincident with the implants in this model. The internal and external graft were added in this way in order to preserve the holes in the alveolar bone. A cavity command was not needed for this graft as the holes required to prevent the overlap of the implants and the graft had already been created in model 6. Similarly to the other models with grafts, the graft did not fill the holes that had previously been created in the alveolar bone.



Figure 5.17 – Model 8

5.3 Finite element analysis

For each of the eight models, a finite element analysis was run using “Simulation” for “SolidWorks”.

5.3.1 Material properties

The material properties used are shown in table 5.3 below. All materials were assumed to be homogenous and linearly elastic. The values used for the bridge and zygomatic implants were based on standard values for commercially pure titanium. The values used for the skull and bone grafts were average values derived from human cadaver studies investigating the cranial bones.⁶⁷⁻⁶⁹ The same values were used for the skull and the bone graft as it has been demonstrated that autogenous bone can develop around zygomatic implants when the sinus membrane is maintained.¹¹

Property	Bridge & zygomatic implant	Skull and bone graft
Elastic modulus	$1.05 \times 10^{11} \text{ Nm}^{-2}$	$1.5 \times 10^{10} \text{ Nm}^{-2}$
Poisson's ratio	0.37	0.34
Mass density	4510 kgm^{-3}	1678 kgm^{-3}

Table 5.3 – Material properties used for the components of the FEA

5.3.2 Discretisation (mesh creation)

For each of the eight models, a finite element mesh was created using Simulation for SolidWorks. Some models initially did not mesh using the default settings. In these cases, refinements to the mesh were added to reduce the element sizes for specific regions. The number of elements, nodes and refinements used for each model are shown in table 5.4 below.

Model	Elements	Nodes	Refinements
1	133179	27455	Implant element size set to 0.5mm
2	44275	10335	Element size for faces that failed to mesh set to 1mm
3	124256	26049	Implant element size set to 0.5mm
4	37703	9167	None
5	33151	8541	None
6	381016	83762	Element size for model set to 1.45mm
7	32631	8531	None
8	27239	7991	Implants and external graft element sizes set to 1.45mm

Table 5.4 - Elements, nodes and refinements used for each model

5.3.3 External forces

Forces were applied to the inferior surface of the bridge for each of the eight models. A circle of diameter 7mm was created and was placed over the inferior surface of the bridge in the molar region. The forces were spread over the area where the circle and the surface of the bridge intersected.

The angle that the forces made with the occlusal surface of the bridge could be varied. This allowed forces to be applied that simulated occlusal biting forces and lateral biting forces.

Forces of different magnitudes were applied varying from 50N to 600N in order to investigate the effect of different biting strengths at angles of 90° (occlusal) and 30° to the horizontal plane. A force of 150N was applied to each model at angles to the horizontal plane of 0° buccally, 30° buccally, 60° buccally, 90° (occlusally), 60° palatally, 30° palatally and 0° palatally. This allowed the effect of force direction to be investigated.

5.3.4 Boundary conditions

The model was fully restrained at the superior faces of the skull. The medial faces of the skull and bridge (at the midline) were restrained using a roller/slider restraint. This allowed no movement in the medio-lateral direction, but allowed movement in the supero-inferior direction and antero-posterior direction. This method was used to simulate the presence of a mirrored right side of the skull.

5.4 Analysis

The finite element analysis was run for all of the forces and models. The von Mises stresses were plotted on the model using a coloured scale. The maximum overall

stress for each model was recorded for each magnitude and direction of force. These were then compared between models.

6. Results

6.1 Distribution of stresses within models

The distribution of stresses within each model are shown in figures 6.1 to 6.24, and reproduced in larger size in Appendix III. Maximum stresses are represented in red, while minimum stresses are represented in blue. As these values vary between models, the scales used to assign colours are also different between models.

Stresses were concentrated in the bridge and coronal ends of the implants. Low stresses were noted consistently in the zygomatic bone. Where stresses were transferred to the skull, they could be seen in the maxilla around the implants, in the lateral wall of the sinus and lateral to the nose. This pattern of stress distribution is similar to that seen in the dentate maxilla.⁷⁸



Figure 6.1 – Model 1 under occlusal loading: (a) anterior, (b) lateral and (c) medial views.



Figure 6.2 – Model 1 under 30° buccal loading: (a) anterior, (b) lateral and (c) medial views.

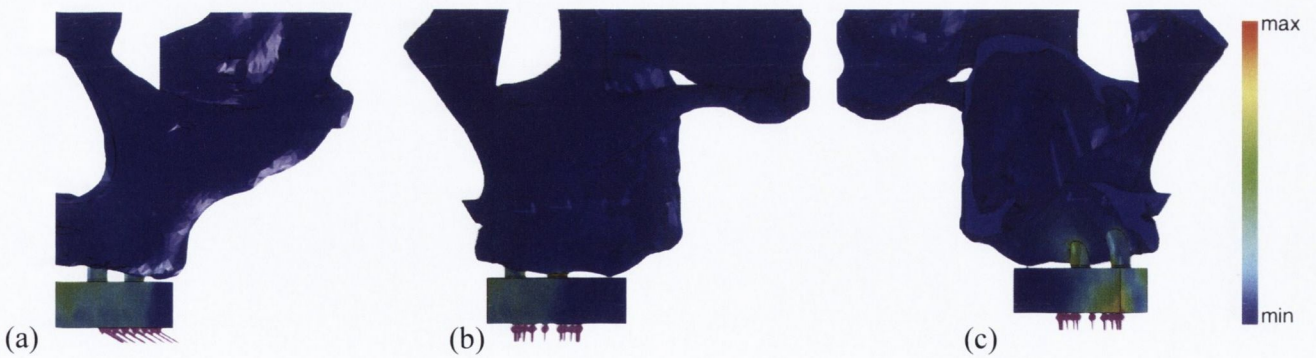


Figure 6.3 – Model 1 under 30° palatal loading: (a) anterior, (b) lateral and (c) medial views.

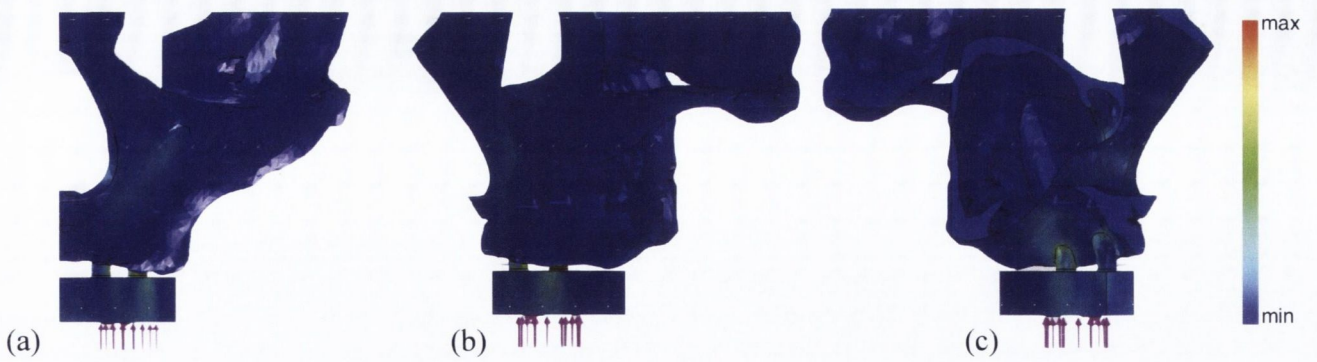


Figure 6.4 – Model 2 under occlusal loading: (a) anterior, (b) lateral and (c) medial views.

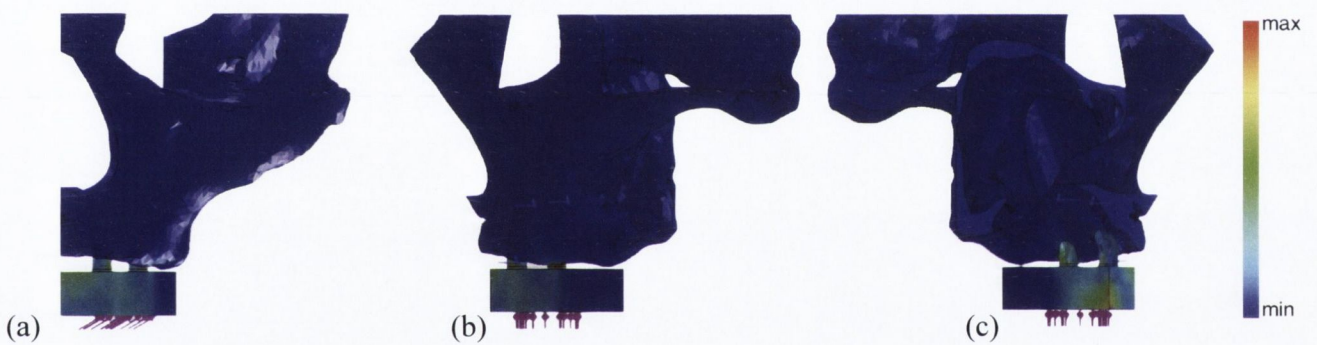


Figure 6.5 – Model 2 under 30° buccal loading: (a) anterior, (b) lateral and (c) medial views.

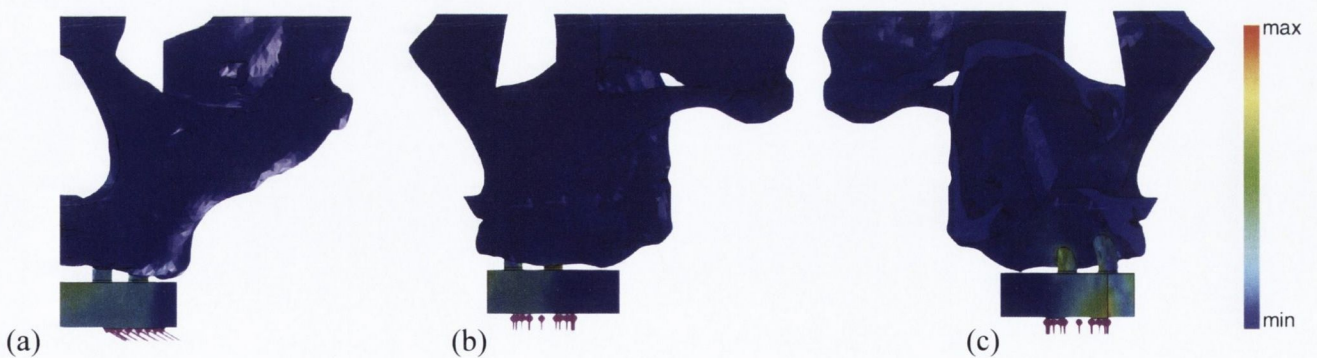


Figure 6.6 – Model 2 under 30° palatal loading: (a) anterior, (b) lateral and (c) medial views.

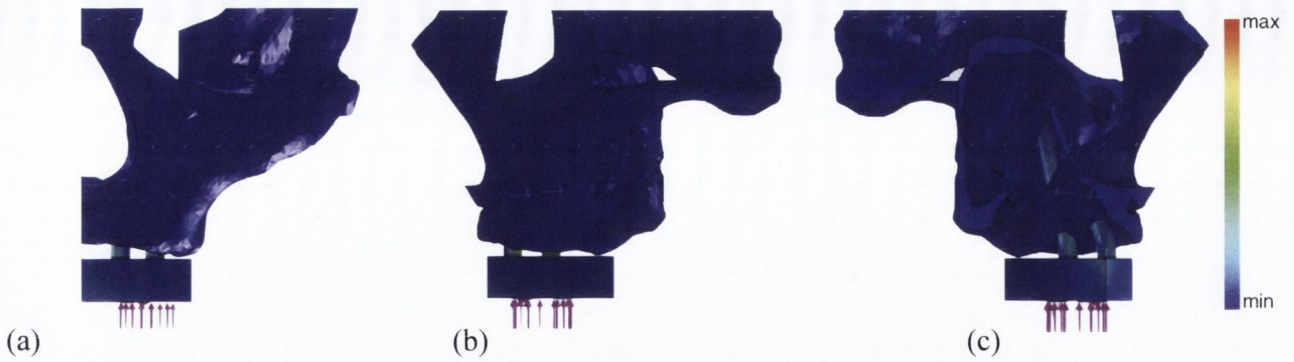


Figure 6.7 – Model 3 under occlusal loading: (a) anterior, (b) lateral and (c) medial views.

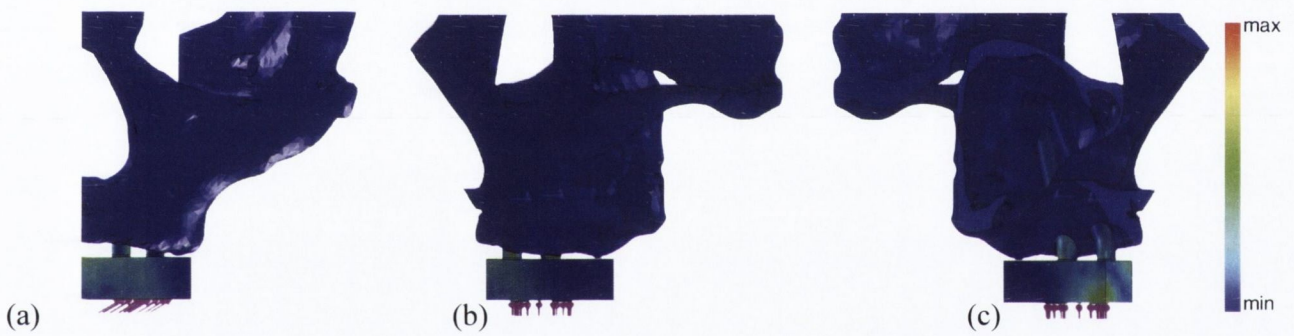


Figure 6.8 – Model 3 under 30° buccal loading: (a) anterior, (b) lateral and (c) medial views.

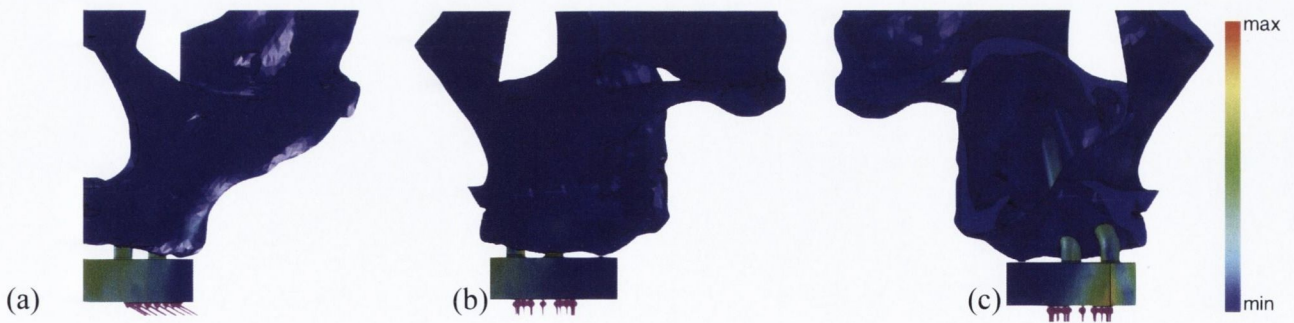


Figure 6.9 – Model 3 under 30° palatal loading: (a) anterior, (b) lateral and (c) medial views.

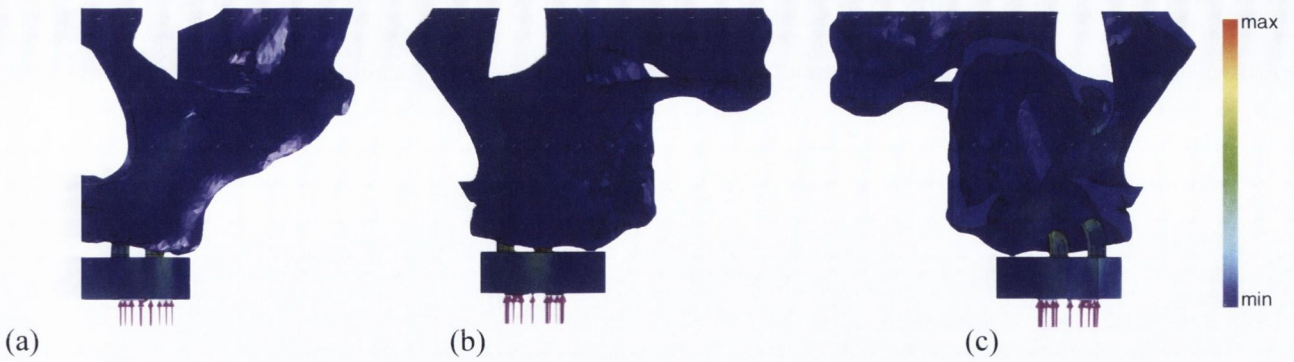


Figure 6.10 – Model 4 under occlusal loading: (a) anterior, (b) lateral and (c) medial views.

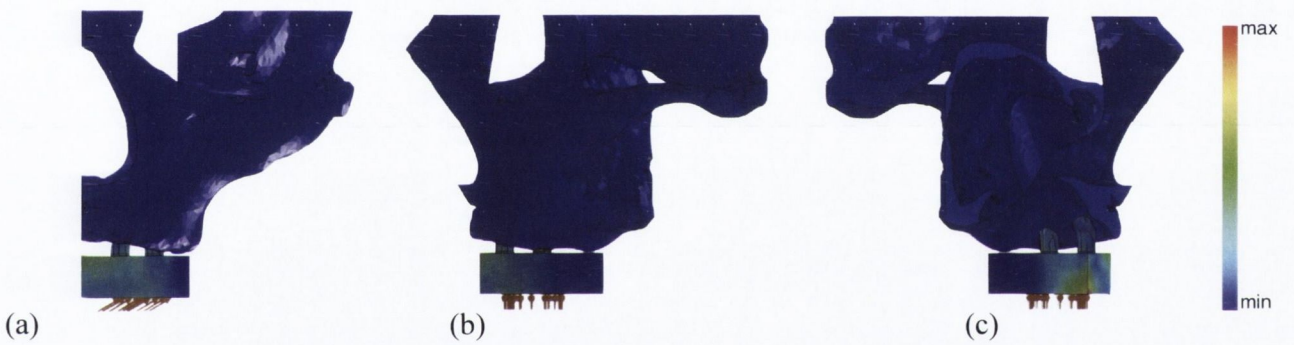


Figure 6.11 – Model 4 under 30° buccal loading: (a) anterior, (b) lateral and (c) medial views.

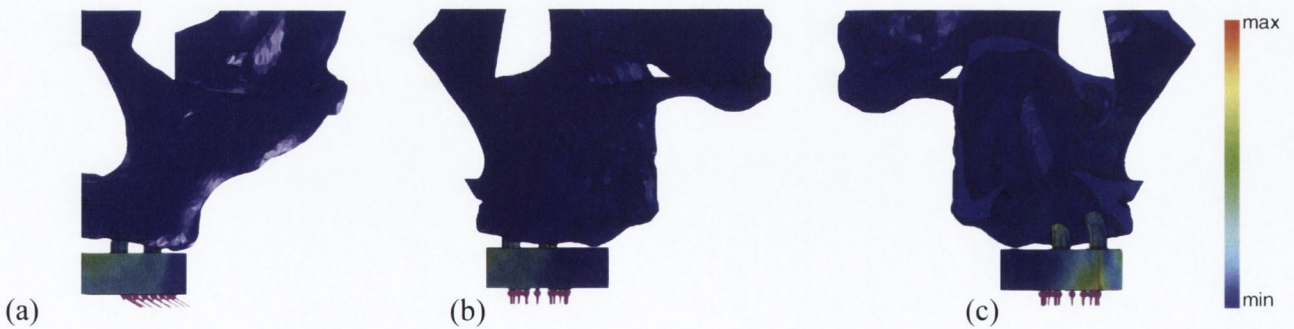


Figure 6.12 – Model 4 under 30° palatal loading: (a) anterior, (b) lateral and (c) medial views.

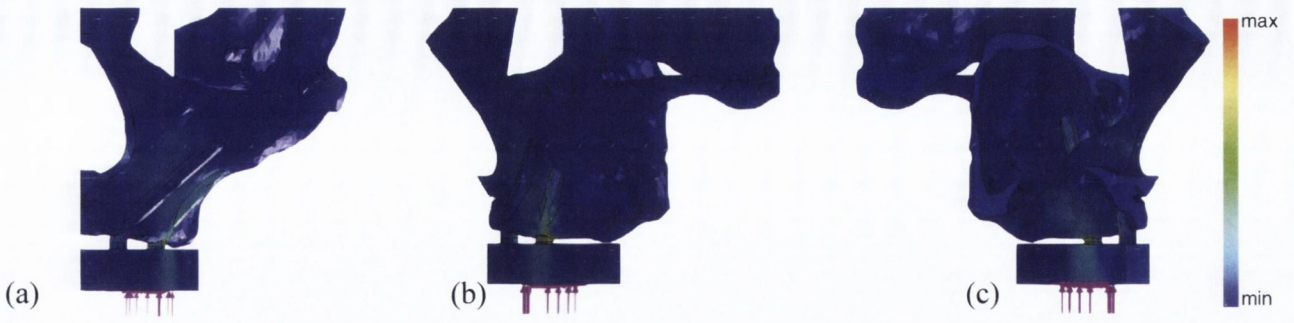


Figure 6.13 – Model 5 under occlusal loading: (a) anterior, (b) lateral and (c) medial views.

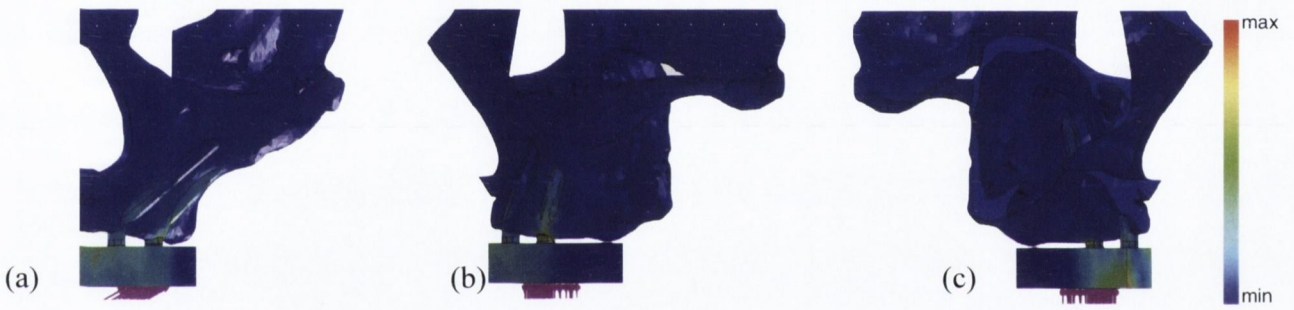


Figure 6.14 – Model 5 under 30° buccal loading: (a) anterior, (b) lateral and (c) medial views.



Figure 6.15 – Model 5 under 30° palatal loading: (a) anterior, (b) lateral and (c) medial views.

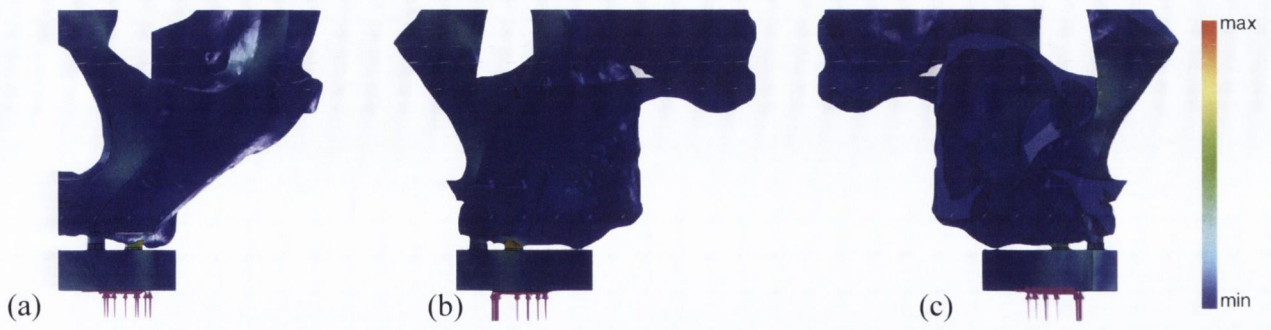


Figure 6.16 – Model 6 under occlusal loading: (a) anterior, (b) lateral and (c) medial views.

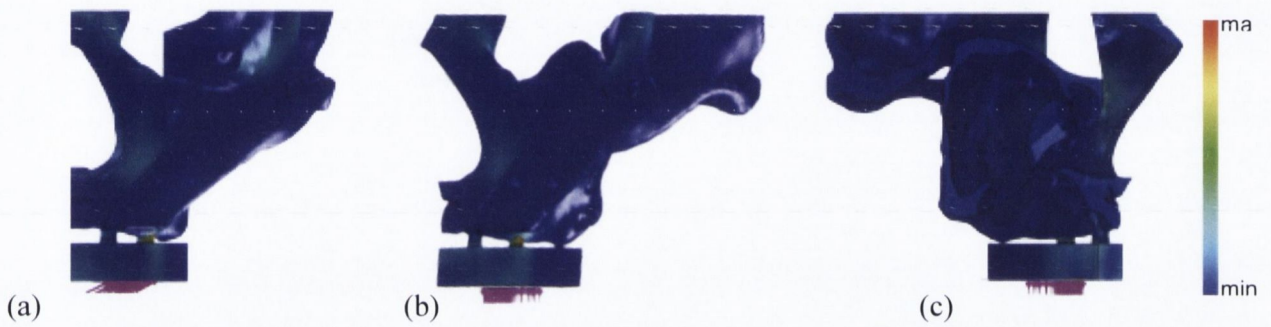


Figure 6.17 – Model 6 under 30° buccal loading: (a) anterior, (b) lateral and (c) medial views.

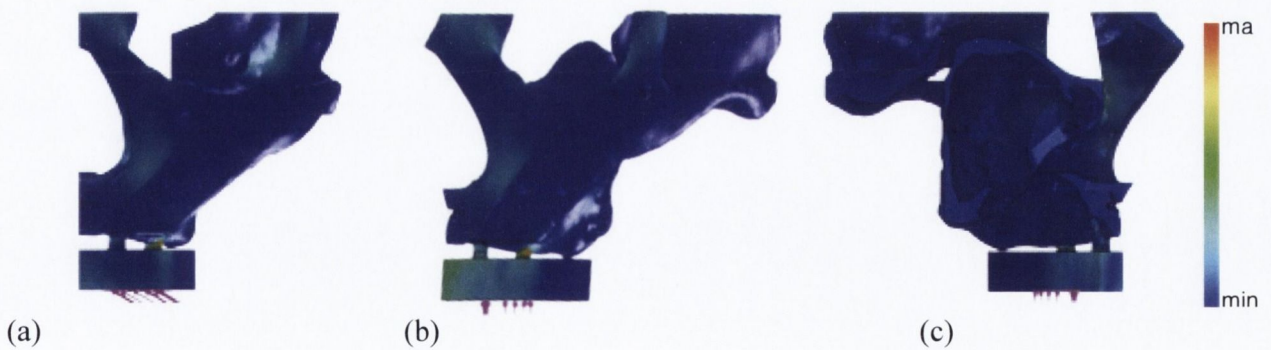


Figure 6.18 – Model 6 under 30° palatal loading: (a) anterior, (b) lateral and (c) medial views.



Figure 6.19 – Model 7 under occlusal loading: (a) anterior, (b) lateral and (c) medial views.

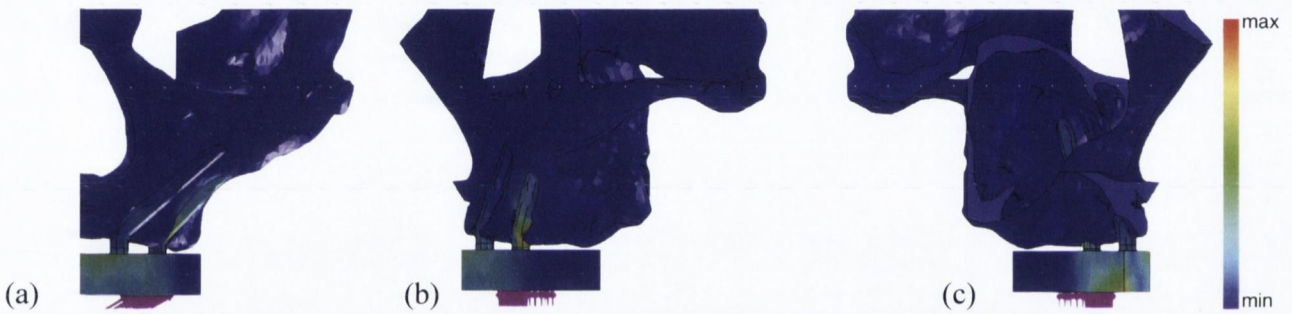


Figure 6.20 – Model 7 under 30° buccal loading: (a) anterior, (b) lateral and (c) medial views.



Figure 6.21 – Model 7 under 30° palatal loading: (a) anterior, (b) lateral and (c) medial views.

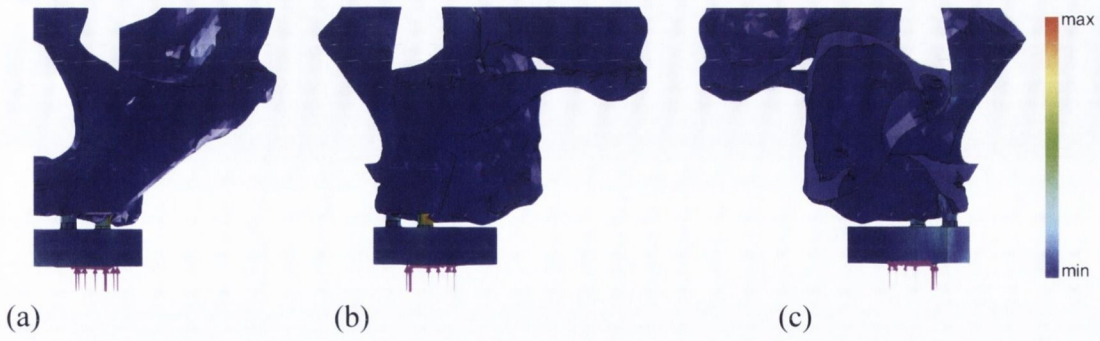


Figure 6.22 – Model 8 under occlusal loading: (a) anterior, (b) lateral and (c) medial views.

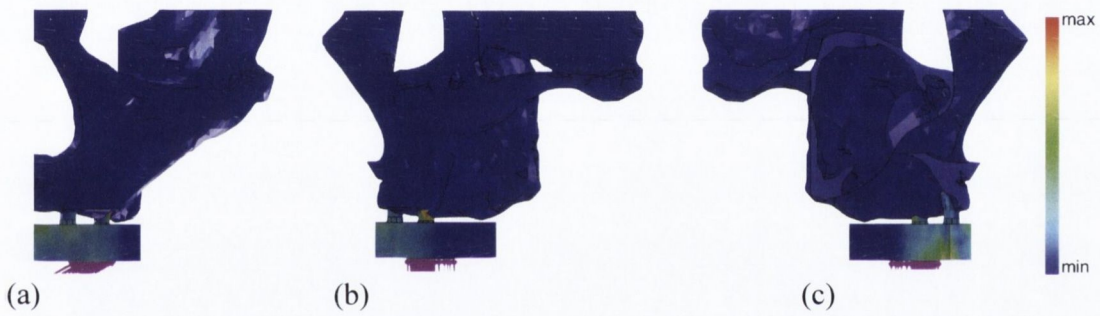


Figure 6.23 – Model 8 under 30° buccal loading: (a) anterior, (b) lateral and (c) medial views.

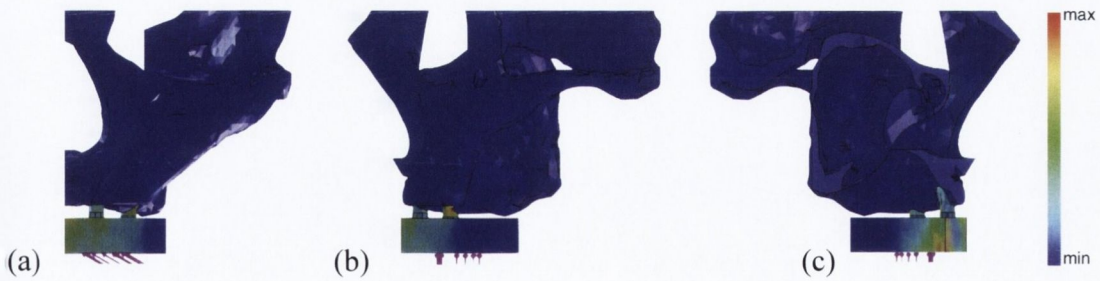


Figure 6.24 – Model 8 under 30° palatal loading: (a) anterior, (b) lateral and (c) medial views.

6.2 Effect of force magnitude

The maximum stress observed in each model varied with the applied force. As the applied force was increased, the maximum stress increased linearly (Figures 6.25 to 6.27). This was true for all models, with occlusal and lateral forces. The distribution of the stresses did not vary as the applied force was increased.

The lowest maximum stress with an occlusally directed force was observed in model 2 (with implants inside the sinus, with alveolar support and with graft). The lowest maximum stress with a 30° lateral force was observed in model 1 (with implants inside the sinus, with alveolar support and without graft).

The highest maximum stress with an occlusally directed force was observed in model 4 (with implants inside the sinus, without alveolar support, with graft). The highest maximum stress with a 30° lateral force was also observed in model 4 (with implants inside the sinus, without alveolar support, with graft).

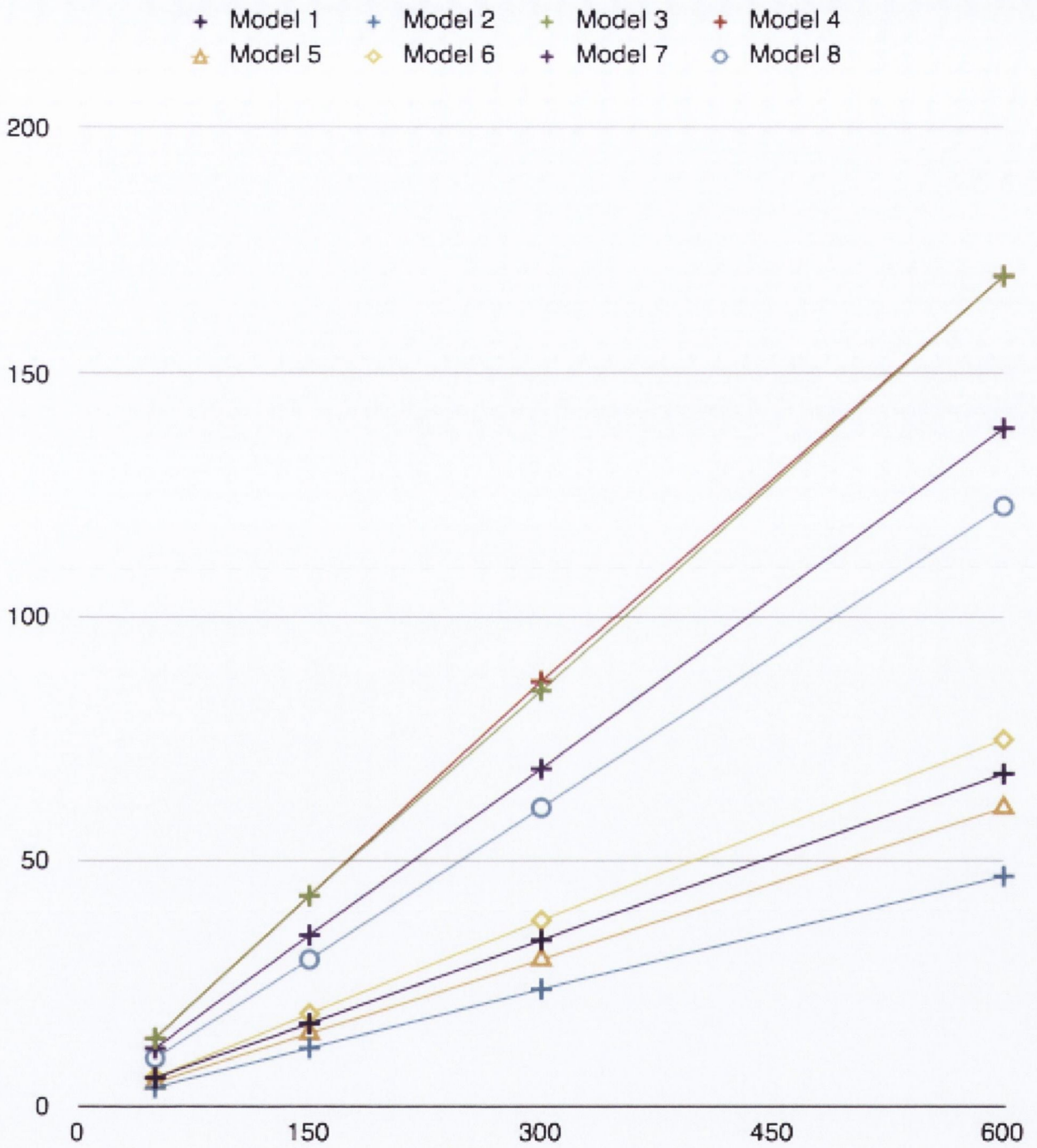


Figure 6.25 – Maximum stress with increasing applied occlusal force.

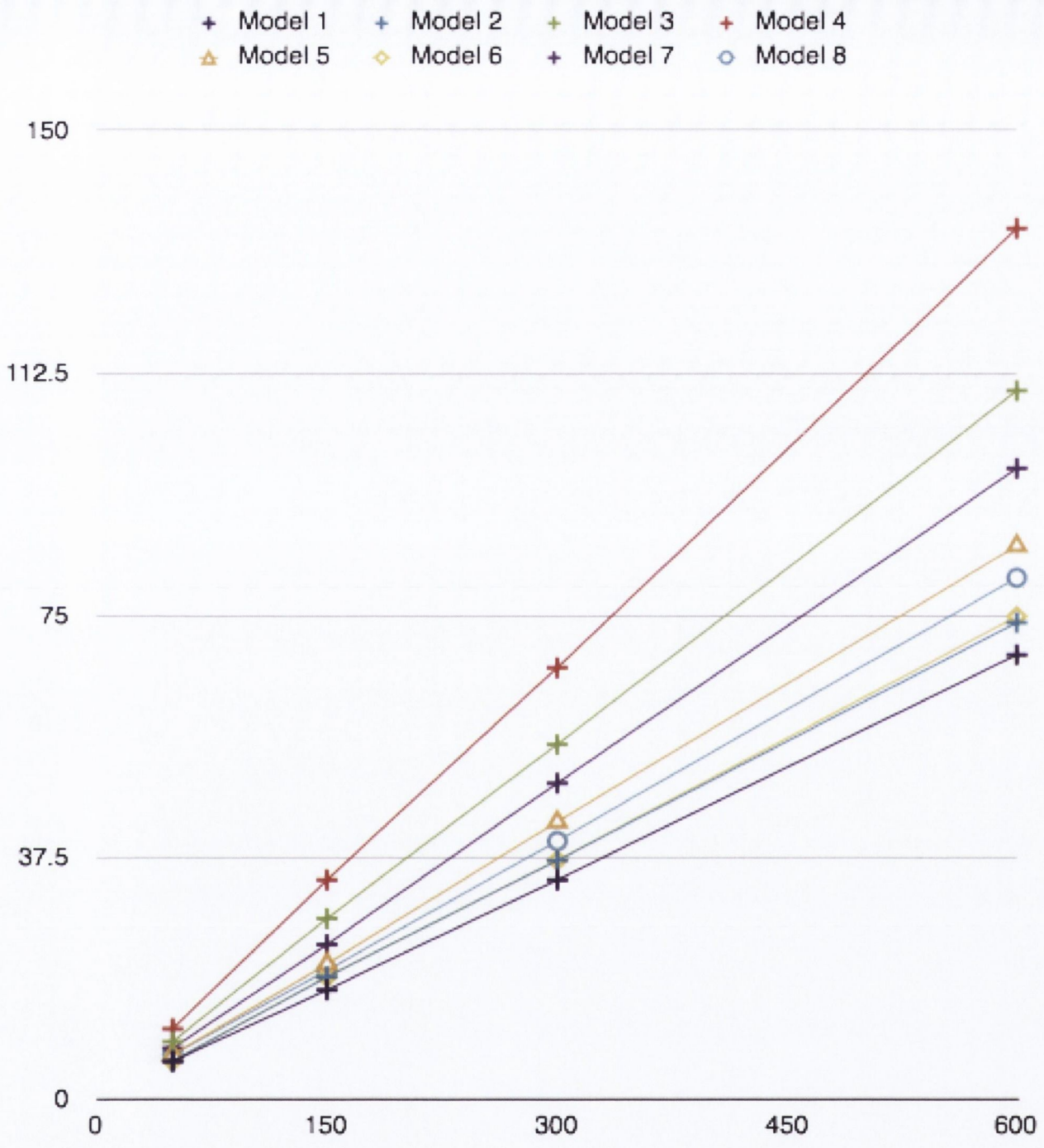


Figure 6.26 – Maximum stress with increasing applied 30° buccal force.

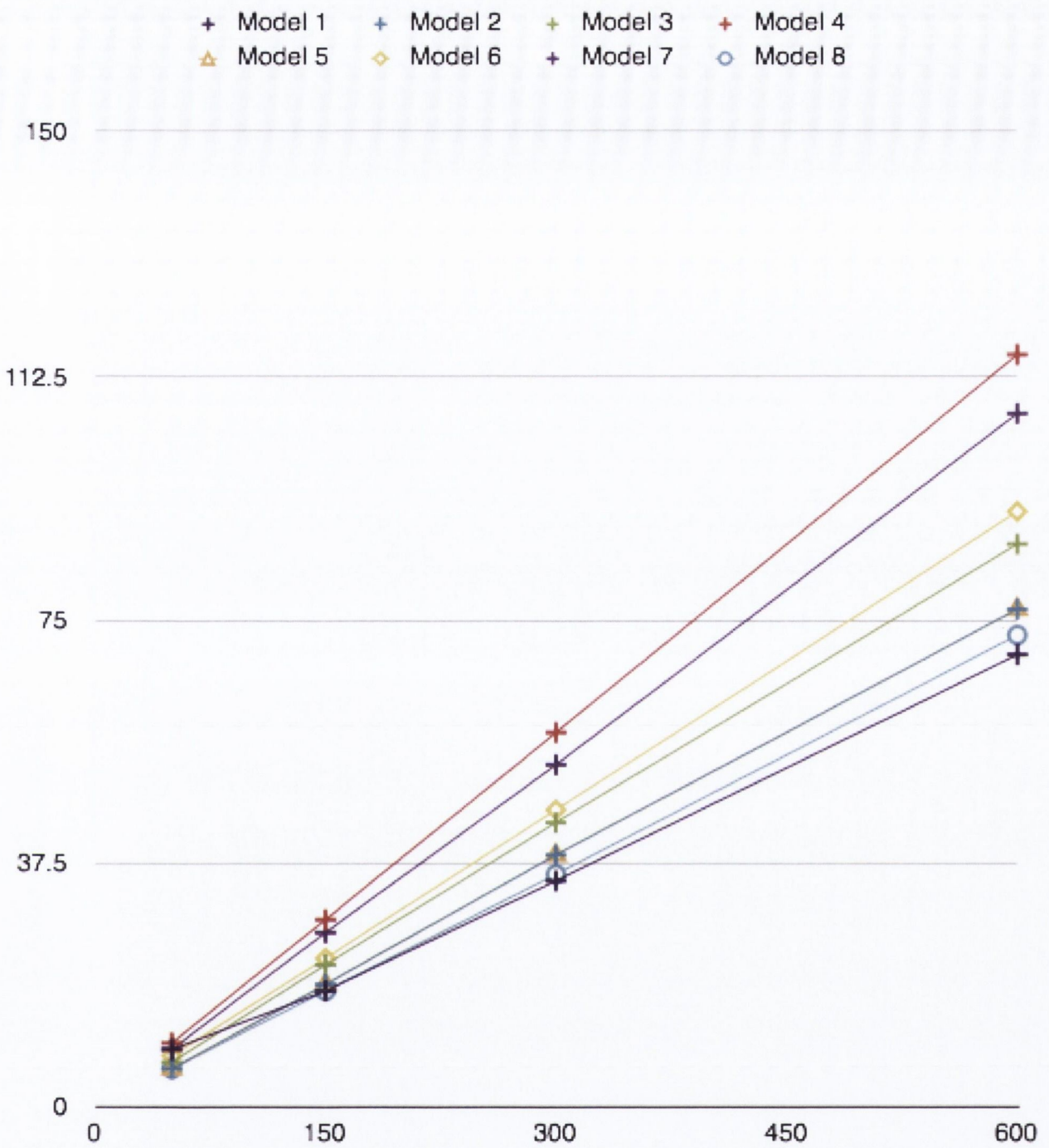


Figure 6.27 – Maximum stress with increasing applied 30° palatal force.

6.3 Effect of force direction

The magnitude of the maximum stress observed in the models varied with the direction of the applied force. In some models, the maximum stress increased as the applied force was directed more occlusally. In others, the opposite occurred, with lower occlusal stresses than lateral stresses noted (Figure 6.28).

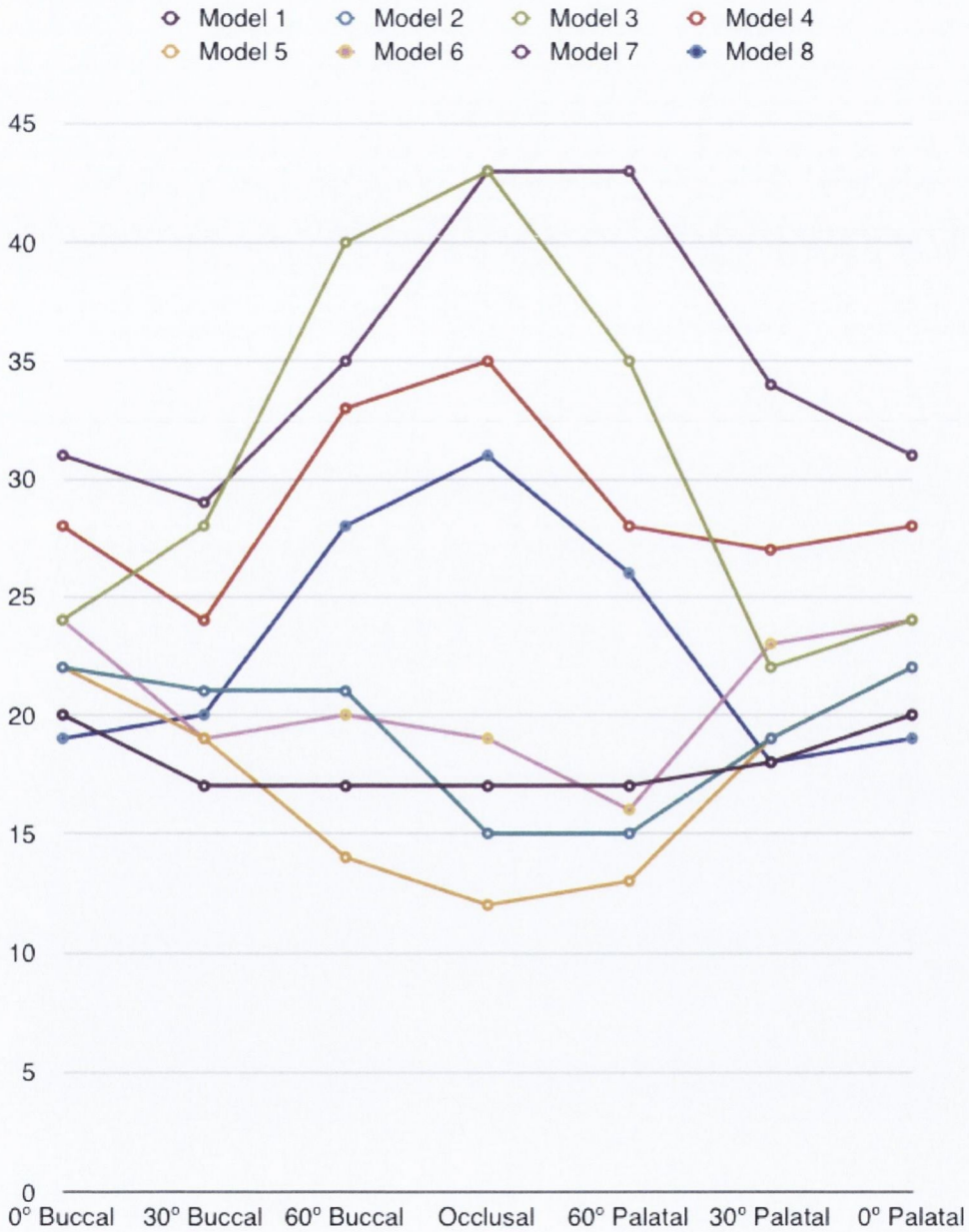


Figure 6.28 – Maximum stresses observed in models with varying force direction.

6.4 Effect of alveolar support

Alveolar bone support had a profound effect on the observed maximum stresses of the models. All of the models without alveolar support showed higher maximum stresses when occlusal forces were applied, compared to when lateral forces were applied. The opposite effect was observed for models with alveolar support. These showed lower maximum stresses when occlusal forces were applied, compared to when laterally directed forces were applied.

The maximum stresses were lower when alveolar support was present in all of the models with an intra-sinus implant position, and when no graft was present in an extra-sinus position.

In the two models with a graft and implants in an extra-sinus position, lower maximum stresses were noted in the model without alveolar support for 0° buccal forces, 0° palatal forces and 30° palatal forces.

The ratios of maximum stresses in models with alveolar support to models without alveolar support are shown in Table 6.1. The range of these ratios was from 0.27 to 1.26. This represents a range from a 73% reduction in maximum stress when alveolar support was present to a 26% increase in maximum stress when alveolar support was present.

150N force / max von Mises stress	0° Buccal	30° Buccal	60° Buccal	Occlusal	60° Palatal	30° Palatal	0° Palatal
No graft, intra-sinus	0.84	0.62	0.43	0.40	0.48	0.80	0.84
No graft, extra-sinus	0.80	0.88	0.63	0.44	0.55	0.73	0.80
Graft, intra-sinus	0.71	0.64	0.41	0.27	0.29	0.57	0.71
Graft, extra-sinus	1.26	0.93	0.69	0.61	0.60	1.26	1.26

Table 6.1 – Ratio of maximum stresses in models with alveolar support to models without alveolar support. Highlighted cells indicate situations where ratio is >1 (no alveolar support > with alveolar support).

6.5 Effect of implant position

The position of the implant had a variable effect on the maximum stresses observed in the models. In the models with alveolar support, an intra-sinus position produced consistently lower stresses when a graft was present. When no graft was present, an intra-sinus position produced lower stresses in lateral forces, but higher stresses in occlusally directed forces when compared to an extra-sinus position.

In the models without alveolar support, an extra-sinus position produced consistently lower stresses when a graft was present. When no graft was present, an extra-sinus position produced lower stresses except when 0° buccal, 0° palatal and 30° palatal forces were applied.

The ratios of maximum stresses in models with an intra- and extra-sinus position are shown in Table 6.2. The range of these ratios was from 0.63 to 1.87. This represents a range from a 37% reduction in maximum stress when an intra-sinus position was used to an 87% increase in maximum stress when an intra-sinus position was used.

150N force / max von Mises stress	0° Buccal	30° Buccal	60° Buccal	Occlusal	60° Palatal	30° Palatal	0° Palatal
No graft, with alveolar support	0.90	0.80	0.81	1.12	1.10	0.90	0.90
No graft, no alveolar support	0.85	1.13	1.19	1.23	1.26	0.82	0.85
Graft, with alveolar support	0.91	0.99	0.73	0.63	0.81	0.84	0.91
Graft, no alveolar support	1.62	1.44	1.23	1.40	1.65	1.87	1.62

Table 6.2 – Ratio of maximum stresses in models with an extra-sinus position to models with an intra-sinus position.

Highlighted cells indicate situations where ratio is >1 (extra-sinus position > intra-sinus position).

6.6 Effect of additional bony support (graft)

The addition of extra bony support to the implants had a variable effect on the maximum stresses observed in the models. In the models with an extra-sinus implant position without alveolar support, the presence of additional bony support consistently reduced the maximum stress. In the models with an extra-sinus position with alveolar support, the presence of additional bony support reduced the maximum stress only with 30° and 60° buccal forces.

In the models with an intra-sinus position, when there was alveolar support, the presence of additional bony support reduced the maximum stress with 60° buccal and palatal forces as well as with occlusal forces. In the same models without alveolar support, this was only the case with a 60° buccal force.

The ratios of maximum stresses in models without additional bony support to those with additional bony support are shown in table 6.3. The range of these ratios was from 0.64 to 1.47. This represents a range from a 36% reduction in maximum stress when additional bony support was absent to a 47% increase in maximum stress when additional bony support was absent.

150N force / max von Mises stress	0° Buccal	30° Buccal	60° Buccal	Occlusal	60° Palatal	30° Palatal	0° Palatal
With alveolar support, intra-sinus	0.91	0.93	1.18	1.44	1.35	0.91	0.91
With alveolar support, extra-sinus	0.93	1.14	1.06	0.81	0.99	0.85	0.93
No alveolar support, intra-sinus	0.76	0.95	1.13	0.99	0.82	0.64	0.76
No alveolar support, extra-sinus	1.47	1.21	1.17	1.13	1.07	1.47	1.47

Table 6.3 – Ratio of maximum stresses in models without graft to models with graft.

Highlighted cells indicate situations where ratio is >1 (without graft > with graft).

7. Discussion

7.1 Model construction

The computer model used in this study was constructed using a similar approach to other FEA studies.^{6, 9, 28} Many studies have assigned cortical thickness to the maxilla and used material properties for the skull derived from other cortical bones in the body.¹² This approach has not been validated and may lead to inaccurate analysis. The maxilla is a membranous bone and has very thin cortical plates. Strait, in 2005, showed that when species and site specific values were averaged for use in FEA of the skull, accurate results could be obtained by treating the bone as isotropic, homogenous and linearly elastic.⁷¹ Therefore, in this study, no distinction was made between cortical and cancellous bone. The bone forming the skull was therefore assumed to be homogenous, which simplified the model construction and analysis.

Material properties were taken from averaged values calculated by Peterson *et al* in 2003 and 2006, and Seong *et al* in 2009 to ensure that the model would accurately simulate reality.⁶⁷⁻⁶⁹

Only half of the skull and bridge were modelled for use in the FEA. Using a slider-roller restraint at the midline of the model simulated the presence of an identical mirrored side. This created a smaller model with reduced complexity. Fewer elements were needed to carry out the FEA, which was less intensive on computer resources. The model was also mirrored initially and a small number of FEAs run to validate this approach. In these cases, stresses travelled across the midline through the bridge and skull as would occur *in vivo*. The stresses observed around the implants were similar to when a slider-roller restraint was used at the midline.

Forces from 50N to 600N were applied to each of the models in occlusal and 30° lateral directions. This range was designed to exceed normal masticatory forces

created during functional movements.^{79, 80} When evaluating the effect of force direction and comparing models to each other, a single force of 150N was used for consistency. This force was chosen as it represents a normal functional load.⁸⁰ As the maximum stresses for all of the models were found to increase linearly as the applied force was increased, similar results would be found for comparisons at higher and lower forces.

The magnitudes of the maximum stresses observed under a force of 150N in this study ranged from 12 MPa to 43 MPa. This represents a similar range to the results found by the groups led by Ujigawa *et al* in 2007 and Miyamoto *et al* in 2010 investigating zygomatic implants.^{6, 28} Tie *et al* in 2005 and Ishak *et al* in 2012 reported significantly higher stresses in the bridge components of their models, but similar stresses in the implants and bony components.^{9, 65} While direct comparisons cannot be made between the studies, the fact that the bony and implant components showed similar results to this study is reassuring, and supports our approach to constructing the models.

7.2 Stress distribution in the skull

Previous studies have suggested that most of the stresses applied via the prosthesis to zygomatic implants are transferred to the zygomatic bone.⁶ This is a reasonable hypothesis, as a larger surface area of the implant is placed in the zygomatic bone than any other area.²³ The results of this study, however, have consistently shown low stresses in the area of the zygomatic bone. Stresses were distributed laterally via the palate and vertically via the lateral maxilla and nasal buttress.

All previous FEA studies investigating the stress distribution around zygomatic implants have incorporated a masseteric force, spread over the zygomatic

bone, usually of 300N.^{6, 9, 28, 65} In the context of normal occlusal loads of 150N, it is much more likely that the high stresses reported in the zygomatic bone in these previous studies are related to the masseteric force, rather than stresses distributed through the implants. Ujigawa *et al* in 2007 presented figures illustrating low stresses at the apical (zygomatic) ends of the implants in their FEA study.⁶ Despite this, they claimed that most stresses were transferred to the zygomatic bone and that the support of zygomatic implants was not influenced significantly by the maxilla. The opposite was shown in our study (without a masseteric force), with stresses being efficiently dissipated via the maxilla and low stresses being noted in the zygomatic bone.

While the inclusion of the muscular components of the skull will improve the accuracy of a model aiming to predict stress distributions in the cranial bones, it will obscure an analysis of the proportion of those stresses arising from implants. There can be no doubt that stresses will be generated in the zygomatic bone, when a masseteric force is applied regardless of the presence of implants.

Alexandridis *et al* in 1985 investigated the stress distribution in the dentate human skull using a photoelastic model.⁷⁸ They found that stresses were propagated along the bony buttresses of the skull, i.e. the nasal, zygomatic and pterygoid areas, in a similar manner to that observed in this study. In the context of the low zygomatic stresses observed, the significance of the maxilla in distributing the forces in and around osseointegrated zygomatic implants is likely to be greater than previously appreciated. The importance of the zygomatic bone in providing a large area of bone for primary stability is not called into question.

The location of the maximum stresses observed in all models was either in the bridge or the implants. Stresses observed in the skull were consistently lower than those in the bridge and implants. When lateral forces were applied, high stresses were

noted at the midline of the bridge. This can be expected as the midline was restrained in the lateral direction as part of the model's boundary conditions. Achieving cross arch stabilisation clinically would allow these stresses to be distributed via the bridge to the contra-lateral implants.

The models used in this study are the first FEA models investigating zygomatic implants that have not included a masseteric force. Our results more accurately portray the distribution of stresses generated by masticatory forces with zygomatic implants. They consistently show low stresses in the zygomatic bone. Even when support at the alveolar end of the implants was removed, stresses were concentrated in the bridge and implants as they deformed, and low stresses were seen in the zygomatic bone. This finding challenges the widely held belief that stresses from zygomatic implants are primarily dissipated through the zygomatic bone.

7.3 Alveolar bone support

The significance of alveolar bone support for zygomatic implants has not been previously studied. Previous research has led to the conclusion that most stresses are transferred from the implants to the zygomatic area. As a result, the quality and quantity of the zygomatic bone has been the focus of previous research.^{21, 22, 25} Our study is the first to investigate the effect that alveolar bone support has on the stress distribution around zygomatic implants.

Two changes were noted in the maximum stresses of the models when alveolar bone support was removed. Firstly, greater maximum stresses tended to occur in the models without alveolar support. The distance from the applied force (at the bridge) to the first point of bony support was increased when alveolar support was absent. This created a longer cantilever and explains the higher stresses seen (Figure 7.1).

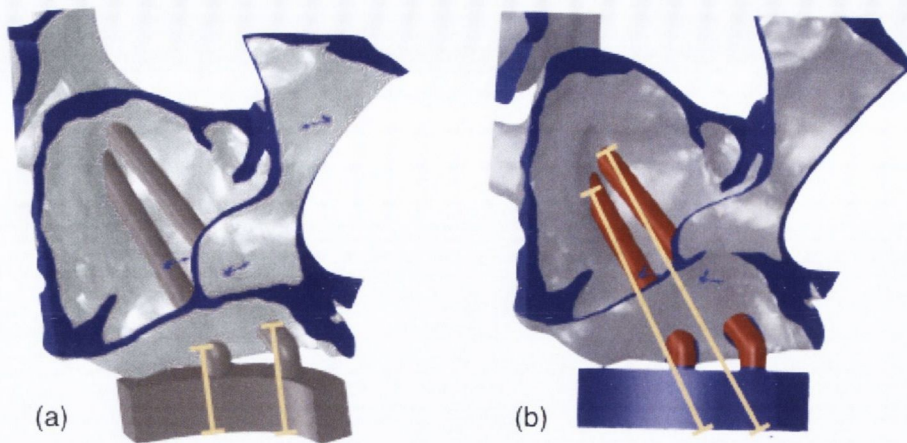


Figure 7.1 - A shorter cantilever arm (orange lines) exists when alveolar bone support is present (a) compared to when it is absent (b).

Secondly, occlusal forces created the highest stresses when alveolar support was absent. Lateral forces created the highest stresses when alveolar support was present (Figure 6.28). Despite this alteration in the pattern of maximum stresses, in most cases the lateral stresses were higher for models without alveolar support than for equivalent models with alveolar support.

The finding that occlusal forces caused an increase in the maximum stresses when alveolar support was absent is important, as most functional masticatory forces are occlusally directed and purely lateral forces seldom occur.⁷⁹ Bony support at the alveolar end of the implant was the factor that most significantly and consistently reduced the maximum stresses observed in the models.

Our results clearly indicate that alveolar bone support has a pronounced beneficial effect on reducing the stresses in and around zygomatic implants. This is the first study, to the authors' knowledge, that has reported this finding. While zygomatic implants have been placed without any maxillary support, the results of

this study highlight the importance of support for zygomatic implants in the palatal or alveolar bone when available.^{5, 81}

7.4 Implant position

Numerous zygomatic implant positions have been documented, ranging from the traditional intra-sinus position to the sinus slot and extra-maxillary positions.^{1, 5, 8} Chrcanovic *et al* in 2012 suggested that the decision regarding which implant position to adopt should be made based on the degree of concavity of the lateral wall of the sinus. They suggested that very concave sinuses are suited to extra-sinus implant positions while less concave or convex sinuses are better suited to an intra-sinus position.³⁴

This study found that implant position had a variable effect on the maximum stresses in the models. In general, for occlusal forces, an extra-sinus position produced lower maximum stresses than an intra-sinus position. Lateral forces generally produced lower maximum stresses when the implants were in an intra-sinus position.

Implants in an extra-sinus position benefitted from the support of the lateral wall of the maxillary sinus. This may explain why occlusal stresses were lower for extra-sinus implants, as the lateral maxilla transfers stresses vertically to the zygomatic area in the dentate skull.⁷⁸ The intra-sinus position may have been more favourable for lateral forces as stresses could be directly transferred from the implants to the palate, which serves as a horizontal buttress.

Ishak *et al* in 2012 used a single zygomatic implant in an FEA model. They concluded that both an intra- and extra-sinus positions produced satisfactory results. In agreement with Ishak *et al's* study, our results show that stresses in and around

zygomatic implants were similar with intra- and extra- sinus implant positions. There is not enough evidence, based on these results, to advocate one implant position over another.

7.5 Additional bony support

The addition of bony support in this study was intended to simulate the presence of an artificial bone graft around the zygomatic implants. Zygomatic implants are often used to avoid the need for a bone graft, or in patients who are not suitable for bone grafting procedures.²⁶ However, it has been demonstrated that when the sinus lining is preserved, new bone formation can occur around the zygomatic implant.¹¹

When comparing models with and without bone grafts in this study it was expected that the addition of support to the implants would reduce the maximum stresses noted. This was not observed. In many cases, the addition of bone graft increased the maximum stress recorded.

The reason why additional bony support did not reduce the stresses observed in all models is unclear. One explanation is that the extra support prevented the implants from flexing along their length. This would have concentrated higher stresses at the head of the implant and the bridge. Another possibility is that adding such a large volume of bone to the lateral wall of the sinus made this area of the skull more rigid. This could have reduced its capacity to distribute the stresses generated by the implants, again concentrating higher stresses at the head of the implant and the bridge.

In all cases where observed stresses were increased by additional bony support, the increase was seen at the coronal end of the implant. In practice, overload

in this area would result in a failure of the abutment or prosthesis. While this is a difficult clinical problem to rectify, it is preferable to failure of the entire implant.

Bone grafting is not suggested as part of any of the protocols for the placement of zygomatic implants and has not been proposed in case reports.³⁴ It would, however, be a simple supplement to the surgical procedure to place a grafting material over the implants as an onlay or sinus lift. This is a routine procedure for conventional dental implants with exposed threads in the alveolus.

The results of this study are inconclusive regarding the value of placing a bone graft. It reduced overall stresses in some models, but not in others. In the absence of clinical data to support bone grafting around zygomatic implants, it should not be routinely advocated.

7.6 Decision tree

Bringing all of the results of the study together for occlusal forces, which make up the majority of masticatory forces, a decision tree can be made to guide the placement of zygomatic implants (Figure 7.2).

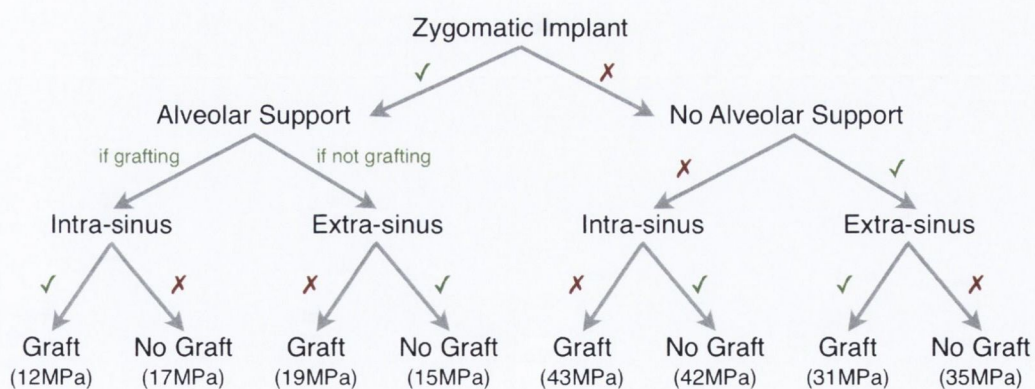


Figure 7.2 - Decision tree for reducing maximum stresses with occlusal forces. Green ticks indicates lower stresses, red crosses indicate higher stresses. Numbers in brackets indicate maximum stress when a 150N occlusal force is applied.

Alveolar support was the variable found to most significantly influence the maximum stresses observed and this study shows that it is the most important factor to consider. If alveolar support is available, the decision to place the implants in an intra-sinus position or an extra-sinus position should be made clinically depending on the shape of the maxilla.³⁴ Grafting will offer additional support along the length of the implant, but was shown to increase the stresses within the bridge and abutment in some models.

7.7 Limitations

As with all FEA studies, the results reported in this study must be interpreted giving consideration to the parameters used to create the model. The model was derived from CT data of one patient. Repeating the study using data from a number of different patients would serve to strengthen its findings. Efforts were made to ensure that accurate material properties were used. However, cranial bones do not behave as isotropic homogenous materials. The comparisons made between models in this study can be said to be valid as the same material properties were used in all models. The magnitudes of maximum stresses observed were similar to those reported by other groups. These values are approximations of the true values that would be observed *in vivo* and would need to be validated by direct clinical measurements in order to transfer them directly to the real world.

8. Conclusion

This study has investigated the stress distribution of a fixed bridge supported by two zygomatic implants per side in an edentulous skull. Finite element models of the edentulous skull, bridge and zygomatic implants were created for different implant positions, and with the implants supported by different components of the skull.

Within the limitations of the study, it was shown that stresses were concentrated in the prosthetic components of the models and the implants. The stresses that were transferred to the skull were lower than those observed in the bridge and implants. These stresses were distributed efficiently along the vertical and horizontal facial buttresses as occurs in the dentate skull. Low stresses were transferred to the zygomatic area of the skull as a result of occlusal and lateral forces applied to the bridge in all of the models studied.

Alveolar bone support was found to have a substantial effect on the maximum stresses observed in the models. The presence of alveolar support consistently reduced the maximum stress regardless of implant position, presence of additional bony support or force direction. Therefore, where possible, alveolar bone support should be maintained when placing zygomatic implants.

Implant position had a variable effect on the maximum stresses observed. It is not possible based on the results of this study to advocate an extra-sinus position or an intra-sinus position for all circumstances. When alveolar bone support is available, a decision regarding the implant position is best made clinically. If alveolar bone support is not available, an extra-sinus implant position produced lower stresses.

The addition of extra bony support (bone graft) also produced a variable effect on the maximum stresses observed. It is therefore not possible to recommend that a

bone graft should routinely be placed around zygomatic implants based on the results of this study. A decision tree was produced to demonstrate which situations were favourable for placing a bone graft based on the results of this study.

The variable effect that was seen with implant position and bone grafting highlights the complexity of the system being investigated. A bridge supported by zygomatic implants represents a sophisticated combination of structures with different shapes and material properties. As forces are applied to the bridge, the system is placed under compression in some areas and tension in others. This occurs as the components bend. Small changes to the support and position of the implants can produce unpredictable changes in the stresses observed. Support for the implant in the alveolar bone is the factor that consistently reduced the maximum stresses observed under functional loading conditions.

The facial skeleton did not evolve to support implants and fixed dental prostheses. The fact that stresses are distributed so efficiently though it and that zygomatic implants have a high clinical success rate is a tribute to the adaptability of a biological system rather than a triumph of any material or design.

9. References

1. Brånemark PI, Grondahl K, Ohnrell LO, Nilsson P, Petruson B, Svensson B, et al. Zygoma fixture in the management of advanced atrophy of the maxilla: technique and long-term results. *Scand J Plast Reconstr Surg Hand Surg* 2004;38(2):70-85.
2. Misch CE. Contemporary Implant Dentistry. 3rd ed: Mosby (Elsevier), Philadelphia, USA; 2008. ISBN 0323043739.
3. Esposito M, Grusovin MG, Felice P, Karatzopoulos G, Worthington HV, Coulthard P. The efficacy of horizontal and vertical bone augmentation procedures for dental implants - a Cochrane systematic review. *Eur J Oral Implantol* 2009;2(3):167-84.
4. Esposito M, Grusovin MG, Rees J, Karasoulos D, Felice P, Alissa R, et al. Effectiveness of sinus lift procedures for dental implant rehabilitation: a Cochrane systematic review. *Eur J Oral Implantol* 2010;3(1):7-26.
5. Malo P, Nobre Mde A, Lopes I. A new approach to rehabilitate the severely atrophic maxilla using extramaxillary anchored implants in immediate function: a pilot study. *J Prosthet Dent* 2008;100(5):354-66.
6. Ujigawa K, Kato Y, Kizu Y, Tonogi M, Yamane GY. Three-dimensional finite elemental analysis of zygomatic implants in craniofacial structures. *Int J Oral Maxillofac Surg* 2007;36(7):620-5.
7. NobelBiocare. Brånemark System® - Zygoma Implant Placement & Prosthetic Procedure.
http://files.nobelbiocare.com/manuals/pdf/ZygomaMan_14650_GB_C8.pdf.

Date accessed 24/6/2012

8. Stella JP, Warner MR. Sinus slot technique for simplification and improved orientation of zygomaticus dental implants: a technical note. *The International journal of oral & maxillofacial implants* 2000;15(6):889.
9. Ishak MI, Abdul Kadir MR, Sulaiman E, Abu Kasim NH. Finite element analysis of different surgical approaches in various occlusal loading locations for zygomatic implant placement for the treatment of atrophic maxillae. *Int J Oral Maxillofac Surg* 2012;41(9):1077-89.
10. Lindhe J, Karring T, Lang NP. Clinical periodontology and implant dentistry: Blackwell Munksgaard Oxford, UK; 2003. ISBN 1405160993.
11. Chow J, Wat P, Hui E, Lee P, Li W. A new method to eliminate the risk of maxillary sinusitis with zygomatic implants. *Int J Oral Maxillofac Implants* 2010;25(6):1233-40.
12. Geng JP, Tan KB, Liu GR. Application of finite element analysis in implant dentistry: a review of the literature. *J Prosthet Dent* 2001;85(6):585-98.
13. Logan DL. A first course in the finite element method: Cengage Learning, Independence, Kentucky, USA; 2011. ISBN 0495668257.
14. Albrektsson T, Brånemark PI, Hansson HA, Lindström J. Osseointegrated titanium implants: Requirements for ensuring a long-lasting, direct bone-to-implant anchorage in man. *Acta Orthopaedica* 1981;52(2):155-70.
15. Brånemark PI, Breine U, Adell R, Hansson B, Lindström J, Ohlsson Ö. Intra-osseous anchorage of dental prostheses: I. experimental studies. *Scandinavian Journal of Plastic and Reconstructive Surgery and Hand Surgery* 1969;3(2):81-100.
16. Esposito M, Coulthard P, Thomsen P, Worthington HV. The role of implant surface modifications, shape and material on the success of osseointegrated

- dental implants. A Cochrane systematic review. *Eur J Prosthodont Restor Dent* 2005;13(1):15-31.
17. Worthington P, Lang BR, Rubenstein JE. Osseointegration in dentistry: an overview: Quintessence Pub. Co.; 2003. ISBN 086715425X.
 18. Babbush CA, MScD JAH, Krauser JT, Rosenlicht JL. Dental implants: Saunders (Elsevier), Philadelphia, USA; 2001. ISBN 0721677479.
 19. Malevez C, Abarca M, Durdu F, Daelemans P. Clinical outcome of 103 consecutive zygomatic implants: a 6-48 months follow-up study. *Clin Oral Implants Res* 2004;15(1):18-22.
 20. Sinnatamby CS, Last RJ. Last's anatomy: regional and applied: Churchill Livingstone Edinburgh; 2006. ISBN 0443100330.
 21. Kato Y, Kizu Y, Tonogi M, Ide Y, Yamane GY. Internal structure of zygomatic bone related to zygomatic fixture. *J Oral Maxillofac Surg* 2005;63(9):1325-9.
 22. Nkenke E, Hahn M, Lell M, Wiltfang J, Schultze-Mosgau S, Stech B, et al. Anatomic site evaluation of the zygomatic bone for dental implant placement. *Clin Oral Implants Res* 2003;14(1):72-9.
 23. Rigolizzo MB, Camilli JA, Francischone CE, Padovani CR, Branemark PI. Zygomatic bone: anatomic bases for osseointegrated implant anchorage. *Int J Oral Maxillofac Implants* 2005;20(3):441-7.
 24. Balshi TJ, Wolfinger GJ, Petropoulos VC. Quadruple zygomatic implant support for retreatment of resorbed iliac crest bone graft transplant. *Implant Dent* 2003;12(1):47-53.

25. Rossi M, Duarte LR, Mendonca R, Fernandes A. Anatomical bases for the insertion of zygomatic implants. *Clin Implant Dent Relat Res* 2008;10(4):271-5.
26. Malevez C, Daelemans P, Adriaenssens P, Durdu F. Use of zygomatic implants to deal with resorbed posterior maxillae. *Periodontol 2000* 2003;33:82-9.
27. Bothur S, Jonsson G, Sandahl L. Modified technique using multiple zygomatic implants in reconstruction of the atrophic maxilla: a technical note. *Int J Oral Maxillofac Implants* 2003;18(6):902-4.
28. Miyamoto S, Ujigawa K, Kizu Y, Tonogi M, Yamane GY. Biomechanical three-dimensional finite-element analysis of maxillary prostheses with implants. Design of number and position of implants for maxillary prostheses after hemimaxillectomy. *Int J Oral Maxillofac Surg* 2010;39(11):1120-6.
29. Penarrocha M, Garcia B, Marti E, Boronat A. Rehabilitation of severely atrophic maxillae with fixed implant-supported prostheses using zygomatic implants placed using the sinus slot technique: clinical report on a series of 21 patients. *Int J Oral Maxillofac Implants* 2007;22(4):645-50.
30. Aparicio C, Ouazzani W, Aparicio A, Fortes V, Muela R, Pascual A, et al. Extrasinus zygomatic implants: three year experience from a new surgical approach for patients with pronounced buccal concavities in the edentulous maxilla. *Clin Implant Dent Relat Res* 2010;12(1):55-61.
31. Periotest. Medizintechnik Gulden e. K., Eschenweg 3, 64397 Modautal, Germany. <http://www.med-gulden.com/periotest.php>. Date accessed 24/6/2012

32. Aparicio C, Ouazzani W, Garcia R, Arevalo X, Muela R, Fortes V. A prospective clinical study on titanium implants in the zygomatic arch for prosthetic rehabilitation of the atrophic edentulous maxilla with a follow-up of 6 months to 5 years. *Clin Implant Dent Relat Res* 2006;8(3):114-22.
33. Miglioranca RM, Coppede A, Dias Rezende RC, de Mayo T. Restoration of the edentulous maxilla using extrasinus zygomatic implants combined with anterior conventional implants: a retrospective study. *Int J Oral Maxillofac Implants* 2011;26(3):665-72.
34. Chrcanovic BR, Pedrosa AR, Custodio AL. Zygomatic implants: a critical review of the surgical techniques. *Oral Maxillofac Surg* 2012. epub ahead of print doi 10.1007/s10006-012-0316-y.
35. Becktor JP, Isaksson S, Abrahamsson P, Sennerby L. Evaluation of 31 zygomatic implants and 74 regular dental implants used in 16 patients for prosthetic reconstruction of the atrophic maxilla with cross-arch fixed bridges. *Clin Implant Dent Relat Res* 2005;7(3):159-65.
36. Zwahlen RA, Gratz KW, Oechslin CK, Studer SP. Survival rate of zygomatic implants in atrophic or partially resected maxillae prior to functional loading: a retrospective clinical report. *Int J Oral Maxillofac Implants* 2006;21(3):413-20.
37. Chow J, Hui E, Lee PK, Li W. Zygomatic implants--protocol for immediate occlusal loading: a preliminary report. *J Oral Maxillofac Surg* 2006;64(5):804-11.
38. Duarte LR, Filho HN, Francischone CE, Peredo LG, Branemark PI. The establishment of a protocol for the total rehabilitation of atrophic maxillae employing four zygomatic fixtures in an immediate loading system--a 30-

- month clinical and radiographic follow-up. *Clin Implant Dent Relat Res* 2007;9(4):186-96.
39. Aparicio C, Ouazzani W, Aparicio A, Fortes V, Muela R, Pascual A, et al. Immediate/Early loading of zygomatic implants: clinical experiences after 2 to 5 years of follow-up. *Clin Implant Dent Relat Res* 2010;12 Suppl 1:e77-82.
40. Bedrossian E, Stumpel LJ, 3rd. Immediate stabilization at stage II of zygomatic implants: rationale and technique. *J Prosthet Dent* 2001;86(1):10-4.
41. Bedrossian E, Rangert B, Stumpel L, Indresano T. Immediate function with the zygomatic implant: a graftless solution for the patient with mild to advanced atrophy of the maxilla. *Int J Oral Maxillofac Implants* 2006;21(6):937-42.
42. Hirsch JM, Ohnell LO, Henry PJ, Andreasson L, Branemark PI, Chiapasco M, et al. A clinical evaluation of the Zygo™ fixture: one year of follow-up at 16 clinics. *J Oral Maxillofac Surg* 2004;62(9 Suppl 2):22-9.
43. Kahnberg KE, Henry PJ, Hirsch JM, Ohnell LO, Andreasson L, Branemark PI, et al. Clinical evaluation of the zygo™ implant: 3-year follow-up at 16 clinics. *J Oral Maxillofac Surg* 2007;65(10):2033-8.
44. Petruson B. Sinuscopy in patients with titanium implants in the nose and sinuses. *Scand J Plast Reconstr Surg Hand Surg* 2004;38(2):86-93.
45. Davo R, Malevez C, Lopez-Orellana C, Pastor-Bevia F, Rojas J. Sinus reactions to immediately loaded zygo™ implants: a clinical and radiological study. *Eur J Oral Implantol* 2008;1(1):53-60.
46. Reychler H, Olszewski R. Intracerebral penetration of a zygomatic dental implant and consequent therapeutic dilemmas: case report. *Int J Oral Maxillofac Implants* 2010;25(2):416-8.

47. Zarb GA, Bolender CL, Eckert SE, Jacob R, Fenton A, Mericske-Stern R. Prosthodontic treatment for edentulous patients: Mosby St Louis, MO, USA; 2004. ISBN 0323022960.
48. Jacobs SH, O'Connell BC. Dental Implant Restoration: principles and procedures: Quintessence UK; 2011. ISBN 1850971013.
49. Harris D, Hofer S, O'Boyle CA, Sheridan S, Marley J, Benington IC, et al. A comparison of implant-retained mandibular overdentures and conventional dentures on quality of life in edentulous patients: a randomized, prospective, within-subject controlled clinical trial. *Clin Oral Implants Res* 2011.
50. Jensen OT, Cottam J, Ringeman J, Adams M. Trans-Sinus Dental Implants, Bone Morphogenetic Protein 2, and Immediate Function for All-on-4 Treatment of Severe Maxillary Atrophy. *J Oral Maxillofac Surg* 2011.
51. Jensen OT, Adams MW. The maxillary M-4: a technical and biomechanical note for all-on-4 management of severe maxillary atrophy--report of 3 cases. *J Oral Maxillofac Surg* 2009;67(8):1739-44.
52. Candel E, Penarrocha D, Penarrocha M. Rehabilitation of the atrophic posterior maxilla with pterygoid implants: a review. *J Oral Implantol* 2011.
53. Huebner K, Dewhirst D, Smith D, Byrom T. The finite element method for engineers: Wiley, New York; 2001. ISBN 0471370789.
54. Hrennikoff A. Solution of problems of elasticity by the framework method. *Journal of applied mechanics* 1941;8(4):169-75.
55. Courant R. Variational Methods for the solution of problems of equilibrium and vibrations. *Bulltin of the American Mathematical Society* 1943;49:1-23.
56. Turner MJ, Clough RW, C MH, J TL. Stiffness and deflection analysis of complex structures. *Journal of Aeronautical Sciences* 1956;23(9):805-24.

57. Greenstadt J. On the reduction of continuous problems to discreet form. *IBM J. Res. Dev.* 1959;3:355-63.
58. Clough RW. The finite element method in plane stress analysis: American Society of Civil Engineers; 1960. p. 345.
59. Saber NR, Phillips J, Looi T, Usmani Z, Burge J, Drake J, et al. Generation of normative pediatric skull models for use in cranial vault remodeling procedures. *Childs Nerv Syst* 2011.
60. NEMA. Digital Imaging and Communications in Medecine (DICOM). <http://medical.nema.org/>. Date accessed 24/6/2012
61. Danaher S. The complete guide to digital 3D design: The Ilex Press Ltd; 2004.
62. Yourtee D, Emery J, Smith RE, Hodgson B. Stereolithographic models of biopolymers. *J Mol Graph Model* 2000;18(1):26-8, 59-60.
63. Garcia-Perez V, Tristan-Vega A, Aja-Fernandez S. NURBS for the geometrical modeling of a new family of Compact-Supported Radial Basis Functions for elastic registration of medical images. *Conf Proc IEEE Eng Med Biol Soc* 2010;2010:5947-50.
64. Van Oosterwyck H, Duyck J, Vander Sloten J, Van der Perre G, De Cooman M, Lievens S, et al. The influence of bone mechanical properties and implant fixation upon bone loading around oral implants. *Clin Oral Implants Res* 1998;9(6):407-18.
65. Tie Y, Wang DM, Wang CT, Wu YQ, Zhang ZY. Biomechanical evaluation of unilateral maxillary defect restoration based on modularized finite element model of normal human skull. *Conf Proc IEEE Eng Med Biol Soc* 2005;6:6184-7.

66. Junker R, Dimakis A, Thoneick M, Jansen JA. Effects of implant surface coatings and composition on bone integration: a systematic review. *Clin Oral Implants Res* 2009;20 Suppl 4:185-206.
67. Peterson J, Dechow PC. Material properties of the human cranial vault and zygoma. *Anat Rec A Discov Mol Cell Evol Biol* 2003;274(1):785-97.
68. Seong WJ, Kim UK, Swift JQ, Heo YC, Hodges JS, Ko CC. Elastic properties and apparent density of human edentulous maxilla and mandible. *International journal of oral and maxillofacial surgery* 2009;38(10):1088-93.
69. Peterson J, Wang Q, Dechow PC. Material properties of the dentate maxilla. *The Anatomical Record Part A: Discoveries in Molecular, Cellular, and Evolutionary Biology* 2006;288A(9):962-72.
70. Cezayirlioglu H, Bahniuk E, Davy DT, Heiple KG. Anisotropic yield behavior of bone under combined axial force and torque. *J Biomech* 1985;18(1):61-9.
71. Strait DS, Wang Q, Dechow PC, Ross CF, Richmond BG, Spencer MA, et al. Modeling elastic properties in finite-element analysis: How much precision is needed to produce an accurate model? *The Anatomical Record Part A: Discoveries in Molecular, Cellular, and Evolutionary Biology* 2005;283A(2):275-87.
72. Materialise Group, Leuven, Belgium. Mimics. <http://www.materialise.com/mimics>. Date accessed 24/6/2012
73. Netfabb GmbH, Parsberg, Germany. Netfabb. <http://www.netfabb.com/>. Date accessed 24/6/2012
74. McNeel North America, 3670 Woodland Park Ave N, Seattle, WA 98103 USA. Rhinoceros. <http://www.rhino3d.com/>. Date accessed 24/6/2012

75. Dassault Systèmes SolidWorks Corporation, Waltham, Massachusetts, USA. SolidWorks. <http://www.solidworks.com/>. Date accessed 24/6/2012
76. Dassault Systèmes SolidWorks Corporation, Waltham, Massachusetts, USA. Simulation. <http://www.solidworks.com/sw/products/fea-cfd-simulation-software.htm>. Date accessed 24/6/2012
77. Autodesk Inc., 55 N University Avenue Ste 223, Provo, UT 84601, USA. T-Splines for Rhino. <http://www.tsplines.com>. Date accessed 26/8/2012
78. Alexandridis C, Caputo AA, Thanos CE. Distribution of stresses in the human skull. *J Oral Rehabil* 1985;12(6):499-507.
79. Hattori Y, Satoh C, Kunieda T, Endoh R, Hisamatsu H, Watanabe M. Bite forces and their resultants during forceful intercuspal clenching in humans. *J Biomech* 2009;42(10):1533-8.
80. Ferrario VF, Sforza C, Serrao G, Dellavia C, Tartaglia GM. Single tooth bite forces in healthy young adults. *J Oral Rehabil* 2004;31(1):18-22.
81. Kreissl ME, Heydecke G, Metzger MC, Schoen R. Zygoma implant-supported prosthetic rehabilitation after partial maxillectomy using surgical navigation: a clinical report. *The Journal of Prosthetic Dentistry* 2007;97(3):121-28.

10. Appendix I - Model numbers and descriptions

Model	Implant Position	Alveolar Support	Graft
1	Inside Sinus	Yes	No
2	Inside Sinus	Yes	Yes
3	Inside Sinus	No	No
4	Inside Sinus	No	Yes
5	Outside Sinus	Yes	No
6	Outside Sinus	Yes	Yes
7	Outside Sinus	No	No
8	Outside Sinus	No	Yes

Table 5.2 reproduced for ease of reference throughout the text

11. Appendix II - Maximum stress tables

Model	50N Occlusal	150N Occlusal	300N Occlusal	600N Occlusal
Model 1	6	17	34	68
Model 2	4	12	24	47
Model 3	14	43	85	170
Model 4	14	43	87	170
Model 5	5	15	30	61
Model 6	6	19	38	75
Model 7	12	35	69	139
Model 8	10	31	62	123

Maximum von Mises (GPa) stresses observed with different applied forces in an occlusal direction.

Model	50N Buccal	150N Buccal	300N Buccal	600N Buccal
Model 1	6	17	36	69
Model 2	6	19	37	74
Model 3	9	28	55	110
Model 4	11	34	67	135
Model 5	7	21	43	86
Model 6	6	19	37	75
Model 7	8	24	49	98
Model 8	7	20	40	81

Maximum von Mises stresses observed with different applied forces in a 30° buccal direction.

Model	50N Palatal	150N Palatal	Palatal	600N Palatal
Model 1	9	18	35	70
Model 2	6	19	39	77
Model 3	7	22	44	87
Model 4	10	29	58	116
Model 5	6	19	39	78
Model 6	8	23	46	92
Model 7	9	27	53	107
Model 8	6	18	36	73

Maximum von Mises stresses observed with different applied forces in a 30° palatal direction.

150N Force / max von Mises stress	0° Buccal	30° Buccal	60° Buccal	Occlusal	60° Palatal	30° Palatal	0° Palatal
Model 1	20	17	17	17	17	18	20
Model 2	22	21	21	15	15	19	22
Model 3	24	28	40	43	35	22	24
Model 4	28	24	33	35	28	27	28
Model 5	22	19	14	12	13	19	22
Model 6	24	19	20	19	16	23	24
Model 7	31	29	35	43	43	34	31
Model 8	19	20	28	31	26	18	19

Maximum von Mises stresses observed with a 150N force applied in varying directions to the horizontal plane

12. Appendix III - Stress distributions

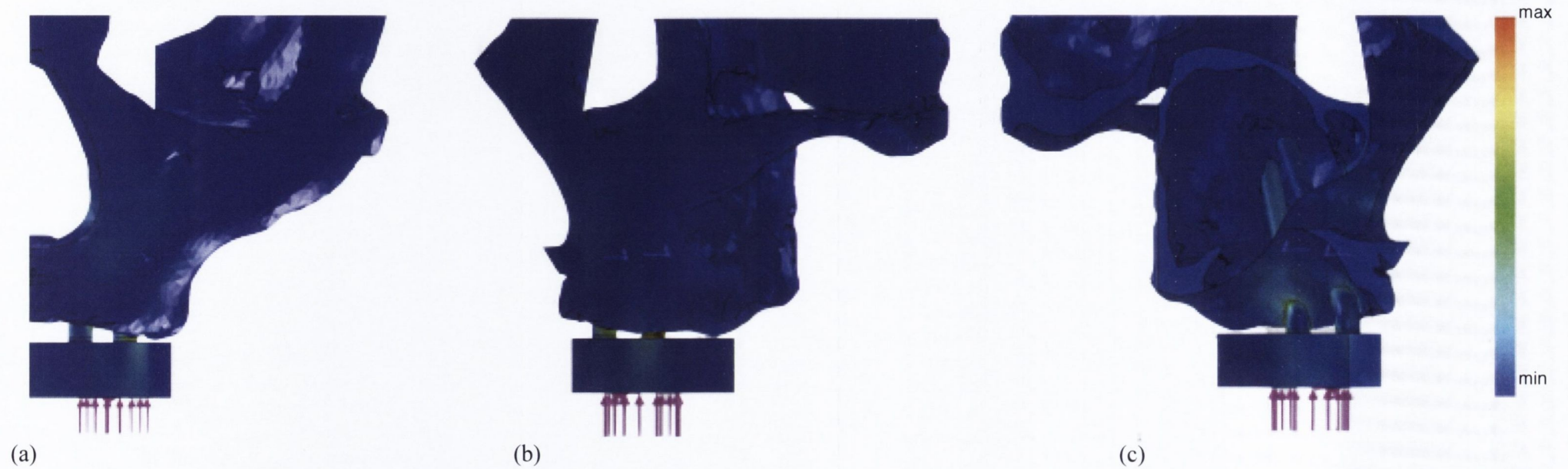


Figure 6.1 – Model 1 under occlusal loading: (a) anterior, (b) lateral and (c) medial views.

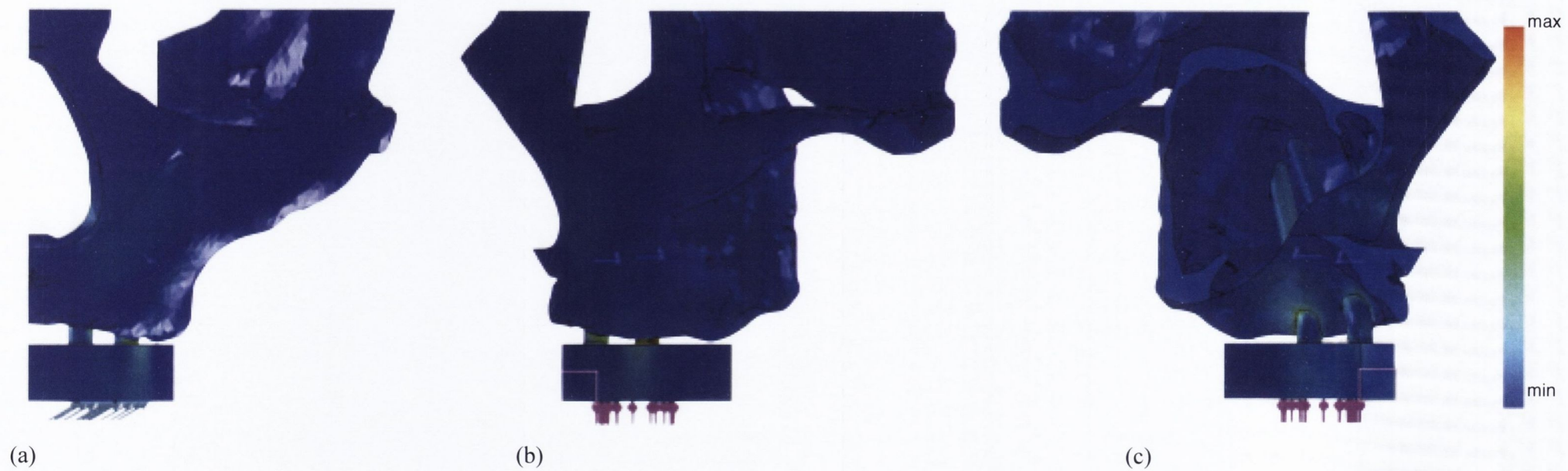


Figure 6.2 – Model 1 under 30° buccal loading: (a) anterior, (b) lateral and (c) medial views.

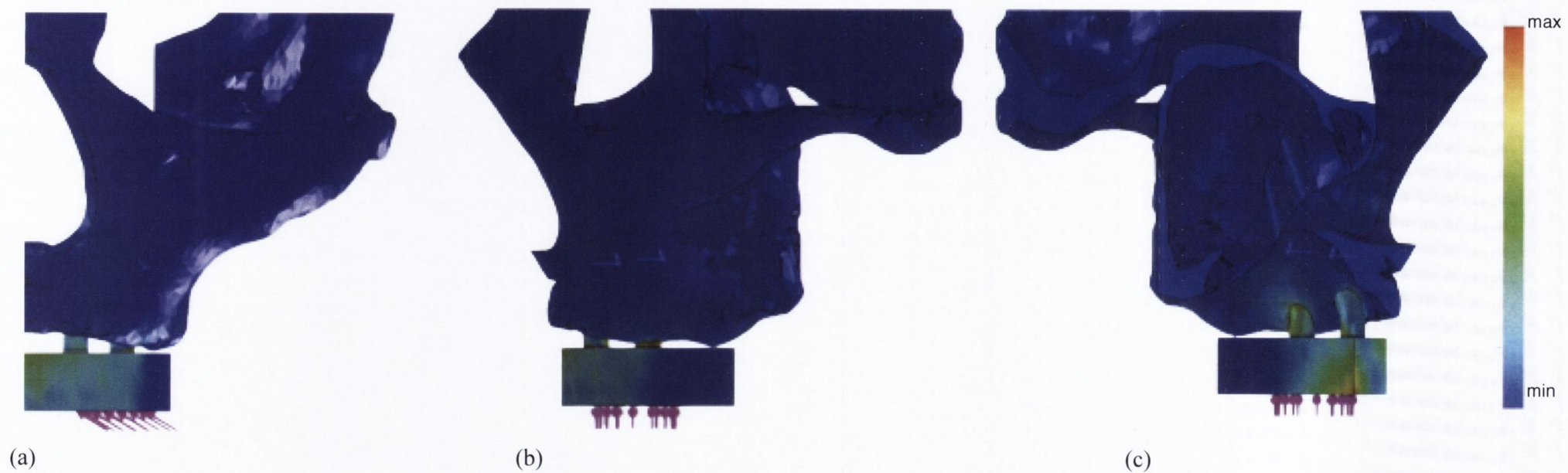


Figure 6.3 – Model 1 under 30° palatal loading: (a) anterior, (b) lateral and (c) medial views.

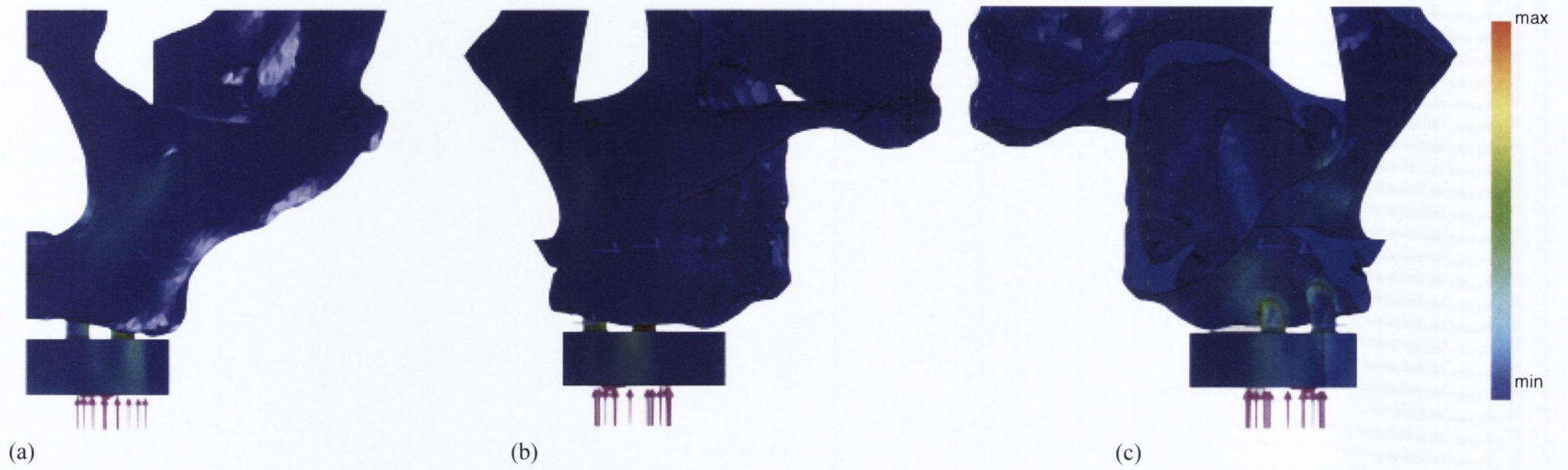


Figure 6.4 – Model 2 under occlusal loading: (a) anterior, (b) lateral and (c) medial views.

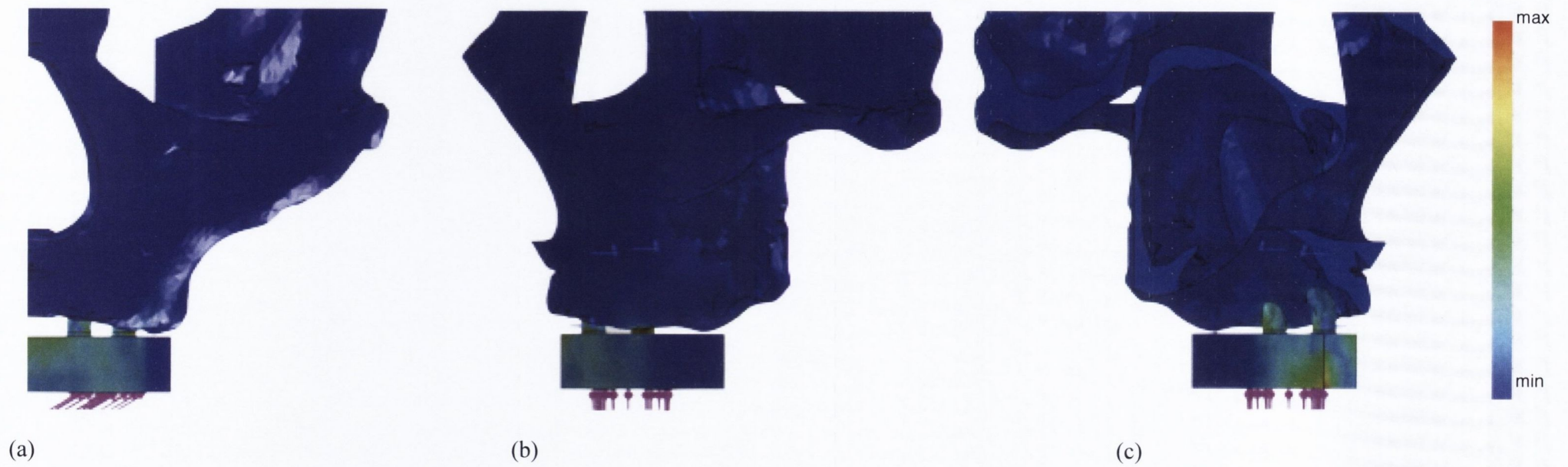


Figure 6.5 – Model 2 under 30° buccal loading: (a) anterior, (b) lateral and (c) medial views.

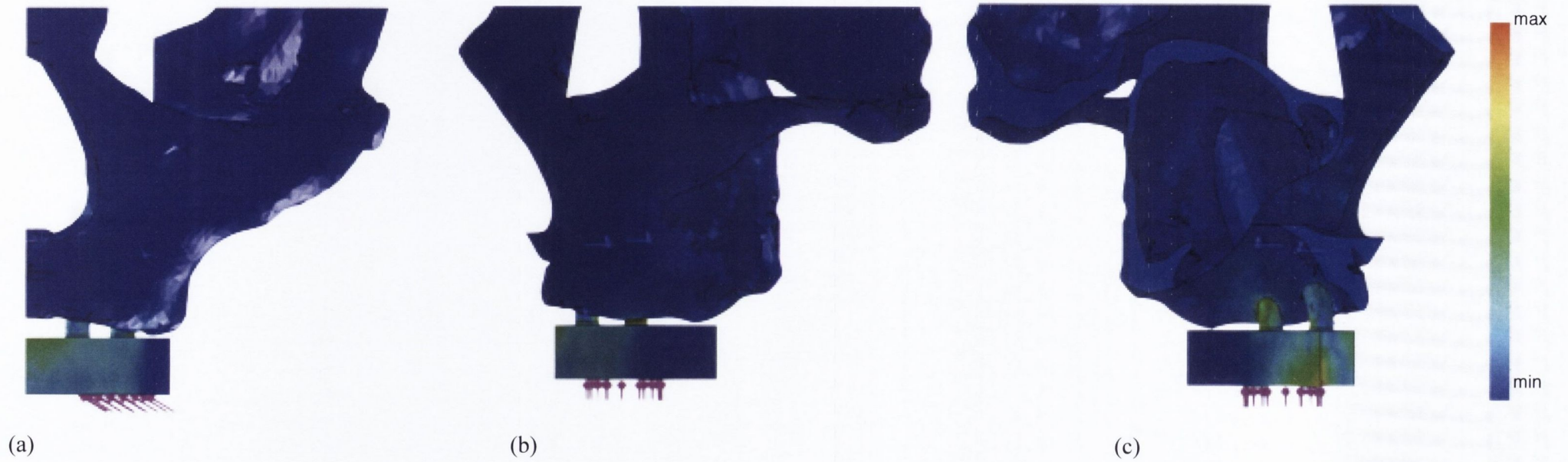


Figure 6.6 – Model 2 under 30° palatal loading: (a) anterior, (b) lateral and (c) medial views.

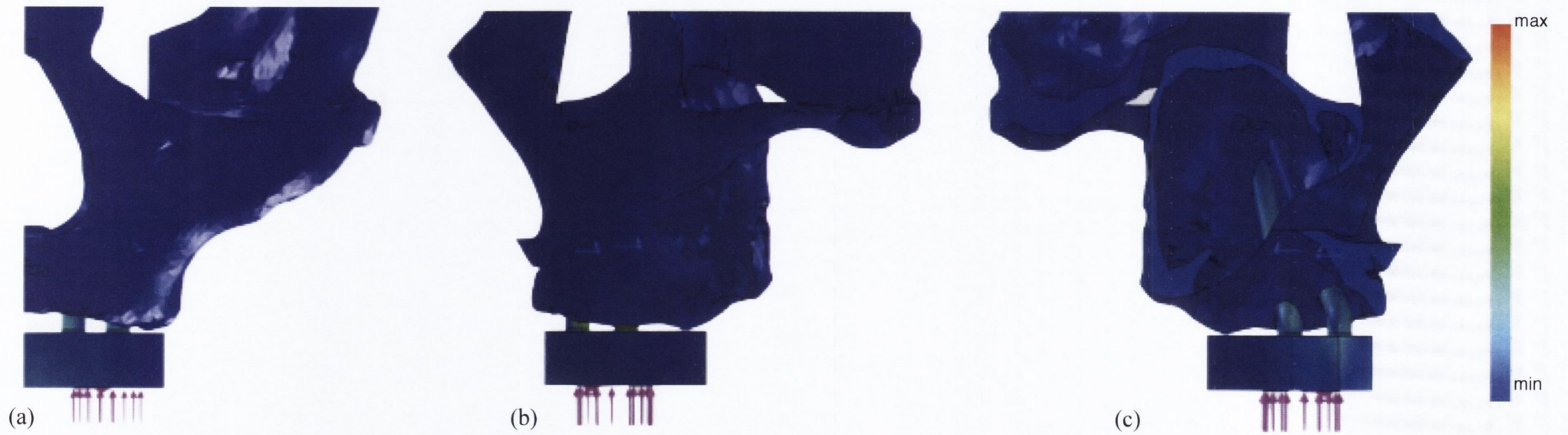


Figure 6.7 – Model 3 under occlusal loading: (a) anterior, (b) lateral and (c) medial views.

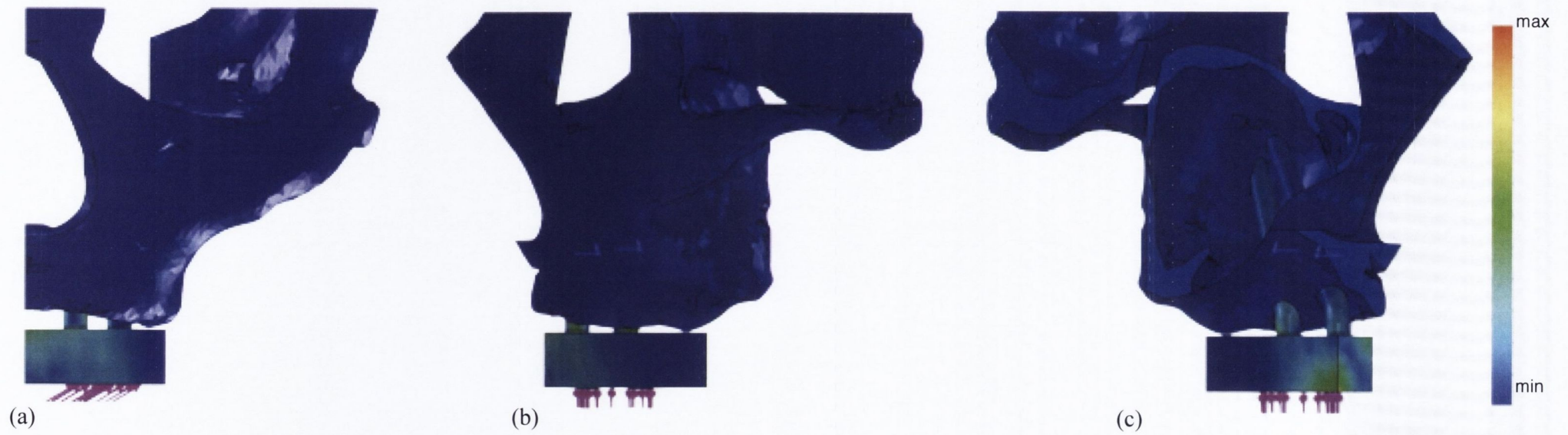


Figure 6.8 – Model 3 under 30° buccal loading: (a) anterior, (b) lateral and (c) medial views.

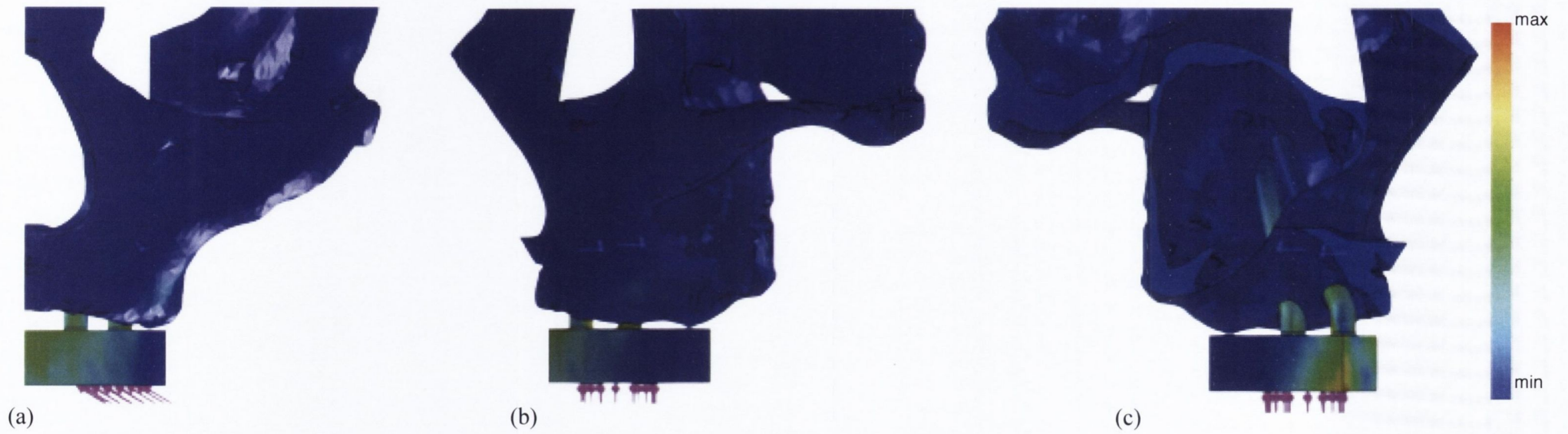


Figure 6.9 – Model 3 under 30° palatal loading: (a) anterior, (b) lateral and (c) medial views.

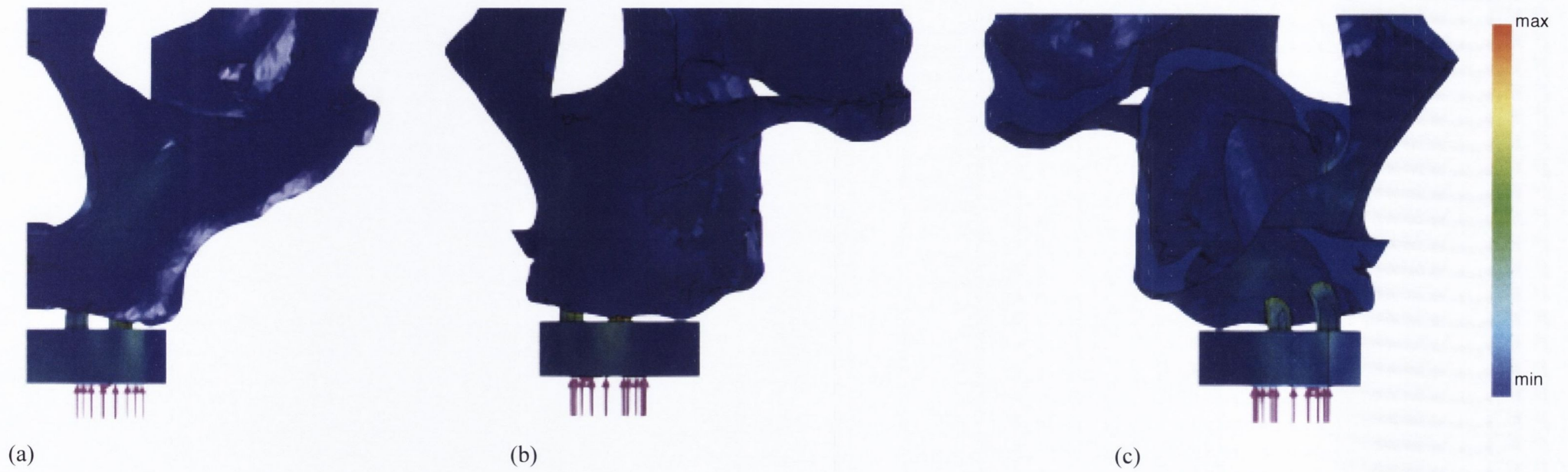


Figure 6.10 – Model 4 under occlusal loading: (a) anterior, (b) lateral and (c) medial views.

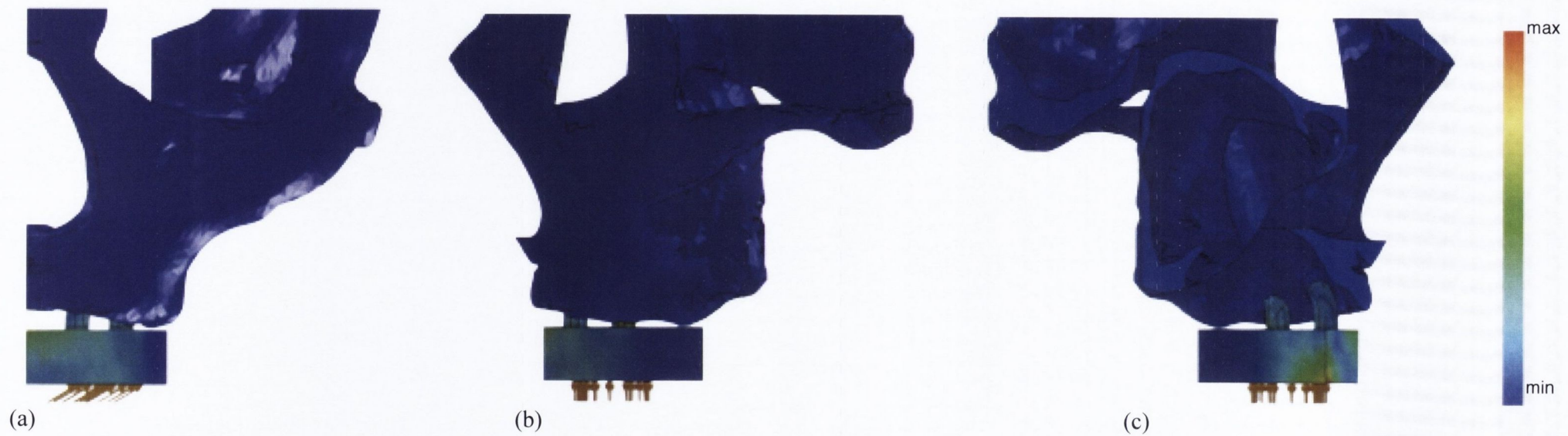


Figure 6.11 – Model 4 under 30° buccal loading: (a) anterior, (b) lateral and (c) medial views.



Figure 6.12 – Model 4 under 30° palatal loading: (a) anterior, (b) lateral and (c) medial views.

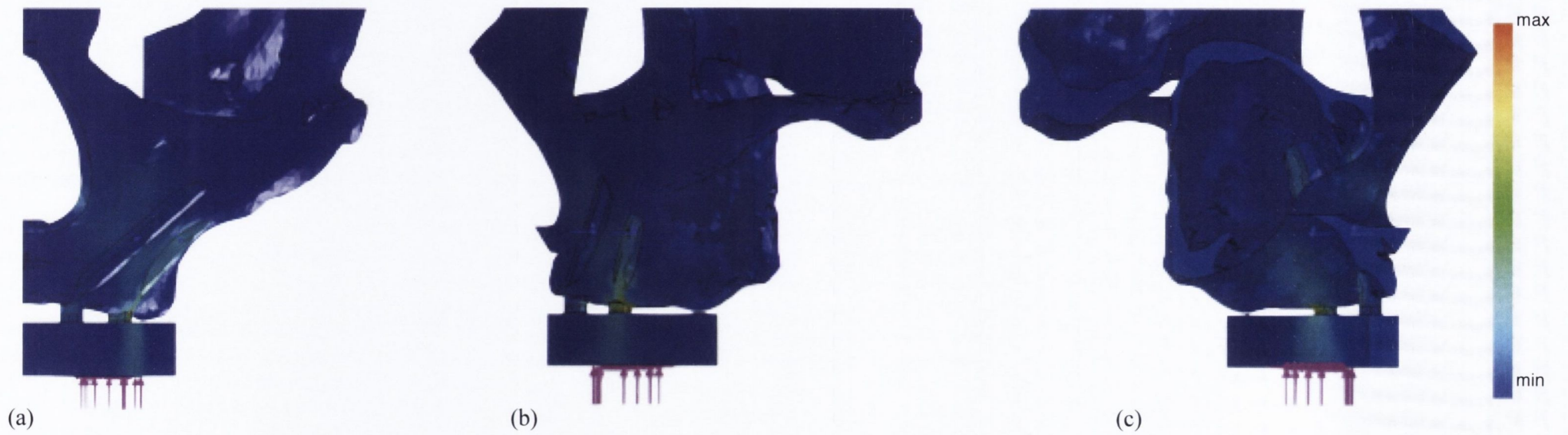


Figure 6.13 – Model 5 under occlusal loading: (a) anterior, (b) lateral and (c) medial views.

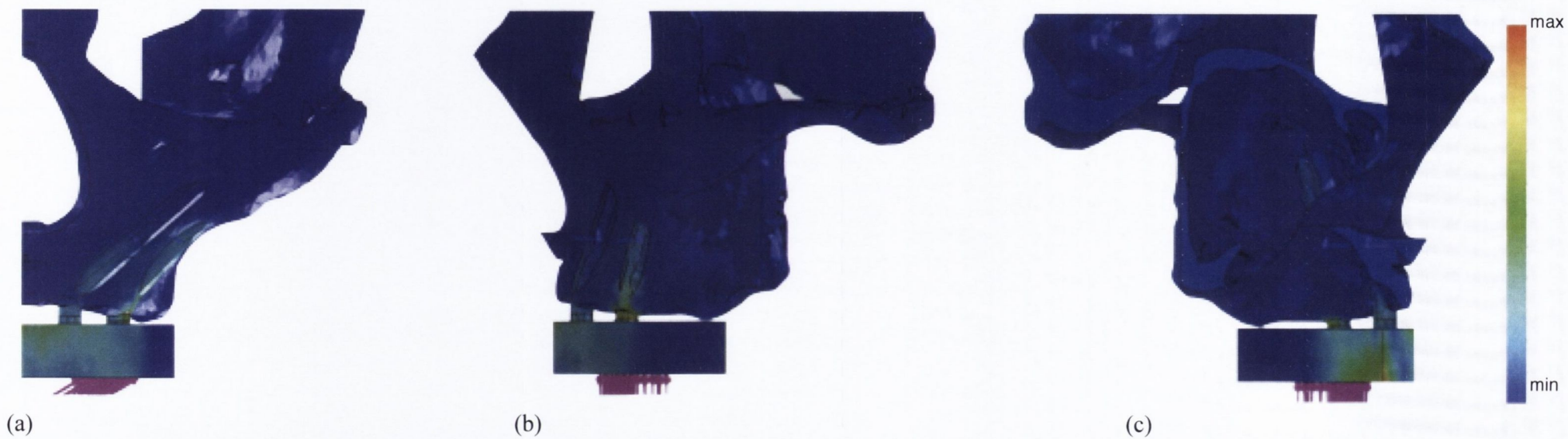


Figure 6.14 – Model 5 under 30° buccal loading: (a) anterior, (b) lateral and (c) medial views.



Figure 6.15 – Model 5 under 30° palatal loading: (a) anterior, (b) lateral and (c) medial views.



Figure 6.16 – Model 6 under occlusal loading: (a) anterior, (b) lateral and (c) medial views.

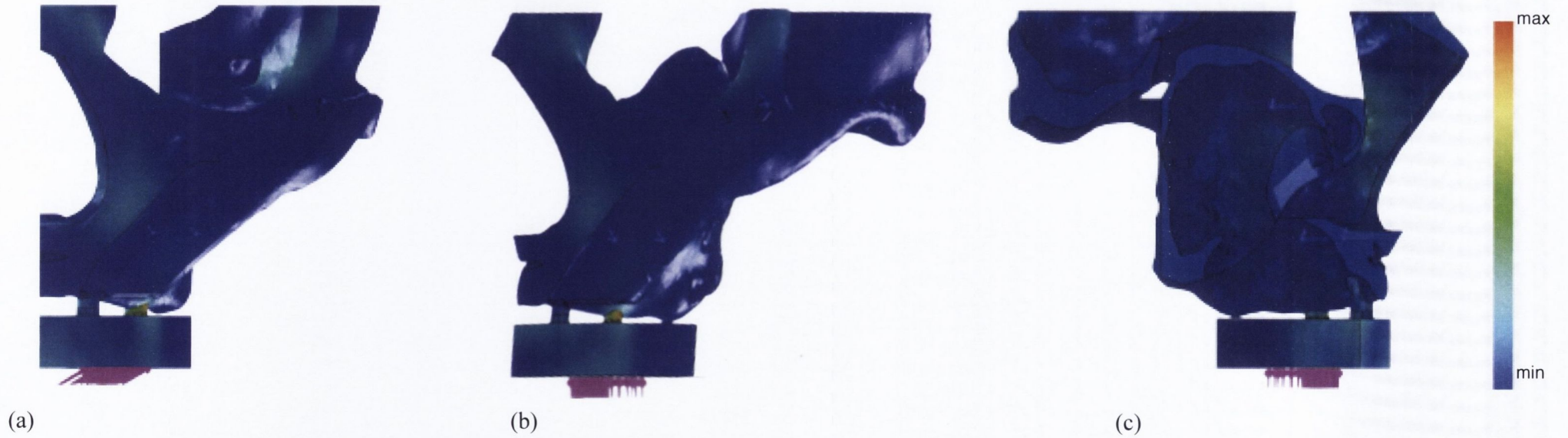


Figure 6.17 – Model 6 under 30° buccal loading: (a) anterior, (b) lateral and (c) medial views.



Figure 6.18 – Model 6 under 30° palatal: (a) anterior, (b) lateral and (c) medial views.

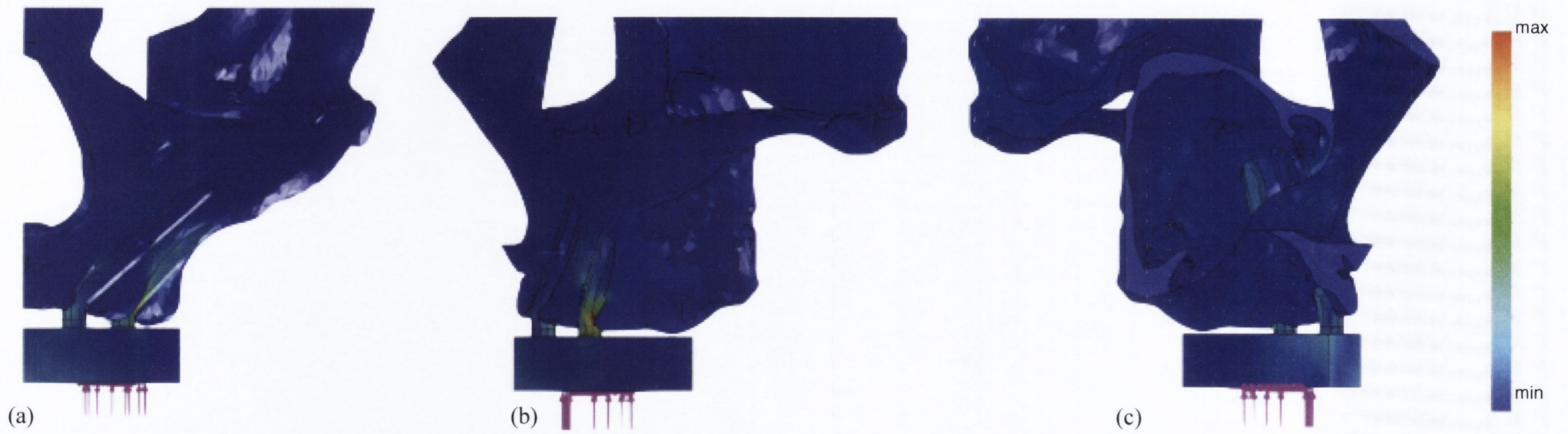


Figure 6.19 – Model 7 under occlusal loading: (a) anterior, (b) lateral and (c) medial views.

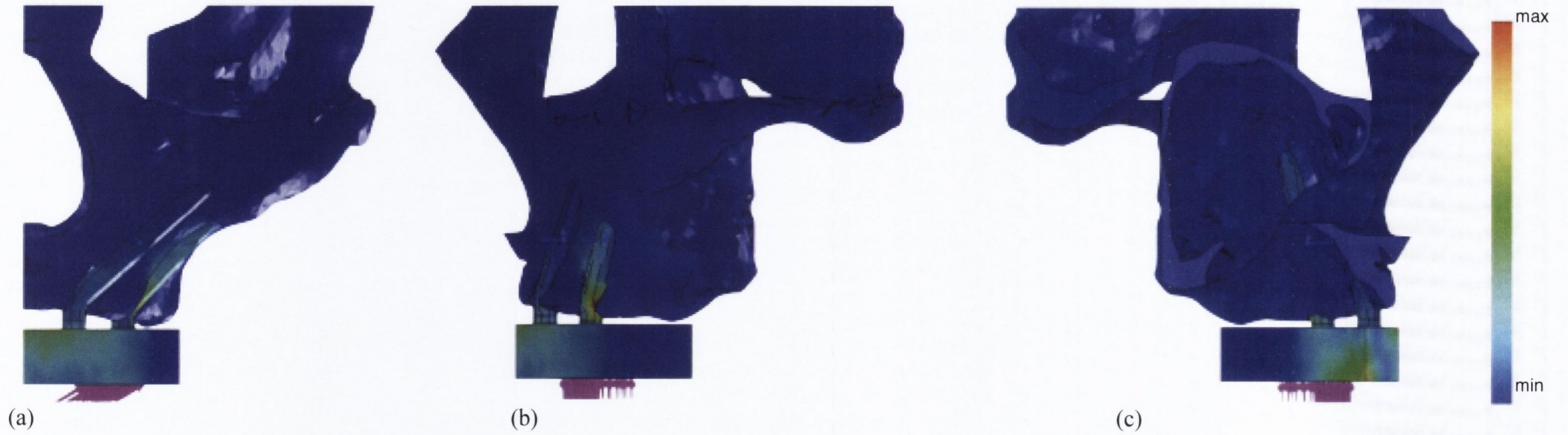


Figure 6.20 – Model 7 under 30° buccal loading: (a) anterior, (b) lateral and (c) medial views.

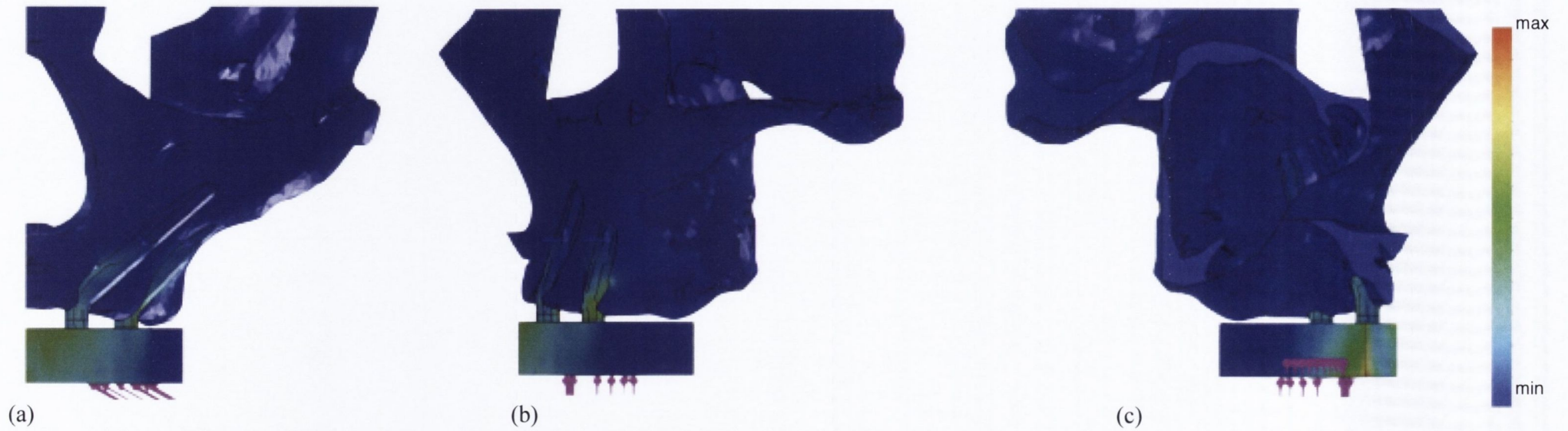


Figure 6.21 – Model 7 under 30° palatal loading: (a) anterior, (b) lateral and (c) medial views.

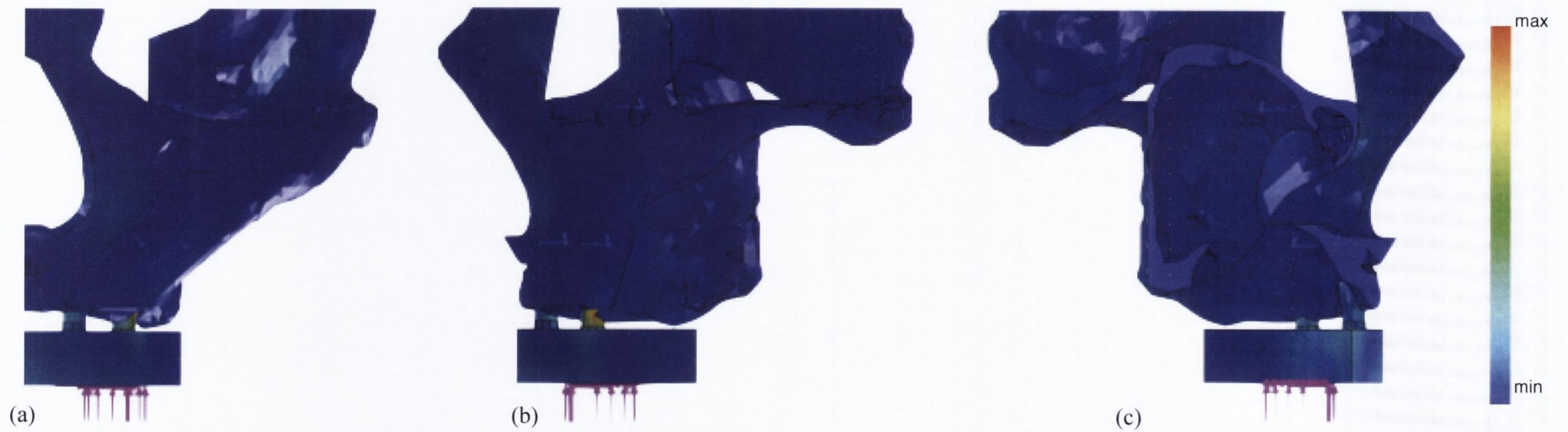


Figure 6.22 – Model 8 under occlusal loading: (a) anterior, (b) lateral and (c) medial views.

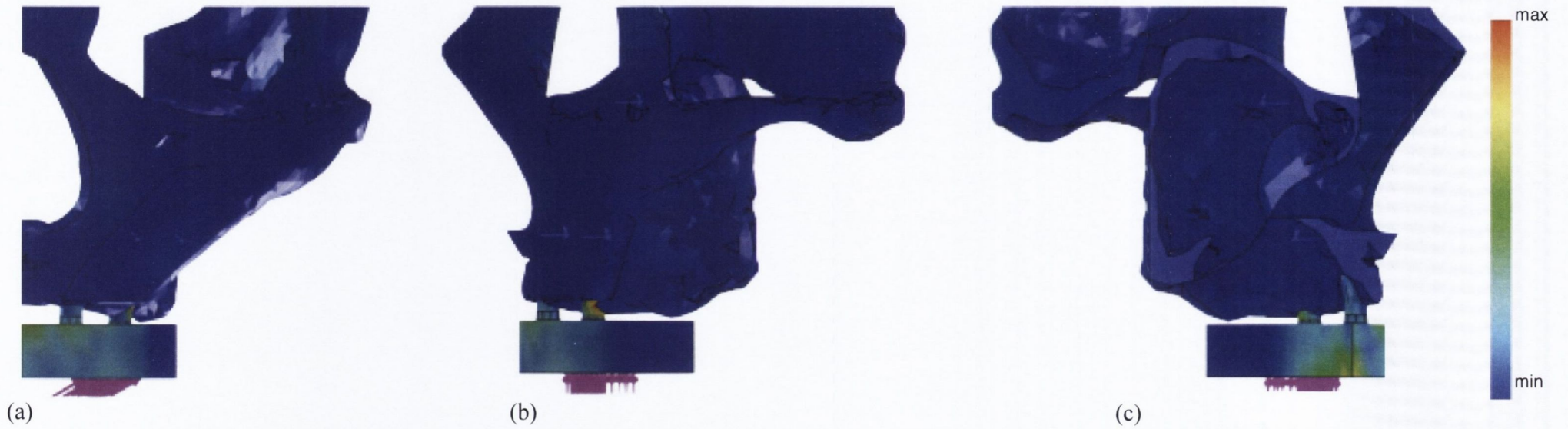


Figure 6.23 – Model 8 under 30° buccal loading: (a) anterior, (b) lateral and (c) medial views.

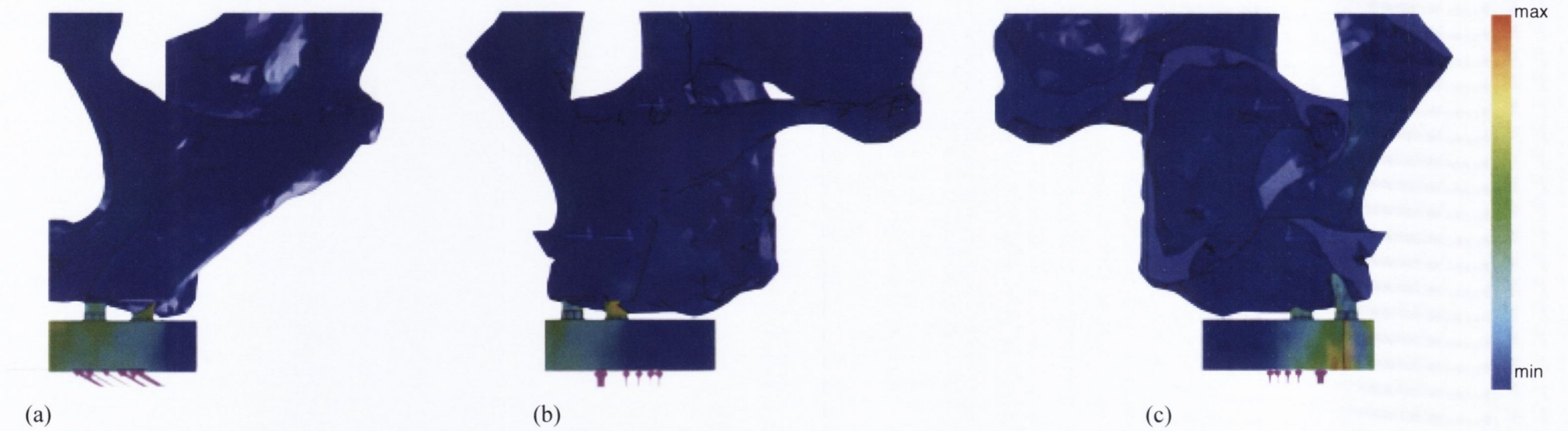


Figure 6.24 – Model 8 under 30° palatal loading: (a) anterior, (b) lateral and (c) medial views.